

# **Low Carbon Sound Absorption**

Creating an optimal noise mitigating product  
for outdoor applications

Loïc Chabus



# Abstract

This research focusses on the creation of sustainable alternatives for acoustic panels and structures in infrastructural and urban environments. Addressing both the environmental impact of current solutions and urban noise stress. Different techniques are applied within material and product development to absorb traffic and urban noise and create a better urban environment.

Initial scientific literature research focusses on noise mitigation strategies, current noise mitigation materials and products, the development of sustainable materials used for the built environment and Key Performance Indicator parameters to assess newly developed materials and products. The focus lies in creating a durable product that forms a valuable alternative to common materials and products made of concrete, glass and perforated aluminium with mineral wool used in outdoor urban situations.

The focus within the material science lies in the creation of porous filler, foamed and perforated materials. Pore size, panel thickness, its surface texture and density all have impact on the sound absorption properties of a material. Different materials have been tested with the Impedance Tube for high, mid and low frequencies. The frequency band where this research focusses on is 400 to 2500 Hz. This is considered the most impactful band width for noise disturbance for humans. First, porous fillers have been produced. Later foamed and perforated samples have been created. Additional literature led to the exploration of these three directions and the decision-making. Sound absorption properties are elaborated further in this research. With the aid of Grasshopper with Aeolus, further decision-making has been made based on design variations to inform the total geometry of the design. Panel geometry suggestions are elaborated further as well.

Various samples were created within this research. All with the aim for maximum sound absorption in the desired frequency bandwidth. Foaming procedures and perforation rates are explored in combination with a sound absorbing backing structure following Helmholtz resonance. The particle size, heating temperature, baking time, filler volume and weight fraction all have a significant impact on the sound absorption and material properties. Temperatures variations between 100 and 160 °C, are researched. Each produced material was evaluated using the grading tool elaborated further in chapter 2.5.

Created material configurations demonstrate findings which indicate that these could be a serious alternative for current sound mitigation products and materials. Existing aluminium sheet materials with a mineral wool absorbent core are compared to the created product. It has been found that perforated materials with a reed structure and a cavity, have significant sound absorption qualities, based on the fundamental acoustic Helmholtz principle. Materials from foamed furfuryl alcohol, specifically furan resin from Biorez, show important sound absorption within the target frequency range. Sound absorption coefficients of 0.8 and 0.9 were achieved for several frequency bands.

Porous filler-based materials were tested on mechanical performance. Flexural strength and impact testing was evaluated. Created foamed materials are tested on moisture uptake and perforated materials on UV and weather resistance.

The best performing final product was a combination of a perforated front panel made from 8040 Fire Hemp with an open area of in between 20-30% and an absorbing material behind it with a cavity of 40 mm. In this research a 100 mm deep reed layer was used. Promising foamed materials varied in sample thickness, with S3 as a cork-based foamed material, showing SACs of 0.85 at 1500 Hz.

A digital acoustic simulation in Grasshopper with Aeolus was explored. This model explores the optimal geometry for different urban scenarios. The focus lies in highly dense urban environments, were not only reflection, but also absorption is required and desired. Literature review, computational acoustics, material development and impedance tube testing present a viable, circular strategy for the development of noise mitigating products in infrastructure and urban settings. The findings point to promising, broader potential for the application of these product configurations and stimulate continuous research in the domain of low carbon sound absorption.

# Low Carbon Sound Absorption

## The Development and Acoustic Evaluation of Low Carbon Materials for Noise Mitigation in Infrastructure and Urban Environments

### TU DELFT

MSC ARCHITECTURE, URBANISM & BUILDING SCIENCES  
BUILDING TECHNOLOGY GRADUATION

### MENTOR TEAM

Prof. Dr. Mauro Overend  
Dr. Gabriele Mirra

### ADVISORY TEAM

Prof. Martin Tenpierik  
Willem Böttger  
Sam Lonis  
Dr. Barbara Lubelli

### STUDENT

Loïc Chabus (5249694)

### PRESENTATION DATE

24th of June 2026

# Acknowledgements

This thesis process has been a great journey. Conducting this research led me towards becoming an engineer and a material researcher with a design and engineering background. Collaboration between the TU Delft and the company NPSP in Delft, which professionally researches and manufactures biocomposite panels, has been a great success.

My gratitude goes to my two mentors from the AE&T department Prof. Dr. Mauro Overend and Dr. Gabriele Mirra, for their guidance along this research and to my supervisors from NPSP, Willem Böttger and Sam Lonis for their consistent advice and refreshing ideas.

It truly was a pleasure to work with you. My excellent first mentor, Prof. Dr. Mauro, always encouraged me to think deeper and in alternative paths to come up and create innovative research. His knowledge on Low Carbon Materials, particularly biocomposites, led to a state-of-the-art knowledge in this field. A field which is globally still considered extremely new and has many aspects that remain to be discovered. I want to thank Dr. Gabriele Mirra for his guidance with building the parametric model within Grasshopper, which helped design the optimal geometry in different urban contexts. His knowledge on parametric design, such as in Grasshopper Aeolus, was greatly appreciated. In particular, the Digipedia page, offers detailed and professional content to create digital designs and workflows.

I thank Sam Lonis for his consistent guidance and critical questions. His background in both Aerospace Engineering and Industrial design, led to a broad knowledge spectrum which further increased the depth of this research. His hands-on approach and knowledge about machinery and working equipment were much appreciated.

Willem Böttger, as partner of NPSP, served as a perfect head of R&D. His suggestions, sometimes truly out of the box, often led to great outcomes. I was able to brainstorm with him regularly to conduct the material development in an efficient and thorough manner. Besides Sam Lonis and Willem Böttger I am thanking all NPSP colleagues for their help and advice.

A word of appreciation goes to Prof. Dr. Ir. Martin Tenpierik for his advice regarding acoustic research and his constant involvement with the real-world acoustical testing. His specialisation in the field of acoustics proved to be inspiring and necessary for this research.

I am thanking Barbara Lubelli for her advice and guidance regarding capillary water absorption testing in the Heritage & Technology Lab at BK.

A thank you to Korneel van Massenhove from the KU Leuven in Brugge, Belgium, for conducting the second Impedance Tube test together with me and Sam and providing key findings in acoustic absorption and product research.

I thank Hans van Ginhoven for his advice regarding the waterjet cutting possibilities within the Glass Lab at BK.

Lastly, I would like to thank my close friends and family who supported me throughout this research journey.

# Table of Contents

## 1. INTRODUCTION

1.1	Research Framework	13
1.1.2	Problem Statement	13
1.1.3	Relevance of Research	16
1.1.4	Objective and Motivation	17
1.1.5	Research Questions	19
1.1.6	Scope and Context of the Research	22
1.2	Approach	22
1.2.2	State-of-the-Art	23
1.2.3	Acoustic Simulations	24
1.2.4	Experimental Investigations	25

## 2. STATE-OF-THE-ART

2.1	Introduction: Outdoor Acoustics	27
2.1.2	Outdoor Sound Propagation Mechanisms	27
2.1.3	Urban Surfaces, Façades & Street Canyons	28
2.1.4	Relevance of Mid-High Frequencies for Traffic-Noise Mitigation	29
2.1.5	Outdoor Constraints for Absorptive Materials	30
2.2	Sound Mitigation Mechanisms	31
2.2.1	Absorption, Reflection, and Scattering as Combined Design Principles	31
2.2.2	Helmholtz Resonance	32
2.2.3	Porous Absorption Mechanisms	32
2.2.4	Layering & Surface Modification	33
2.2.5	Requirements	33
2.3	Conventional Products & Systems	34
2.3.2	Conventional Outdoor Systems	35
2.3.3	Low-Noise Road Surfaces & Porous Asphalt	36
2.3.4	Conventional Sound Absorption Systems	36
2.3.5	Perforated Aluminium with Mineral Wool Core Production Process & EOL	38
2.4	Low Carbon Solutions	40
2.4.2	Natural-Fibre & Biobased Acoustic Materials	40
2.4.3	Natural Elements	41
2.4.4	Biocomposites	41
2.4.5	Emerging Acoustic Metamaterials & Structured Systems	45
2.4.6	Nature Inclusivity	47
2.4.7	Positioning this Research within Existing Products	47
2.5	Strategic KPI's	48

## 3. EXPERIMENTAL INVESTIGATIONS

3.1	Materials & Methods	50
3.2	Production Process & Observations	52
3.3	Test Results	61
3.3.2	Porous Fillers	62
3.3.2.2	Mechanical Testing (3-point bending test)	64
3.3.3	Foamed Materials	65
3.3.3.2	Digital Microscope Imaging	68
3.3.3.3	Capillary Water Absorption	70
3.3.3.4	Freeze-Thaw Testing	71
3.3.4	Perforated Materials	72
3.3.4.2	Geometry Research	76
3.3.4.3	QUV-Testing	77
3.4	Simulations Acoustic Modelling	78
3.5	Discussion	82

## 4. CASE STUDY

4.1	Introduction	84
4.2	Acoustic Analysis of Existing Situation	84
4.3	Parametric Model with Shape Variations	86
4.4	Optimisation & Validation	88
4.5	Grasshopper Components and Design Logic	90
4.6	Reflection Simulations	91
4.7	Design	92

## 5. CONCLUSIONS

5.1	Scientific Findings	95
5.2	Societal Impact (Perforations & Total Product)	100
5.3	Future Research	102

## 6. REFLECTIONS

6.1	Research Approaches	105
6.2	Moral & Ethical Considerations	105
6.3	Evaluation of Societal Impact	105

## References

## Appendix

## Glossary:

Biocomposite(s): biocomposites are composite materials consisting of a matrix (resin) and natural fibre reinforcement derived from biological entities (Mondal et al., 2022)

Sound absorption coefficient:  $\alpha(f)$  (ranging from 0 – 1)

Noise Reduction Coefficient: Value measured in specific internals (250, 500, 1000 & 2000 Hz)

CO<sub>2</sub>e/m<sup>2</sup>: Carbon Dioxide Equivalent per square metre

## Acronyms:

BA: Blowing Agent

BC: Binder Concentration

BMC: Bulk Moulding Compound

EOL: End-Of-Life (usually used for material assessment after its lifespan)

EPD: Environmental Product Declaration

EU: European Union

FS: Flexural Strength

GHG: Green House Gas

GH: Grasshopper (software)

KPI: Key Performance Indicator

LCA: Life Cycle Assessment

LCM: Low Carbon Material(s)

MPa: Mega Pascal (a unit of pressure)

MPP: Micro Perforated Panel

NRC: Noise Reduction Coefficient (Committee, 2023)

SAC: Sound Absorption Coefficient

SI: Sound Interference

SPL: Sound Pressure Level

STC: Sound Transmission Class

STI: Speech Transmission Index

RIVM: Rijksinstituut voor Volksgezondheid en Milieu

TGV: The Green Village (TU Delft)

UV: Ultraviolet

WA: Water Absorption

WHO: World Health Organisation

# List of Figures & Tables

## Figures:

- Figure 1: A noise map of Amsterdam, Netherlands (source: Park, Lee, et al., 2010)
- Figure 2: Cumulative noise map of the Netherlands (source: Schreurs et al., 2010)
- Figure 3: Different SPL (=Sound Pressure Levels) of different vehicles on different frequency bands (source: Cai et al., 2017)
- Figure 4: Different strategies of noise mitigation (source: Cox & D'Antonio, 2004)
- Figure 5: topology optimised acoustic Hamburg concert hall (source: Electricbloomhosting, 2017)
- Figure 6: Overview global carbon emissions (%) for different sectors; building materials represent 12% of total global emissions (source: Why Buildings – Architecture 2030; ISA; Statista)
- Figure 7: Information structure for product design (source: Author)
- Figure 8: Graduation research flowchart (source: Author)
- Figure 9: Overview research gap (source: Author)
- Figure 10: Impedance tube at BK (source: Author)
- Figure 11: Impedance tube set-up (source: Rakesh et al., 2026)
- Figure 12: Outdoor sound propagation mechanisms (diffraction – black, ground reflection – blue, façade reflections/urban canyon effect – red) (source: Author)
- Figure 13: Frequency range focus in this research; frequencies between 400 and 2500 Hz are especially responsive to porous and fibrous absorption and are strongly related to perceived sharpness, speech interference, and tyre-road noise (source: Author)
- Figure 14: Multiple sources of traffic noise categorised into three groups, namely, propulsion, tyre-pavement, and aerodynamic noise, Modelling of Traffic Noise Along Urban Corridor: A Case Study of Amman. (Younes et al., 2021)
- Figure 15: Reflection, absorption, diffusion and transmission of sound (source: Author)
- Figure 16: Different strategies for sound absorption (source: Arenas and Crocker, 2010)
- Figure 17: Placement of the porous absorbent layer (source: Author)
- Figure 18: Porous sound absorption principles (source: Author)
- Figure 19: Perforated aluminium sheet with mineral wool core product (source: [Hot Item] Acoustic Perforated Rock Wool Sound Insulation Sandwich Panel, n.d.)
- Figure 20: Aluminium highway absorptive barrier (source: Perforated Aluminium Acoustic Sheet for Highway Noise Barrier and Buildings, n.d.)
- Figure 21: Perforations on an industrial scale with the (punch method) (source: IndiaMART, n.d.)
- Figure 22: Production process mineral wool (source: Chen et al., 2011)
- Figure 23: Random incidence absorption coefficient for Rockwool of two different thicknesses on a rigid backing (source: Cox & D'Antonio, 2004)
- Figure 24: An overview of natural fibrous materials (source: Author)
- Figure 25: A three-part material diagram showing resin matrix + fibres + fillers, with indications of the functions of each constituent: "load transfer", "reinforcement", "volume/cost/fire/surface tuning", "durability", and "circularity" (source: Author)
- Figure 26: NPSP biocomposite production process (source: NPSP)
- Figure 27: Production process furfural (Catrinck et al., 2020)
- Figure 28: Placement of Furan Resin relative to plastics, and other composite materials (source: Odiyi et al., 2023)
- Figure 29: A scheme showing how sugarcane bagasse is processed and how furan resin is obtained (source: Author)
- Figure 30: Lattice structure for sound absorption (source: Lattice Structures for Acoustics Applications – Zhai Group At NUS, n.d.)
- Figure 31: Metamaterial designs based on natural and bio inspired shapes (source: Lu et al., 2025)
- Figure 32: Fractals inspired acoustic sound absorption design (source: Wan et al., 2020)
- Figure 33: Nature Inclusive design system (source: Studio Marco Vermeulen)
- Figure 34: Flowchart production, testing & evaluation of material development (source: Author)
- Figure 35: Equipment needed in the lab for different produced materials (porous fillers, foamed materials and perforated materials) (source: Author)
- Figure 36: Porous Filler Production Process (source: Author)
- Figure 37: Foamed Material Production Process (source: Author)
- Figure 38: Foaming process using a BA (source: Karger-Kocsis, József; Bárány, Tamás (2019). Polypropylene Handbook (Morphology, Blends and Composites) // Foams., 10.1007/978-3-030-12903-3(Chapter 10), 579–641)
- Figure 39: Potential foaming agents (source: left to right: American Society of Baking, n.d.; Cereals & Grains Association, n.d.; MIT OpenCourseWare, 2012; Lehmann & Voss & Co. KG, 2024; Reglero Ruiz et al., 2015)
- Figure 40: Foamed material production S9 (source: Author)
- Figure 41: S9 foamed material (source: Author)
- Figure 42: S13 foamed material (source: Author)
- Figure 43: Perforated biocomposite 8040 Hemp Fire (20% perforation rate)
- Figure 44: Impedance Tube test – Absorption Coefficient Rice Husk, Rubber, Cork Bio-polyester & Cork Furan (source: Author)
- Figure 45: Impedance Tube test – Absorption Coefficient Glass Bubbles on different pressures & Cork Furan on low pressure (source: Author)
- Figure 46: Impedance Tube test – Absorption Coefficient S9-S13 & Sanded Material full spectrum 0–6400 Hz (source: Author)
- Figure 47: Sanded Cork Furan Material D (source: Author)
- Figure 48: B3 Cork & Bio-Polyester 3-point bending test (source: Author)
- Figure 49: B3 (Cork filler-based material) (source: Author)
- Figure 50: B2 (Cork filler-based material) (source: Author)
- Figure 51: Overview of the best performing foamed materials (S3, S9, S10, S11 & S13) (source: Author)
- Figure 52: Impedance Tube test – Absorption Coefficient S1-S8 Large Samples (100 mm) (source: Author)
- Figure 53: Impedance Tube test – Absorption Coefficient S1-S8 Small Samples (29 mm) (source: Author)

Figure 54: Impedance Tube test – Absorption Coefficient S9–S13 (source: Author)

Figure 55: S3 Porosity Assessment (source: Author)

Figure 56: S3 Depth Assessment Colour (source: Author)

Figure 57: S10 Porosity Assessment (source: Author)

Figure 58: S10 Depth Assessment Colour (source: Author)

Figure 59: S11 Porosity Assessment (source: Author)

Figure 60: S11 Depth Assessment Colour (source: Author)

Figure 61: S13 Depth Assessment 3D (source: Author)

Figure 62: S11 Depth Assessment 3D (source: Author)

Figure 63: Capillary water absorption of 5 samples

Figure 64: Close-up of samples with tape wrapped around the materials (source: Author)

Figure 65: Amount of water (capillary) absorbed for each sample after 8h (A1=S10, A2=S3, A3=S9, B1=S12, B2=S11) (source: Author)

Figure 66: Early-stage freeze-thaw assessment S11 (source: Author)

Figure 67: Impedance Tube with and without a cavity (source: Adjusted from Ďuriš & Labašová, 2021)

Figure 68: different perforated materials C1, C2, C3 & Reed

Figure 69: Illustration on different setups tested with the impedance tube. The behaviour of the soundwaves and Helmholtzresonance is visible (source: Author)

Figure 70: Impedance Tube Test Result: Sound Absorption Coefficient perforated samples 10% open area. (Cav stands for Cavity) (source: Author)

Figure 71: Impedance Tube Test Result: Sound Absorption Coefficient perforated samples 20% open area. (Cav stands for Cavity) (source: Author)

Figure 72: Impedance Tube Test Result: Sound Absorption Coefficient perforated samples 30% open area. (Cav stands for Cavity) (source: Author)

Figure 73: Different steel perforated geometries (source: Okhrimenko, 2022)

Figure 74: Different set-up configurations for the perforated external material (20%) and S3 (left), 100mm reed (middle) & 100mm mineral wool (right) (source: Author)

Figure 75: Perforated Hemp Fire 8040 material (A2) & 8012 Bio-polyester (A1) QUV-testing (source: Author)

Figure 76: Simulation of the expected sound absorption curve on whole octave subdivisions based on the values in table 10 and table 11 (source: Porous Absorber Calculator, n.d.-b)

Figure 77: Simulation of the expected sound absorption curve on whole octave subdivisions based on the values in table 10 and table 12 (source: Porous Absorber Calculator, n.d.-b)

Figure 78: Simulation of the expected sound absorption curve on whole octave subdivisions based on the values in table 10 and table 13 (source: Porous Absorber Calculator, n.d.-b)

Figure 79: Absorption Coefficient simulation Acoustic Modelling using Table 14 and 15 (source: Helmholtz Calculator, n.d.-c)

Figure 80: Absorption Coefficient simulation Acoustic Modelling using Table 14 and 15 (source: Helmholtz Calculator, n.d.-c)

Figure 81: Noise barrier system installation locations A10 Zuidas (source: (Zuidasdok & Zuidasdok, 2026)

Figure 82: A10 highway Amsterdam West Surinameplein (source: 3DBAG Viewer, n.d.)

Figure 83: Urban situation diagrams (source: Author)

Figure 84: An impression of acoustic barriers on the chosen location (source: own)

Figure 85: Close-up impression of reflecting sound in the parametric model (source: Author)

Figure 86: An impression of the sound reflections on the two chosen traffic lanes (source: Author)

Figure 87: The evaluation of the SPL on the target surface (source: Author)

Figure 88: The evaluation of the SPL on the target surface (source: Author)

Figure 89: Workflow diagram digital simulation (source: Author)

Figure 90: SPL visualisation with N= 3 (5715 dB total) (source: Author)

Figure 91: SPL visualisation with N = 2 (5710 dB total) (source: Author)

Figure 92: illustration on allocation of absorptive façade elements (source: Author)

Figure 93: impression of sound waves and barrier geometry in the urban landscape (source: Author)

Figure 94: impression of sound waves and barrier geometry in the urban landscape (source: Author)

Figure 95: Design variations 600x600 panels (source: Author)

Figure 96: Quantitative 2D Stress Distribution (source: Author)

Figure 97: Potential design variations with different back structures; from left to right: mineral wool, reed, foamed furan resin, reed higher density, nature inclusive (e.g. birds) (source: Author)

Figure 98: Current production process at NPSP for pressed biocomposites and a possible upscale perforation device added (source: Author)

Figure 99: Current production process for foamed biocomposites (source: Author)

Figure 100: Impact comparison of different applied materials for noise mitigation infrastructure in the Dutch context (CO<sub>2</sub> in kilotonnes) (source: Author)

**Tables:**

*Table 1: (sources: a: Jacksons Fencing, n.d., b: Acoustic Supplies, n.d.; c: First Fence, n.d.; d: GlasBoertje, n.d.; e: Ornitolink, n.d.; f: Solosar, n.d.; g: SteelProfil, n.d.; h: Lacasta et al., 2016)*

*Table 2: (sources: a: Saint-Gobain Ecophon, 2023; b: CertainTeed, n.d.; c: Rockfon, 2025a, 2025b; d: PlafondPlaza, n.d.; BASF SE, 2025; e: Post Acoustics, n.d.; f: Plastocell Kunststoff, n.d.; g: Yamamah Smart, n.d.; h: EUROPUR, 2025; i: ABM Trade, n.d.; Fibers & Foams, n.d.; j: Topakustik AG, 2025; SCS Global Services, 2024; k: Eckel Industries, n.d.; l: Acoustic Measurement, 2025; m: VTT Technical Research Centre of Finland, 2012; n: Vicoustic, n.d.; o: Thomann, n.d.; m: Yang & Sheng, 2023)*

*Table 3: Overview common resin types used for biocomposites and their main properties (source: Li et al., 2007; Mohammed et al., 2023; Odiyi et al., 2023)*

*Table 4: Biogenic content in Nabasco Façade Panels, per FU (1 m<sup>2</sup>) (source: Nabasco EPD).*

*The kg C/FU is taking the entire lifetime of the product into account*

*Table 5: Grading tool (source: Author)*

*Table 6: Controlling Parameters Material Development (source: Author)*

*Table 7: Porosity Analysis S10, S11 & S3 (source: Author)*

*Table 8: Production Overview Material Development (source: Author)*

*Table 9: S9-S13 (source: Author)*

*Table 10: Perforated panel (source: Porous Absorber Calculator, n.d.-b)*

*Table 11: a: flow resistivity taken on 40,000 with M. Tenpierik (source: Porous Absorber Calculator, n.d.-b)*

*Table 12: a: flow resistivity taken on 40,000 with M. Tenpierik (source: Porous Absorber Calculator, n.d.-b)*

*Table 13: a: flow resistivity taken on 40,000 with M. Tenpierik (source: Porous Absorber Calculator, n.d.-b)*

*Table 14: Perforated panel (source: Helmholtz Calculator, n.d.-c)*

*Table 15: a: flow resistivity taken on 40,000 with M. Tenpierik (source: Helmholtz Calculator, n.d.-c)*

*Table 16: a: flow resistivity taken on 40,000 with M. Tenpierik (source: Helmholtz Calculator, n.d.-c)*

*Table 17: z: 3-point average is taken for the NRC of S13 (500, 1000 & 2000 Hz) Note: comparison can only be made if values are compared in the correct unit: EN 15804 is used; w: a prediction based on the curve of S3 has been made; y: based on Nabasco EPD data, see references*

*To assess the area and compare the materials optimally, an estimation on the curvature on the frequencies in between 1600 (the end of large 100 mm samples in the impedance tube) and 2500 Hz (the end of the focus frequency range), is made.*

*Obtained values for established materials are retrieved from the Literature Review chapter and the same as applied in table 1 and 2. (source: Author)*



01

INTRODUCTION

## 1.1 Research Framework

### 1.1.2 Problem Statement

Environmental noise exposure is widely recognized as one of the most significant and persistent environmental stressors affecting public health in modern societies.

The main long-term contributor of environmental noise comes from traffic noise. This is both in urban and peri-urban areas, particularly in regions characterised by infrastructural networks and high mobility regions (World Health Organization [WHO], 2011, 2018; European Environment Agency [EEA], 2020). In the Netherlands alone, around 3.5 million people experience discomfort from traffic noise yearly (Bureau Sanering Verkeerslawaa, 2025). Traffic noise has a chronic and repetitive nature. This leads to prolonged exposure that accumulates over time and affects many residents. In policy and health literature, this chronicity is decisive. The public health relevance of noise is not merely that it is loud at certain moments, but that it is continuously present, structurally embedded in everyday environments, and difficult for residents to avoid (WHO, 2018; EEA, 2023).

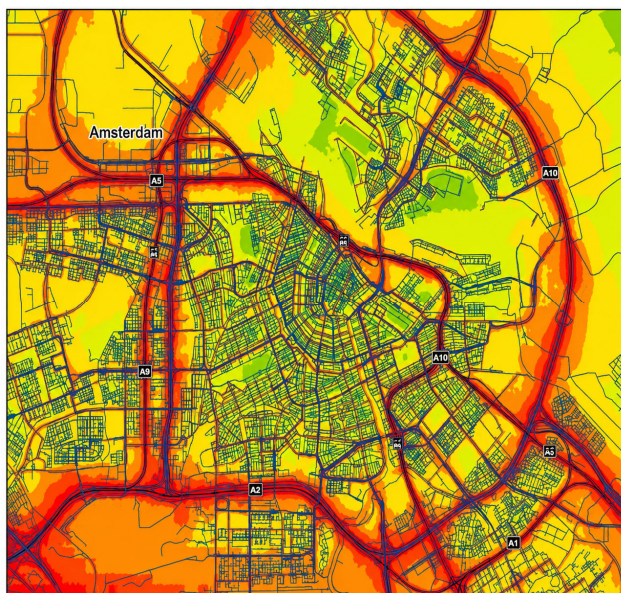


Figure 1: A noise map of Amsterdam, Netherlands (source: Park, Lee, et al., 2010)

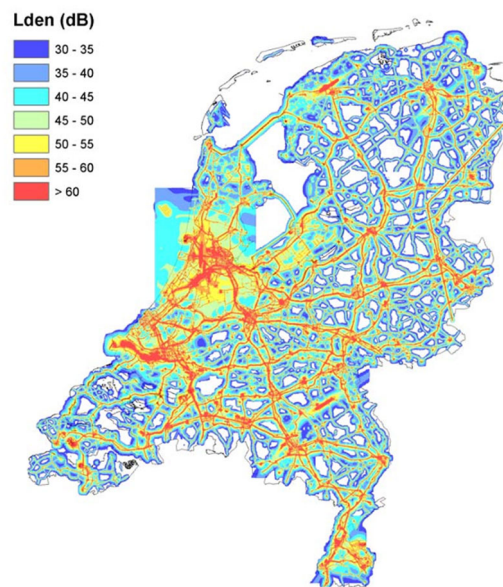


Figure 2: Cumulative noise map of the Netherlands (source: Schreurs et al., 2010)

Epidemiological research outlines that long term exposure to higher noise levels is associated with larger ranges of health issues. Increased physiological stress responses, sleep disturbance, heightened risk of cardiovascular disease, impaired cognitive functioning, and increased numbers of premature mortality (van Kempen et al., 2018; Khomenko et al., 2022). It is important to note that some of the health concerns were also present in noise levels that were historically seen as acceptable. This showcases the need to review regulatory thresholds and mitigation strategies (WHO, 2018). The WHO research emphasizes that noise stress can be subdivided into the following categories: direct physiological stress, indirect behavioural disruption, mainly sleep, and cumulative psychosocial strain. These factors make it a complex issue (WHO, 2011, 2018; van Kempen et al., 2018). The National Institute for Public Health and Environment (RIVM) researched environmental noise related topics within the Netherlands. It is found that a substantial proportion of the population is exposed to noise levels that exceed health-based guidelines. The main sources for the noise stress are major roads and junctions, proximity to highways and dense urban corridors (RIVM, 2014, 2018, 2022).

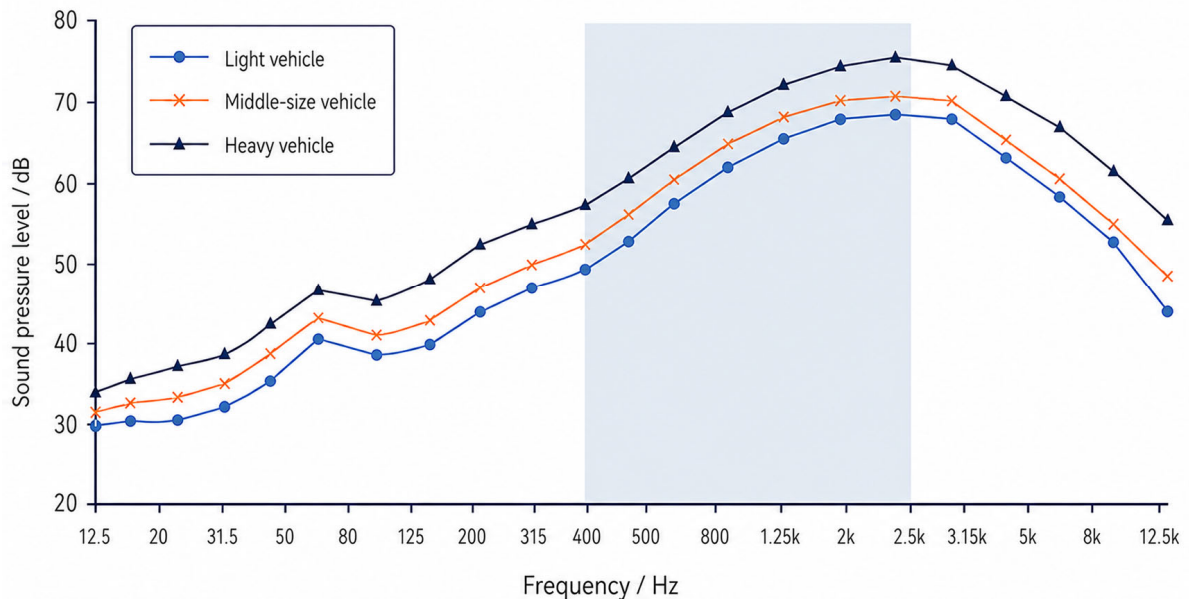


Figure 3: Different SPLs (=Sound Pressure Levels) of different vehicles on different frequency bands (source: Cai et al., 2017)

According to research conducted by the Atlas Leefomgeving (2025) and the RIVM, noise exposure is unevenly distributed. Inhabitants residing near large-scale infrastructure experience disproportionately high exposure levels. Following research findings from Hayward & Helbich., 2024, concluding that exposure correlates with socioeconomic and demographic characteristics. Suggesting noise pollution is not only a health problem, but also a spatial and equity issue.

Effects of decades long policies on mitigation of existing noise factors remain limited. Noise barriers, low-noise road surfaces, and building envelope improvements are common approaches. The Dutch Bureau Sanering Verkeerslawaaai (2025) outlines the formal institutional framework for the traffic noise interventions. These interventions show local reductions in noise levels, however conventional materials consist of concrete, glass, mineral wool and synthetic polymers. These examples usually have high embodied carbon, are energy intense and are limited in recyclability. Especially considering their full life cycle (Carruthers, 2012; Ahmad et al., 2025).

The choice to focus on innovative and sustainable building materials comes from the desire to create wider impact. When looking at carbon emissions worldwide. The building sector is responsible for around 37% of total emissions (United Nations Environment Programme & Yale Centre for Ecosystems + Architecture, 2023). Out of the total emissions, construction materials account for 11% of the total and 37% of the building sector's share (Röck et al., 2020). Therefore, research into composites with a biobased share is worth to be researched.

Awareness on sustainability, climate change, and resource depletion has increased over the past decades. Therefore, the common materials used for noise mitigation are outdated and problematic. Global and national accords on the reduction of fossil-based and mineral intensive materials force governments to adopt innovative solutions. Discussions around waste flows, circular processing, and material valorisation within the Netherlands, show how infrastructure sectors are being asked to reduce waste and adopt circular material strategies (Afval Circulair, 2022). Noise mitigation will increasingly be treated as a fixed part of sustainable infrastructure projects and not only as a technical issue (Ahmad et al., 2025; Afval Circulair, 2022).

As a result, societies face a dual challenge. This being chronic noise-related health concerns which need to be addressed, and the current unsustainable materials used for noise reduction. This graduation project addresses the dual challenge by researching bio inspired materials for noise

mitigation. Specifically, the development of low carbon materials for acoustic evaluation. The aim is to produce, test, and simulate biocomposites to achieve a product, which can be implemented in the real world, with a TRL matching this goal. The research assumes the product(s) will be applied both in infrastructural settings and urban networks with a high need for noise control. Requirements for safety, weather resistance, manufacturability, and lifecycle performance will shape what is feasible.

### 1.1.3 Relevance of the Research

#### Scientific relevance

This scientific research combines environmental acoustics, material science, and sustainable construction. In the field of acoustics, it is general knowledge that sound absorption is mainly achieved through viscous and thermal losses in porous and fibrous materials. Internal structures enhance dissipation of acoustic energy across various frequencies (Jaouen et al., 2025). From an environmental perspective, fibrous materials are being researched. These have a high capacity of sound absorption due to their high surface area and intricate pore networks. This property translates acoustic oscillations into heat (due to boundary-layer losses).

Translating laboratory level testing to real-world standards remains a challenge. The characterization of porous media is however progressing (Jaouen et al., 2025). This is especially important for biocomposites, where microstructures are more variable compared to mineral wools and polymer foams.

This project focusses on frequencies which are seen as most affecting for noise stress, being in between the range of 400 Hz and 2500 Hz (Lu et al., 2025). While humans perceive sounds from 20 Hz to 20,000 Hz, this research considers measures in between the 400-2500 Hz range. Traditional noise control measures usually include sound absorption and reflection. As transmission is usually extremely low for common façade materials. This comes from the ability to convert acoustic energy into thermal energy (Lu et al., 2025).

Material thickness and surface treatment are other factors influencing sound absorption in natural fibre materials. These materials are especially interesting for traffic noise mitigation, as they perform well in this frequency range. Research from Shankar et al., 2025 underscores the importance of design variables alongside microstructural porosity as a measure to improve noise control.

Mineral wool and synthetic materials are historically researched for their predictable acoustic performance and ease of industrial production. These materials often perform best for sound absorption. This is confirmed by the thorough research from Cox and D'Antonio on absorbers and diffusers and discussed in the review from 廣澤邦 (2008). This research also demonstrates that combination of diffusion and absorption can lead to improved reflections and reverberation.

The past years have shown a surge in research in natural fibres and biobased composites, leading to increasing research in the domain of natural fibres and acoustics. Coir and rice husk promise serious sound absorption according to empirical studies. These materials show promising results when manufactured in suitable thickness, density and pore structure (Lekshmi et al., 2023). Research done by Mohammadi et al., 2024, proves that within research on natural-fibre composites for sound absorption materials, fibre morphology, porosity, and material selection are the main factors for the optimal performance. Bamboo proves to be a high performing option for indoor acoustic comfort and having the ability to tune acoustic targets (Irvani et al., 2025).

To conclude, these sources demonstrate plausibility that low carbon materials and biobased materials can deliver serious acoustic absorption if designed and manufactured with appropriate microstructural and macrostructural control (Lekshmi et al., 2023; Mohammadi et al., 2024; Irvani et al., 2025).

This scientific research focusses on an application ready product, which can be implemented in the built environment for noise mitigation. While existing research often focusses on natural fibre acoustic panels for indoor applications, this project explores the outdoor context. In indoor spaces, room acoustics, reverberation, and mid to high frequency management is dominant (Bozkurt, 2022). Often low- and mid-frequency energy is the main exposure in traffic dominated areas and infrastructural environments. Low frequency absorption is more challenging for porous absorbers. Contamination, weathering, structural limitations all change effective porosity and impedance. Shankar et al. (2025) demonstrates that thickness and surface modifications are relevant to the performance. Stating that indoor strategies cannot directly be implemented in outdoor environments. This research advances the understandings of how biocomposites perform under conditions faced in outdoor infrastructural environments such as highways or urban centres. This domain remains less represented in current biobased acoustics research (Jaouen et al., 2025; Mohammadi et al., 2024).

Even though biocomposites are increasingly forming a sustainable alternative for mainstream building materials, research gaps remain regarding (long-term) performance under real-world conditions, and integration into the circular economy (Ahmad et al., 2025; Nwankwo & Mahachi, 2025). Natural fibres form an alternative with multiple sustainable arguments. Being reduced embodied energy, renewable production, drastically improved end-of-life scenarios in comparison with commonly used construction materials (Przybek, 2025a). As stated above, this research contributes to biocomposite material innovation in performance-driven applications. Focusing on real-world application.

## Societal Relevance

Noise pollution has large effects on societies. WHO guidelines for the environment state that noise is a health determinant and that prevention is required for both source control and interventions along exposure paths (WHO, 2018). According to European environmental health reports, environmental noise is a persistent risk factor and a public health burden (EEA, 2020, 2023). As confirmed in the introduction, the RIVM in the Netherlands, further demonstrates the link between noise exposure, health, well-being, and psychosocial effects (RIVM, 2014, 2022).

Research from Hayward & Helbich, 2024, show a relation between environmental noise exposure and socioeconomic and demographic characteristics across Dutch neighbourhoods. Highlighting the urge to combat noise pollution. Urban development and infrastructure placement expose noise pollution in disfavoured neighbourhoods with fewer means to combat this issue. This confirms the need for interventions (Hayward & Helbich, 2024; RIVM, 2014).

Due to international agreements (such as the Paris Agreement, 2015), on sustainable goals, societal priorities shift more towards circular considerations and the circular economy. Waste reduction, material reuse, and the development of biobased material chains.

The Dutch waste and circularity organization analyses waste processing and translates the measurements into statistics (Afval Circulair, 2022). Bio-based materials reduce fossil fuel resource dependency and enables the renewable material economy. NPSP B.V., the company this research is executed with, has their own network of suppliers, which will be elaborated later in the report. It is important to understand the focus of the research towards an application specific validation (Przybek, 2025a; Ahmad et al., 2025; Nwankwo & Mahachi, 2025).

To conclude, the societal relevance of this research is demonstrated in both the aim to reduce important public health burdens, namely noise stress, and the continuing development of sustainable material solutions for the circular economy and climate targets. This would result in improved liveability and health for urban areas, while also reducing the carbon footprint of current mitigation infrastructure.

## Professional and Practical Relevance

For this research, collaboration with a Delft based firm named NPSP B.V. is established. This company is specialised in the development and production of biocomposites.

Translating lab results to implementable designs is a key factor for the professional relevance of this research. Topics which will be researched for the product are safety, durability, cost, maintenance, standard compliance, and public acceptance.

The testing of water absorption has been conducted at NPSP itself and in the Heritage and Technology Lab at the TU Delft through a water basin and timely measurements.

The Bureau Sanering Verkeerslawaaai shapes the boundaries for the solutions which could be implemented in practice within the Dutch context.

Moreover, the professional practice increasingly demands digital workflows for planning and evaluation. Traffic noise maps, exposure assessments, and decision support tools, are now standard features of environmental planning; interactive mapping environments used in the Netherlands exemplify this (RIVM & Atlas Leefomgeving, 2025). Beyond mapping, advanced data management, visualisation, and simulation increasingly use cloud and GIS tools, as evidenced by work on cloud computing for online visualisation of GIS applications in urban contexts (Park et al., 2010). This proposal aligns with that professional direction by emphasizing measurable performance, data-driven interpretation, and integration of case context through mapping and digital analysis workflows.

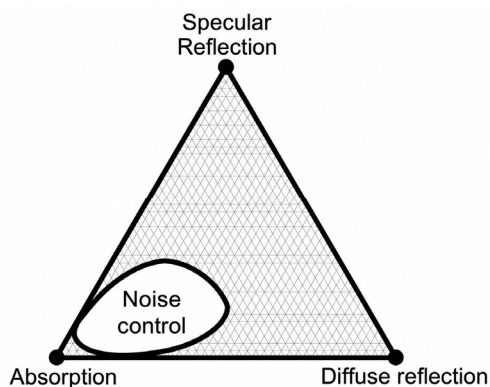


Figure 4: Different strategies of noise mitigation (source: Cox & D'Antonio, 2004)

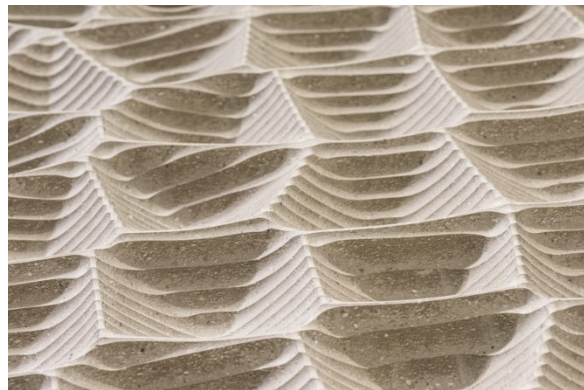


Figure 5: topology optimised acoustic Hamburg concert hall (source: Electricbloomhosting, 2017)

### 1.1.4 Objective and Motivation

The main objective of this graduation master thesis is to develop and evaluate low carbon materials for effective sound absorption for noise mitigation in infrastructure and urban environments. This directly contributes to solutions for noise-related health impacts combined with the environmental limitations of conventional acoustic materials. Within the realm of sustainable construction and circular economy strategies, this also responds to calls to broaden low carbon material applications beyond conventional structural or aesthetic uses and to demonstrate functional performance in demanding settings (Ahmad et al., 2025; Nwankwo & Mahachi, 2025).

To achieve the desired objective, the project is divided in several steps. The first step is to analyse the needed acoustical characteristics required for noise mitigation in urban areas with noise pollution. The frequency bands most important for noise stress, and how scattering and absorption should be balanced for the most optimal noise reduction, are explored (Jaouen et al., 2025; WHO, 2018).

The second step would be to investigate biobased fibres, binders, and composite combinations suitable for acoustic applications. Using the state-of-the-art scientific research within this domain. Research on coir, wool, rice husk, bamboo, hemp composites all play a key role in this development (Lekshmi et

al., 2023; Mohammadi et al., 2024; Irvani et al., 2025). Current biocomposites from NPSP are measured using the impedance tube to categorise these and draw conclusions on which material combinations are an indication of promising materials for acoustics. Specifically for absorption and the scattering of noise.

The third step focuses on the development and design of biocomposite materials. Looking into parameters like density, porosity, fibre fraction and the layering of the fibres and matrix. These choices are backed by theory and processing considerations (Jaouen et al., 2025; Ma et al., 2015).

Fourth, standard measurement techniques are used to evaluate acoustic performance of existing materials. Also, the benchmarking results will be compared with conventional solutions and literature. Understanding of room and building acoustics is mandatory (Bozkurt, 2022).

Finally, application in real-world contexts in urban areas will be assessed (RIVM, 2014, 2022; Atlas Leefomgeving, 2025).

The personal motivation for this research comes from a profound conviction of the importance and impact biocomposites have on the total global carbon emissions. To make an impact, building materials become an increasingly dominant factor within the built environment. In figure 6, the share building materials have on the total global carbon emissions is illustrated. From a societal perspective, health impacts of environmental noise need innovative and sustainable solutions (WHO, 2018; EEA, 2023; Khomenko et al., 2022). Regarding the professional perspective, collaboration with NPSP opens an opportunity to connect academic research with real-world implementation through mock-ups.

The research is limited by constraints related to scale, planning and timeframe, and available facilities, focusing on laboratory-scale development and testing first, rather than full industrial implementation. These boundary conditions are not only limiting; they encourage a focus on generating strong, interpretable relationships between material design and acoustic performance.

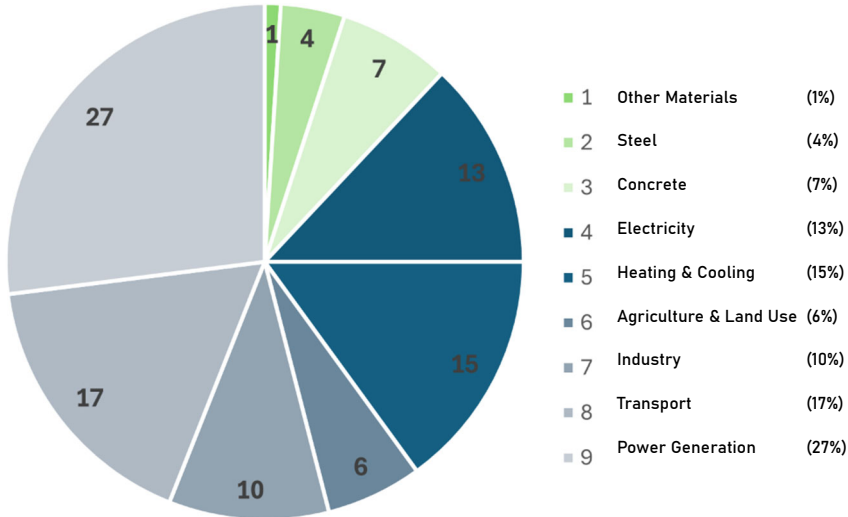


Figure 6: Overview global carbon emissions (%) for different sectors; building materials represent 12% of total global emissions (source: Why Buildings – Architecture 2030; ISA; Statista)

### 1.1.5 Research Questions

The central research question guiding this project:

**How can low carbon materials be designed and optimised to provide effective acoustic performance for noise mitigation in infrastructure and urban environments?**

This overarching question is supported by sub-questions addressing important parts of the problem. These include the following questions:

- (a) What are requirements for traffic noise reduction?
- (b) How do biobased fibre composite configurations affect sound absorption and attenuation?
- (c) How do material parameters such as density, porosity, and binder type control acoustic response?
- (d) How do the developed biocomposite concepts compare with conventional mitigation materials?
- (e) How can numerical and laboratory results can be interpreted in relation to real-world highway and urban contexts?

Foundational knowledge required to answer the sub-questions, include the characteristics of traffic noise and its health risk (EEA, 2020; RIVM, 2022), the theoretical principles of porous acoustics, absorption, and diffusion (Jaouen et al., 2025; 廣澤邦, 2008), and limitations of existing used material solutions (Carruthers, 2012; Ahmad et al., 2025). To select materials, research on waste flows and biobased design strategies is issued from (Afval Circulair, 2022; Groene Bouwmaterialen, 2025).

The following hypotheses are made for this research;

Firstly, it is stated that LCM (low carbon materials) engineered with controlled porosity and fibrous networks and fibres can achieve sound absorption coefficients comparable to established porous absorbing materials. Comparable to absorbers in mid-frequency range (Lekshmi et al., 2023; Mohammadi et al., 2024; Irvani et al., 2025).

Second, it is hypothesised that material designs such as graded density, layered assemblies, or surface texture modification could potentially improve broadband performance and potentially extend effectiveness into lower frequency ranges, consistent with porous material and absorber design principles (Jaouen et al., 2025; 廣澤邦, 2008).

Thirdly, it is established that material selection with circular design that can produce solutions that are not only acoustically effective, but environmentally sustainable compared to fossil based or mineral intensive materials. This follows the framing of biocomposites in construction (Ahmad et al., 2025; Nwankwo & Mahachi, 2025).

### 1.1.6 Scope and Context of the Research

The research places itself within the broader context of sustainable infrastructure development and environmental health. To make the scope of the research realistic, the focus in this project lies in the development and evaluation of biocomposites rather than making suggestions for a systemic infrastructural redesign. Exploring the relationship between material development and acoustics while keeping the boundaries of time, resources and production capacity in mind is key in this research.

The A10 highway in Amsterdam forms the practical application area. Through simulations in Grasshopper, an optimal design can be found for this case study. As seen in the introduction, highway

networks and urban transportation infrastructure create the highest noise exposure. Research from the RIVM, 2014 and Atlas Leefomgeving, 2025, provide requirements for the significance of absorption results.

These aims are important, but acknowledging the limitations is as important. The research's value lies in the exploration of new material combinations for optimal noise mitigation and an exploration how digital simulations could support the design and application potential. The research positions itself alongside ongoing developments in sustainable construction and material engineering, where low carbon materials are proposed as promising but still under-standardised solutions (Ahmad et al., 2025; Nwankwo & Mahachi, 2025). The overview of the research domains to achieve the desired product, is illustrated in figure 9.

This research is embedded in a network of academic, industrial, and institutional stakeholders. This context is important because outdoor noise mitigation is not implemented through solely laboratory testing. A successful material design must align with production capabilities, infrastructure requirements, safety expectations and environmental policy.

Academic stakeholders include supervisors, researchers, laboratory staff, and domain experts in acoustics, material science, sustainability, and infrastructure design. Their role is to support methodological rigor, theoretical coherence, and interpretation of results. The academic network is also important for access to testing facilities, including impedance tube testing and, where relevant, reverberation-room knowledge or other acoustic laboratories. While this thesis focuses primarily on laboratory-scale evaluation, the broader TU Delft context supports the translation between material testing, design research and built-environment application.

Overall, the institutional context strengthens the applied relevance of the research. NPSP provides material-development expertise, Rijkswaterstaat provides infrastructural relevance, public-health institutions define the urgency of noise mitigation, and academic facilities support experimental validation. An elaborated overview of the production of the product and the parameters involved are illustrated in figure 8. The institutional network enables the research to move beyond isolated material testing and toward an application-oriented understanding of biocomposite acoustic products.

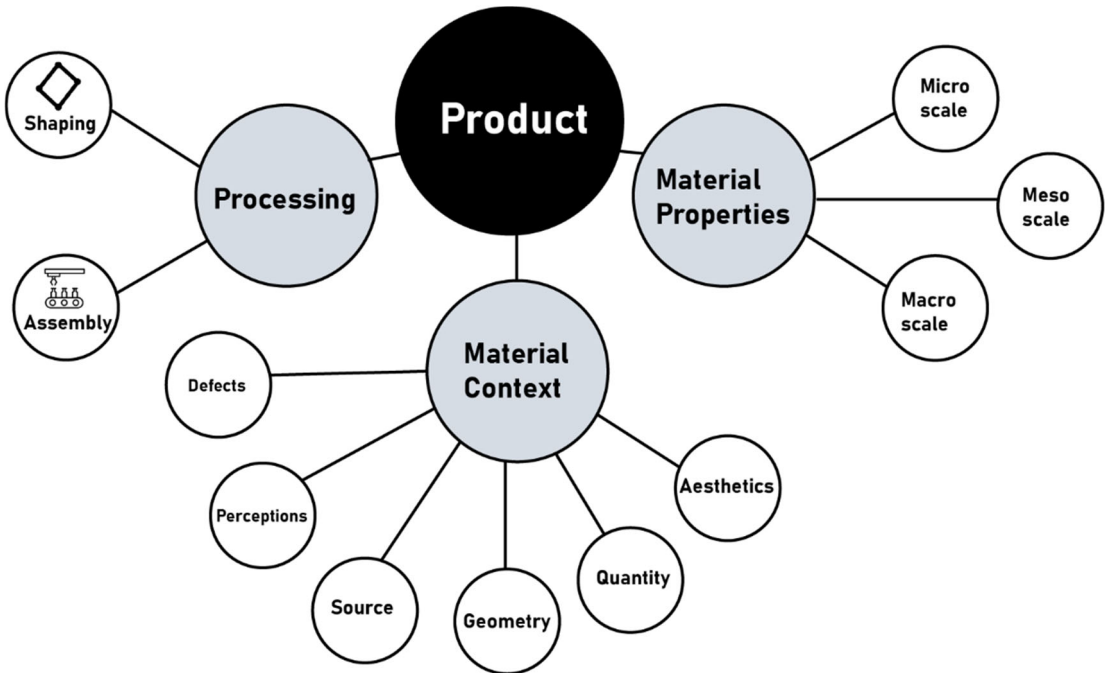


Figure 7: Information structure for product design (source: Author)

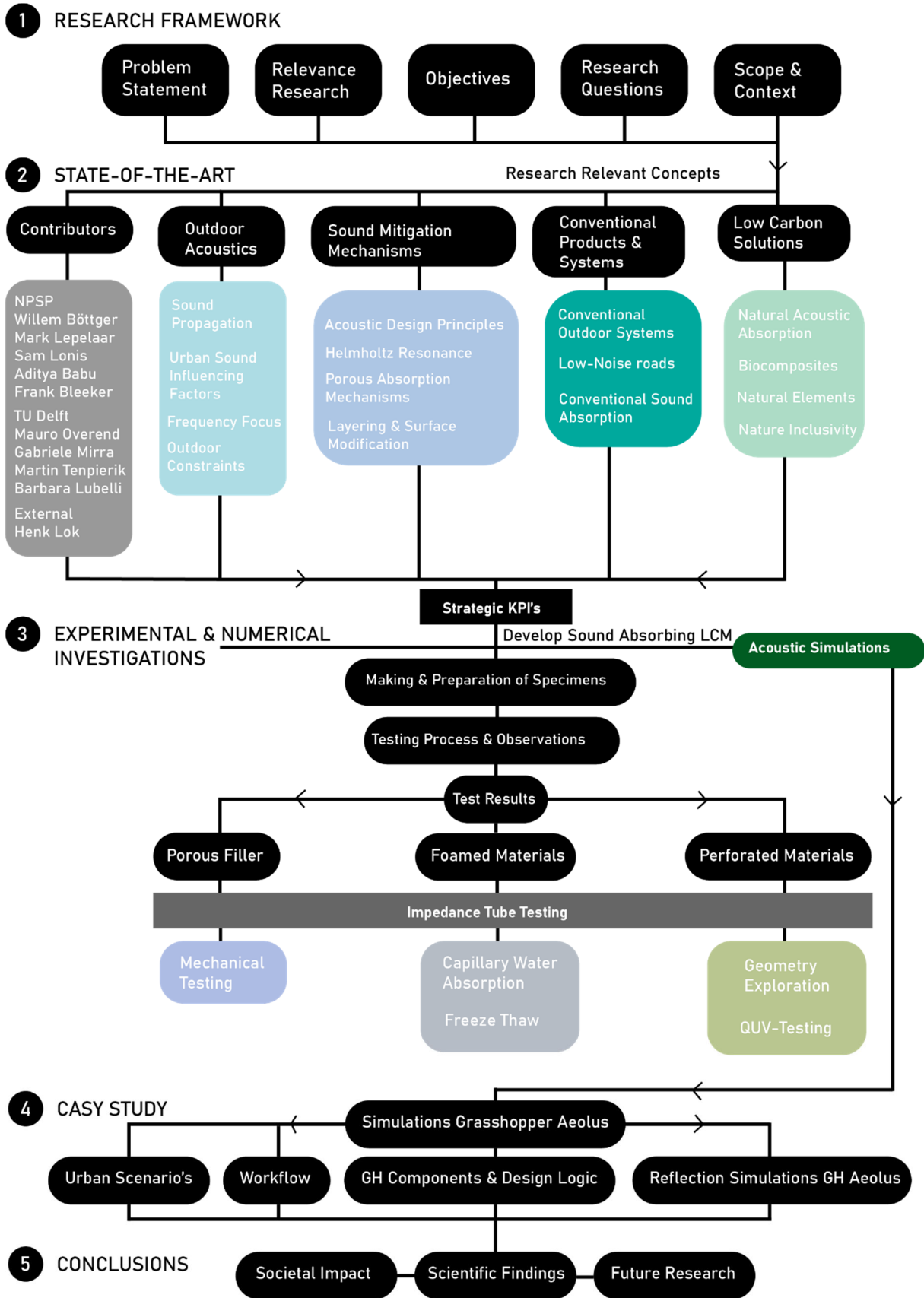


Figure 8: Graduation research flowchart (source: Author)

## 1.2 Approach

This research investigates how low carbon materials can be designed and evaluated for acoustic noise mitigation in outdoor infrastructural urban environments. The study is positioned at the intersection of environmental acoustics, material science, sustainable construction, and applied product development.

Traffic noise can be classified as both a health concern and a material/product challenge. Therefore, multiple experimental material testing, are conducted. With the use of simulations in a case study, the application potential of the design can be elaborated.

Spatial context is researched, as outdoor noise mitigation differs per location. Highways, urban streets and areas in traffic infrastructure, vary in noise pollution. Important parameters to research are the distance to the receiver, reflection, and the space available for interventions. By taking the spatial context into account, the material research stays connected to real world situations.

The following part focuses on the material requirements. Traffic noise is broadband. As the produced noise covers multiple frequencies. Humans can perceive mid-frequencies best. This is also the frequency band in which vehicles produce most noise, as stated in the first part of the introduction. Porous and fibrous absorbers perform effectively in the mid to high frequency range. Lower frequency noise can be absorbed by applying thicker materials.

Characterisation of porous media is central to the material development of this research. Specific parameters to focus on are thickness, porosity, airflow resistivity, density and boundary conditions Jaouen et al. (2025).

Useful information on absorption and diffusion can be found in the work of Cox and D'Antonio. This work provides a framework for the deeper understanding of how materials and surface geometries influence absorption, scattering, reflection, and diffusion (Cox & D'Antonio, 2016). This research is about outdoor acoustics and uses the general acoustic design references. Outdoor sound absorbing products not only absorb sound but should also redirect sound in complex urban settings.

In the third stage, the material selection is made. Promising materials from previous research can be implemented. Natural sound absorbing materials include coir, rice husk, bamboo, sheep wool, sunflower stem and other natural fibres. Thickness, porosity, density and fibre morphology are essential for the sound absorbing properties (Asdrubali, 2006; Chabriac et al., 2016; del Rey et al., 2017; Irvani et al., 2025; Leksmi et al., 2023; Mohammadi et al., 2024).

Additional parameters for the material development include fibre fraction, fibre type, binder content, density, thickness, porosity, fibre orientation, layered configuration and surface openness.

The material production will be conducted at laboratory scale. By using existing aluminium moulds, or create new ones, the materials can be manufactured. The mould geometry and fabrication method will influence the material production consistency and reproducibility.

Fibre mass, binder ratio, pressing pressure and curing conditions are expected to heavily influence the acoustic performance of the created materials.

The fourth stage is about providing acoustic characterisation. With the use of impedance tube measurements, the materials can be compared using the normal-incidence absorption coefficients across relevant frequency bands. Additional measurements like water absorption, surface observation and preliminary fire testing are planned.

Understanding the physical structure of the created materials is necessary to understand the acoustic results. Repeated measurements and consistent sample production will ensure quality scientific documentation.

The research compares the newly created materials against data from mainstream, and environment intensive absorptive materials. Absorbing materials like mineral wool, PET fibre, fibreglass, wood wool

cement boards, porous concrete and melamine foam, are investigated (Amran et al., 2021; Kapicová et al., 2024; Knauf Insulation, n.d.; Sağlı et al., 2019; Sound Acoustic Solutions, 2018).

Preliminary testing for durability is the aim in this research. This includes capillary moisture testing, UV radiation ageing and manufacturability. Durability and standardisation are key barriers for broader application (Ahmad et al., 2025; Faruk et al., 2012; Nwankwo & Mahachi, 2025; Przybek, 2025).

## 1.2.2 State-of-the-Art

The research combines state-of-the-art knowledge from the following three domains: urban noise mitigation, theory on acoustic materials and low carbon material development. By combining these fields, a full picture of sustainable noise mitigation can be formed. The research explores sustainable material systems that absorb sound to a meaningful extent. It is investigated if the foreseen product is technically, environmentally and durably considerable.

Starting with outdoor noise mitigation, societal, spatial and research relevance are investigated. Traffic noise is a dominant contributor to environmental stress (European Environment Agency, 2023; WHO, 2018). The RIVM (Rijksinstituut voor Volksgezondheid en Milieu) and Atlas Leefomgeving have precise data on noise exposure and health in the Netherlands. (Atlas Leefomgeving 2025; Rijksinstituut voor Volksgezondheid en Milieu, 2022).

Acoustic material theory is the second domain, which explains how materials modify sound. The focus lies in porous absorption. Porous and fibrous materials can dissipate sound through viscous and thermal losses. Air particles oscillate through the interconnected pores of such networks. Thickness, density, porosity, tortuosity, airflow resistivity and surface openness influence the extent to which the materials can absorb sound (Allard & Atalla, 2009; Jaouen et al., 2025).

The work of Cox and D'Antonio on absorbers and diffusers consider how surface structures influence reflection and scattering. The research underlines the complexity of sound mitigation, where sound absorption is not the sole strategy. Although it is the most influential strategy to combat the foreseen noise stress. Sound scattering and diffusing are still important influencing factors (Cox & D'Antonio, 2016). Facades near traffic or urban areas with high sound production influence both absorption and the direction of reflected sound. The research explores different geometries to further optimise the product design.

Sustainable low carbon material development is the third domain. This includes biobased content, binders, durability, energy consumption and end-of-life options. Biobased thermosetting resins are key to sustainable design (Ma et al., 2015). This is an important element of this research. Studies on natural-fibre and waste-based materials promise the potential of technically sound biocomposites. Examples of promising materials are e.g. coir, reed, rice husk, bamboo, sheep wool, sunflower stem. These fibres have acoustic potential in early-stage development (Chabriac et al., 2016; del Rey et al., 2017; Irvani et al., 2025; Lekshmi et al., 2023; Mohammadi et al., 2024; Namakka et al., 2025; Yang et al., 2020). Outdoor application of these materials remains under researched. Discovering strategies to be able to apply these materials for outdoor applications is central. Literature on the circular economy provide selection on materials which goes further than selection based solely on technical properties (Afval Circulair, 2022; Argalis et al., 2024; Ioannou & Konijnenberg, 2026). By incorporating this thinking strategy, sustainability is an active assessment element of the production of innovative, well performing acoustics mitigation materials. A material that absorbs sound well, but is environmentally intensive, difficult to recycle, or unsuitable for long-term outdoor use, would not satisfy the full research objective.

In summary: environmental noise research defines the need for mitigation; acoustic material theory explains how absorption and scattering can be achieved; and biocomposite material science provides the basis for developing lower-carbon alternatives. The research is located at the intersection of these three domains.

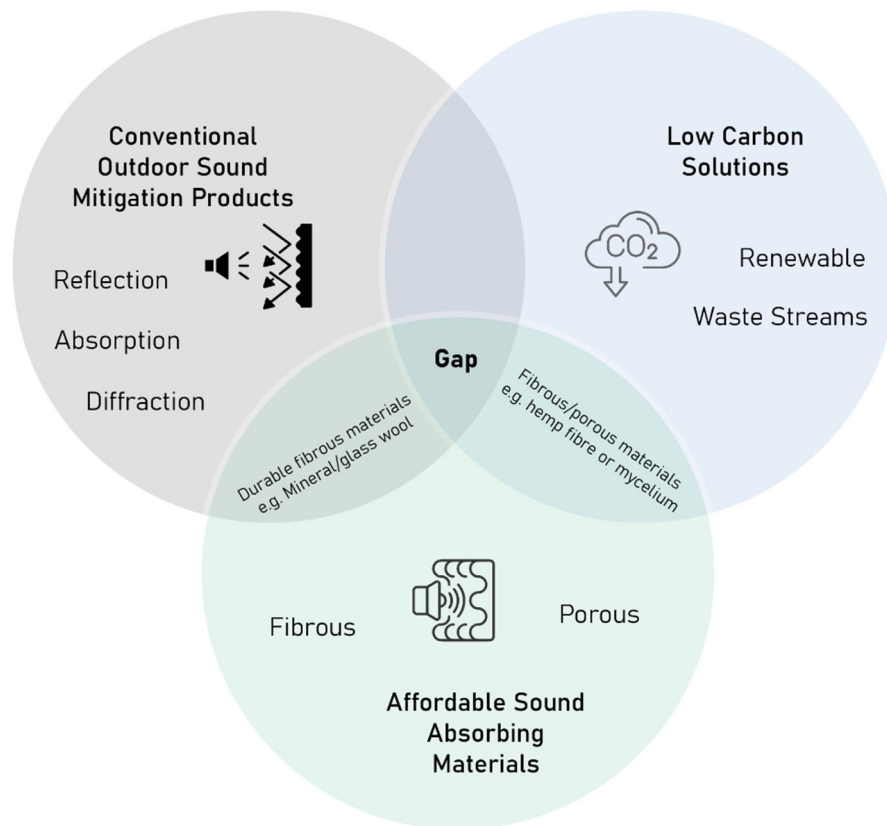


Figure 9: Overview research gap (source: Author)

### 1.2.3 Acoustic Simulations

A digital workflow for urban acoustics has been set up to simulate material-based noise absorber design. The Grasshopper Aeolus plugin is effective in early-stage design to simulate how sound travels, reflects and propagates in urban geometries. Examples of these geometries are facades, courtyards, streets and canopies. One of the strengths of Aeolus is that acoustic feedback remains in the parametric design environment. Quick modifications can be made. Identification of reflective zones is key in the application of this tool. Sound-pressure patterns can be evaluated.

Acoustic Modelling Helmholtz calculator can be consulted to simulate what the effect of different perforations in a front sheet can have in combination with a certain back structure. Cavities, slot size, and absorptive materials can be adjusted in the parameters of the wall setup. The absorption curve can be tuned for specific frequencies this way. Scientific research on perforated absorbers state that the dimensions strongly influence the resonance frequency and absorption performance.

By combining the workflows, the research can inform itself on the geometry and panel placement in space and the optimal perforation rate, cavity and geometry on the product level. The Acoustic Modelling especially helps in early-stage design decisions. For product level validation, reverberation room testing should be conducted. At TU Delft, a minimum of 7 m<sup>2</sup> should be used for reverberation room testing for meaningful results. The official ISO 354:2003 requires 12 m<sup>2</sup> for product scale validation. Simulations are always a simplified representation of reality. It is important to test manufactured prototypes to validate the data.

## 1.2.4 Experimental Investigations

The approach for the experimental investigations is elaborated in this paragraph. Based on the literature, the first applied strategy is to use porous fillers within the material mixture. Porous fillers within the material can be exposed to the outside by sandblasting the materials. It will be discovered if these materials will absorb sound for lower frequencies as well. As small soundwaves can be oscillated by small porous particles, the larger soundwaves are harder to absorb with porous fillers. Material processability is an important aspect of this approach. As the kneader blades do not allow large granulate fillers to mix.

In a second step, porous foamed materials will be investigated as an alternative method for achieving a more continuous porous structure within the material. This approach allowed the influence of foam-based porosity on the overall material characteristics to be studied and compared with the filler-based mixtures. Finally, geometry variations are explored. Panel shapes, but also perforation types can influence the absorption coefficient. This is especially the case when the Helmholtz principle is applied. For each of these approaches, specific experimental procedures will be developed to evaluate their feasibility.

The materials are tested with the impedance tube to gain information on their sound absorption coefficients. The impedance tube testing is one of the first acoustic real-world testing. Impedance tube testing at the TU Delft under the supervision of Prof. Martin Tenpierik is conducted. These tests are conducted at the KU Leuven in Brugge in Belgium to compare data and draw conclusions.

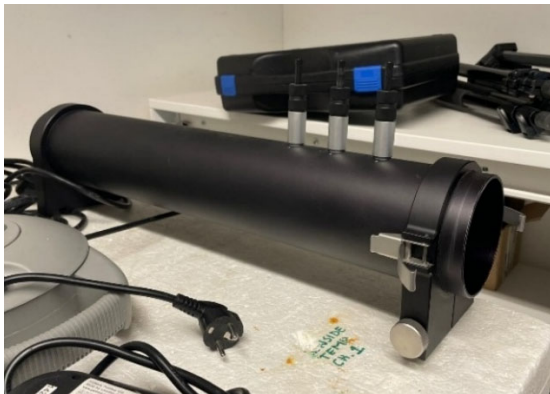


Figure 10: Impedance tube at BK (source: Author)

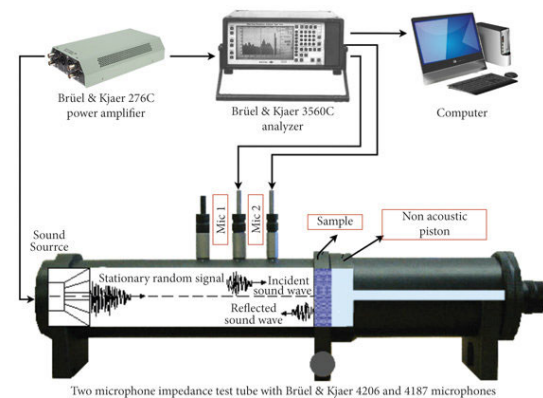


Figure 11: Impedance tube set-up (source: Rakesh et al., 2026)



02

THEORETICAL  
FRAMEWORK

## 2.1 Introduction: Outdoor Acoustics

Sound propagation in outdoor environments is governed primarily by open-air mechanisms. Geometrical spreading, atmospheric absorption, interaction with ground surfaces, diffraction, reflection from facades and scattering are the most influential factors. The spatial relationship between various sources defines the acoustic behaviour in outdoor spaces. The acoustic behaviour should therefore not be seen as a single enclosed volume. Atmospheric conditions play another role in the sound propagation in outdoor environments.

The distinction between room acoustics and outdoor acoustics is essential for traffic noise mitigation. Outdoor spaces such as streets, courtyards, squares and highways do not propagate sound directly to the receiver. Road surfaces, ground impedance, facades, vegetation, street geometry and barriers affect the propagation. Placement, orientation, surface geometry, durability all plays a key role in the final sound mitigation. In this research the focus lies on sound absorption, but overall geometry of the design is considered (Attenborough et al., 2007; Kang, 2006; ISO, 2024).

Irregular geometries and hard surfaces complicate urban acoustics. This is especially the case in dense cities. Asphalt, concrete, brick, glass, metal and stone dominate the acoustic field. By reflecting the sound energy, several reflection paths are created. This is key in street-canyon conditions. Noise mitigation products must therefore be considered within a wider acoustic system.

### 2.1.2 Outdoor Sound Propagation Mechanisms

The first principle of outdoor sound propagation is geometrical spreading. As sound travels away from a source, acoustic energy is distributed over a larger area, causing sound pressure level to decrease with distance. In free field conditions, a point source decreases by approximately 6 dB per doubling of distance. Road traffic can be considered a line source. SPL (=sound pressure levels) decrease by approximately 3 dB per doubling of distance. These theoretical reductions are rarely achieved in dense urban environments. This is because reflections, barriers, ground effects, façade geometry, and meteorological conditions influence the propagation field (Attenborough et al., 2007; ISO, 2024).

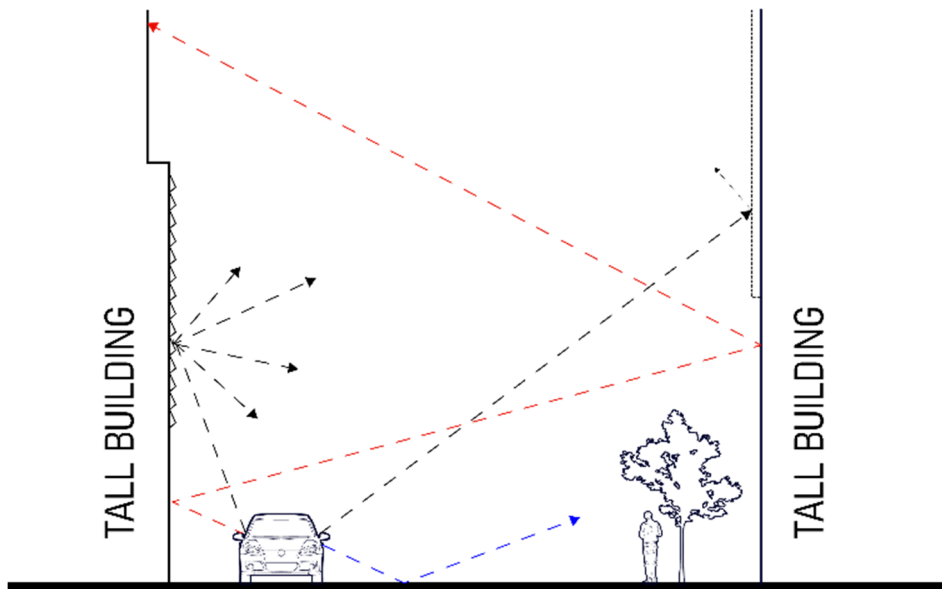


Figure 12: Outdoor sound propagation mechanisms (diffraction – black, ground reflection – blue, façade reflections/urban canyon effect – red) (source: Author)

Another important outdoor acoustic phenomenon is atmospheric absorption. Parts of sound energy is dissipated as it travels through molecules in the air. Sound frequency influences the amount of dissipated energy. Temperature, humidity and atmospheric pressure are important factors. High-frequency sound is absorbed more easily by air compared to low-frequency sound. Distant noise sources lose some of their sharpness during propagation (ISO, 1993). In densely populated urban environments, distances between sound sources and receivers are shorter. Reflections on harder surfaces reduce the effect and importance of atmospheric absorption. Leading to the need for additional noise mitigation strategies.

As mentioned before, ground effects have an important role in the behaviour of outdoor sound propagation. The interaction between direct and reflected sound from the ground is important to investigate. Source and receiver height, the frequency, the distance and acoustic impedance of the surface play a role. Examples of hard surfaces are asphalt, concrete, stones and water. A large part of the incident sound energy is reflected in these cases. More porous surfaces such as soil, grass, planted substrates or porous pavements absorb more sound and reduce the reflected energy. Smaller sound waves can penetrate these surfaces and therefore decrease the reflected energy. This is particularly the case for mid and high frequencies (Attenborough et al., 2007).

Another important outdoor acoustic mechanism is diffraction. Noise barriers often have bending sound effects. The soundwaves bend around these noise barriers, buildings, walls, terrain edges, etc. Low frequency sound diffracts more easily because of their longer wavelengths. Mid- and high-frequency sound is blocked more effectively by barriers (ISO, 2024; Rijkswaterstaat, n.d.-b).

### 2.1.3 Urban Surfaces, Façades & Street Canyons

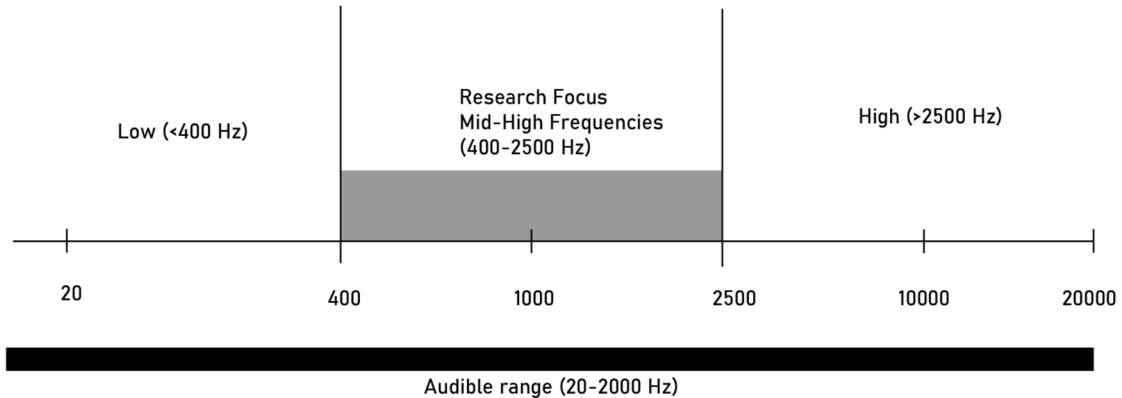
The acoustic street canyon phenomenon occurs when streets are bordered by continuous lines of buildings. Produced noise by traffic reflects continuously in between facades. This forms a semi enclosed space, which leads to increased sound pressure levels for pedestrians and in higher buildings. Specular reflections are strongest from smooth facades. Common materials for smooth facades are glass, concrete, brick, stone and metal cladding. The reflected sound is redistributed leading to increased overall noise pollution.

Facades therefore play a key role in outdoor noise mitigation. The geometry, material, surface roughness and depth are the key influencing factors. Facades can act as reflectors, absorbers or scattering sound. Balconies, vegetation, texture or porous cladding reduce the strength of the urban canyon effect and direct reflection, as confirmed in Kimm's work. Façade design plays an important role in outdoor acoustic mitigation, further than only visual, structural or thermal behaviour (Krimm, 2018).

The research from Cox and D'Antonio elaborates on absorbers and diffusers. Reflection redirects sound in a predictable way. Scattering distributes sound energy in several directions due to the surface roughness or complex geometry. Even if that research is focussed on indoor acoustic contexts, physical behaviour principles can be translated to urban acoustics. The prevention of strong, concentrated reflection is key in outdoor environments. Complete elimination is the most effective measure, but geometry cannot be ignored. Strong reflections lead to perceived loudness and noise stress (Cox & D'Antonio, 2016).

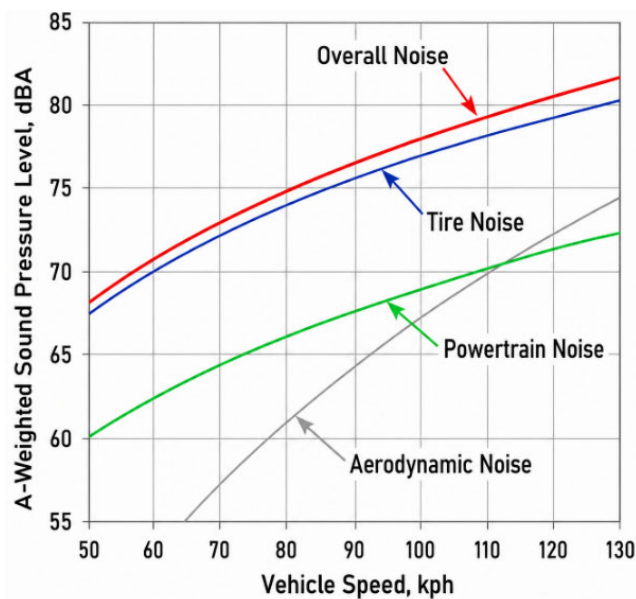
## 2.1.4 Relevance of Mid-High Frequencies for Traffic-Noise Mitigation

Traffic noise in the frequency range of 400–2500 Hz is strongest for human perception and as a result, annoyance. This is also the range which has a large mitigation potential. As mid-high-frequency sound absorption can be achieved with porous and fibrous materials. A relative thin, porous or fibrous layer can interact effectively with sound in this frequency bandwidth. This range is also more realistically targeted by biocomposite systems compared to exceptionally low frequencies, which typically require greater thickness, cavities, resonant systems, or hybrid acoustic structures (Jaouen et al., 2025; Lu et al., 2025; Sandberg & Ejsmont, 2002).



*Figure 13: Frequency range focus in this research; frequencies between 400 and 2500 Hz are especially responsive to porous and fibrous absorption and are strongly related to perceived sharpness, speech interference, and tyre-road noise (source: Author)*

Even if the Mid and High frequency band is most impactful, Low frequency noise is not irrelevant. Heavy vehicles and engines form an important source of low frequency noise production. Low frequency sound absorption is difficult for thin, porous materials because the wavelengths are much longer. Porous biocomposites are likely to be effective for sound mitigation in the desired frequency range. Porous networks and fibrous structures could perform well with a relatively thin thickness. In figure 14, it is visible what the dominant source of sound pollution from traffic is and how it increases with vehicle speed. In a future with more electric or hydrogen powered vehicles, noise pollution will remain a key environmental pollution phenomenon.



*Figure 14: Multiple sources of traffic noise categorised into three groups, namely, propulsion, tyre-pavement, and aerodynamic noise, Modelling of Traffic Noise Along Urban Corridor: A Case Study of Amman. (Younes et al., 2021)*

## 2.1.5 Outdoor Constraints for Absorptive Materials

Indoor and outdoor absorptive materials have different requirements. Outdoor materials have stricter requirements. They must remain acoustically open, while resisting UV exposure, moisture, pollution, clogging, biological growth, freeze-thaw, wind load, vandalism and mechanical damages. Later in this research, nature inclusivity is elaborated. This is another consideration potentially influencing sound absorption as pores can be clogged eventually.

Porosity, airflow resistivity, surface openness, stiffness and long-term performance are all influenced by the previously mentioned factors. Laboratory testing cannot be translated to real-world performance directly. The stated challenge is important in biobased material development. Commonly used natural fibres are sensitive to moisture uptake, biological degradation, expansion and fire-safety requirements. Even if their embodied carbon is lower, this forms a challenge.

The development of outdoor low carbon materials requires durability besides absorbing properties for the desired frequency band. Surface treatment and protective layers may improve durability. It is important to emphasise that the pore structure should be exposed to the outside when being manufactured to be able to absorb sound. The tension between durability and acoustic permeability is the central design challenge for outdoor biobased noise mitigation products (Ahmad et al., 2025; Nwankwo & Mahachi, 2025; Przybek, 2025).

### Key takeaways:

Outdoor urban acoustics is shaped by open-air propagation. In cities, traffic noise is influenced by distance, atmospheric absorption, ground reflection, diffraction, façade reflection, scattering, and weather conditions. Hard surfaces such as asphalt, concrete, brick, glass, metal, and stone often reflect sound, creating multiple sound paths. This is especially problematic in street canyons, where continuous building façades trap and amplify traffic noise. As a result, façades should be considered as active acoustic elements, not only as visual, structural, or thermal components. Surface roughness, balconies, vegetation, porous cladding, and complex geometries can reduce strong reflections and scatter sound more effectively. For traffic-noise mitigation, the frequency range between 400 and 2500 Hz is particularly relevant because it strongly affects human perception, annoyance, tyre-road noise, and speech interference. Porous and fibrous biocomposite materials are promising for absorbing sound in this mid- to high-frequency range. However, low-frequency traffic noise remains difficult to mitigate with thin, porous materials because it requires thicker or more complex acoustic systems. Therefore, the main challenge for outdoor biobased noise-mitigation products is to combine acoustic permeability with long-term durability against moisture, UV exposure, pollution, clogging, biological growth, freeze-thaw cycles, wind, vandalism, and mechanical damage.

## 2.2 Sound Mitigation Mechanisms

### 2.2.1 Absorption, Reflection, and Scattering as Combined Design Principles

The acoustic strategy of this research is based on the idea that outdoor noise mitigation should not rely on absorption alone. As stated before, in infrastructure and urban environments, sound travels through complex paths involving direct propagation, ground reflection, façade reflection, diffraction, and scattering. Therefore, effective acoustic design should consider how a material or product absorbs, reflects, scatters, and redirects sound. The primary principles for sound mitigation are illustrated in figure 15.

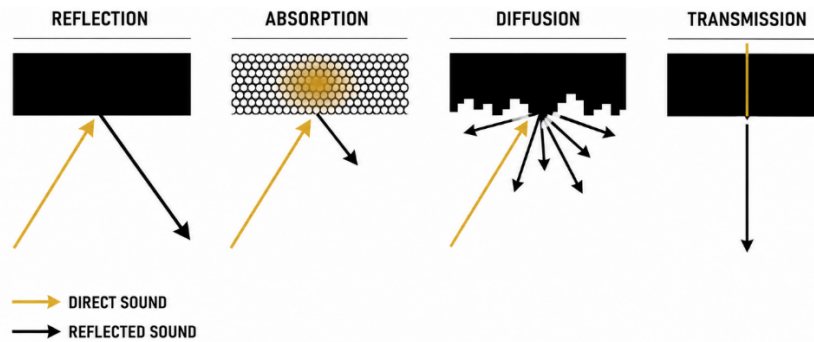


Figure 15: Reflection, absorption, diffusion and transmission of sound (source: Author)

In the work from Cox and D'Antonio, absorption and diffusion are largely elaborated. Absorption removes the energy from the sound field. Diffusion redistributes reflected energy more evenly/ in multiple directions. Their work is especially inspiring as the focus is on architectural applications (Cox & D'Antonio, 2016).

For this research, the most relevant implication is that low carbon materials should not only be evaluated as flat absorptive panels. Their surface geometry, texture, layering, and potential structuring may also influence scattering and reflection behaviour. This opens the possibility of designing acoustic products that combine porous absorption with controlled surface form. For this research, only impedance tube testing has been conducted. In figure 16, 4 important absorption techniques are shown. Cellular absorption makes use of connected cells. Fibrous networks dissipate sound. Granular materials have a similar effect. Perforated materials can make use of the Helmholtz principle. Which is elaborated further in this chapter.

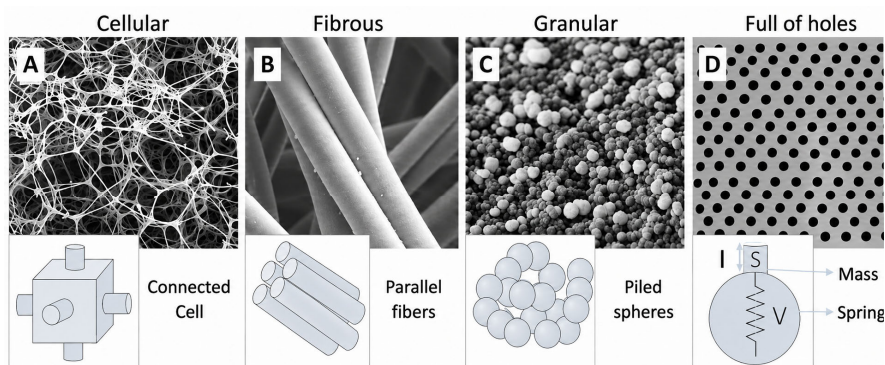


Figure 16: Different strategies for sound absorption (source: Adjusted form: Arenas and Crocker, 2010)

## 2.2.2 Helmholtz Resonance

A Helmholtz resonator is seen as a lumped mass–spring–damper system within acoustics (D in figure 16). The plug of air in the neck behaves like oscillating mass, while the compressible air in the cavity behaves like the spring that provides the restoring force. When sound excites the resonator near its natural frequency, the neck air moves back and forth against the cavity's acoustic compliance, producing a strong resonance that can be used to amplify, absorb, or attenuate sound. For an ideal rigid resonator, the resonance is commonly approximated by:

$$f_0 = \frac{c}{2\pi} \sqrt{\frac{S}{VL_{\text{eff}}}}$$

where  $c$  is the speed of sound,  $S$  is the neck cross-sectional area,  $V$  is the cavity volume, and  $L_{\text{eff}}$  is the effective neck length including end correction; this captures why a larger cavity lowers the resonant frequency, while a larger neck area raises it. Academic treatments describe this directly as a mass–spring analogy, with the cavity acting as acoustic compliance and the neck acting as acoustic mass, often with viscothermal losses represented as damping (Lopez et al., 2024). The Helmholtz resonance principle is applied in the perforated façade panels within this research. Different absorptive layer placements behind a perforated sheet are illustrated in figure 17.



Figure 17: Placement of the porous absorber layer (source: Author)

## 2.2.3 Porous Absorption Mechanisms

Well performing porous materials from a sound absorption point of view have interconnected pores, fibres, or cellular networks through which air can move. For material comparison the weighted sound absorption coefficient is taken ( $\alpha_w$ ). This is common for interior acoustic material performance assessment. It evaluates the values to a standard curve according to ISO 11654 standards.

When sound waves enter the porous material, oscillating air particles receive viscous friction against the pore walls and the fibres. Air compression and expansion cause thermal exchanges within small cavities. Viscous and thermal losses are transformed into heat. This leads to less sound being reflected (Allard & Atalla, 2009; Jaouen et al., 2025).

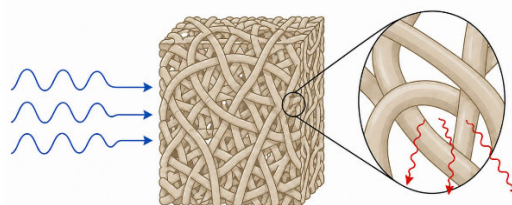


Figure 18: Porous sound absorption principles (source: Author)

Porous absorbers perform based on the following parameters. Thickness, which covers low frequency absorption when the materials become thicker. Density and airflow resistivity, determine how easily air moves through the material. In models described later in the research, the (static) airflow resistivity has been taken as 40,000 Pa.s/m<sup>2</sup>. Some outdoor porous absorber applications require an additional membrane in front of the material. This membrane decreases airflow on high frequencies. As these frequencies cannot enter the porous material. For airflow resistivity, a slice of the porous material can

be considered of thickness  $d$  subject to a mean steady flow velocity  $U$ . Sensors are used to measure the air flow and pressure drop to atmospheric pressure, and hence the flow resistivity is obtained. Porosity and tortuosity influence the path where oscillating air travels through. A too open material leads to sound passing through with little energy loss. A material which is too dense causes sound to be reflected. Optimal porous absorption requires a balance between resistance, openness, fibre structure, granulate size and material depth (Allard & Atalla, 2009; Jaouen et al., 2025).

Fibre morphology, binder content, compaction (density), processing methods all influence the performance of natural fibre or natural granulate based low carbon materials. Based on recent studies, coir, rice husk, hemp, bamboo, sheep wool and sunflower stem are examples of biobased materials which can achieve significant sound absorption, considering thickness, pore structure and density (Asdrubali, 2006; Chabriac et al., 2016; del Rey et al., 2017; Irvani et al., 2025; Lekshmi et al., 2023; Mohammadi et al., 2024; Yang et al., 2020).

Natural fibres often have irregular shapes, hollow structures, high surface area and complex pore networks which make them considerable for sound absorption. Internal friction can be maximised to improve sound absorption (Chabriac et al., 2016; del Rey et al., 2017; Irvani et al., 2025; Lekshmi et al., 2023; Mohammadi et al., 2024; Namakka et al., 2025; Yang et al., 2020). Moisture content could be a destructive factor. The adhesion between the fibres and resin is optimal if the surface area does not contain remaining water.

## 2.2.4 Layering & Surface Modification

Layered systems have the advantage that they could absorb a variety of frequencies and are not limited to a specific frequency range. A more open top layer can allow sound to enter the material, where a denser sub layer could energy dissipation. Air cavities can have a large absorption as sound is trapped in the cavity and reflected inside the material. Usually, products with an absorptive core have a cavity in front of this layer. The cavity depth can ensure lower frequencies can also be absorbed.

Shankar et al. describes surface modification. Thickness and surface treatment influence sound transmission losses in materials made from natural fibres. In outdoor applications a durable top layer could reduce acoustic performance. This can prove to be a challenging development area. Commercially available façade panels ensure surface pores are enclosed for optimal durability. This is different from the desire to have an open structure to allow sound to enter the material to eventually be absorbed. More about furan-based resins will follow sub chapter 2.4.

## 2.2.5 Requirements

Outdoor noise-mitigation products must satisfy mechanical, durability and sustainability requirements. On the mechanical performance level: safety, wind resistance, impact resistance, stiffness, vandalism resistance and safe failure should be considered.

Acoustic porosity may reduce stiffness and strength. It is a common phenomenon that increased porosity (and improved absorption), decrease mechanical performance.

As sustainability is a key component for the material development in this research, acoustic performance alone is not the focus. LCA estimates are made to assess whether a created solution is truly one to be considered. Within Life Cycle Assessment, feedstock, waste valorisation, repairability, recyclability and responsible end-of-life paths are investigated (Ahmad et al., 2025; Nwankwo & Mahachi, 2025; Przybek, 2025).

Waste-based materials are also relevant, as shown by research into manufacturing waste and food-waste-based façade cladding (Argalis et al., 2024; Ioannou & Konijnenberg, 2026). These studies support the idea that acoustic biocomposites could contribute to circular construction if they combine

acoustic performance with robust material design. Within this research the focus remains on biobased and grown materials integrated in the final product. Pumice (volcanic byproduct) and rubber granulate were considered in this research.

Testing and Performance Indicators are necessary to compare newly created materials on the full spectrum of sound absorption, carbon footprint, price and durability. As mentioned in the introduction, impedance tube testing, is used to measure normal-incidence sound absorption. ASTM C423 and ISO 354 are commonly used to assess sound absorption in reverberation rooms. ISO 9613 is used for outdoor propagation modelling (ASTM International, 2023; ISO, 2024; Jaouen et al., 2025).

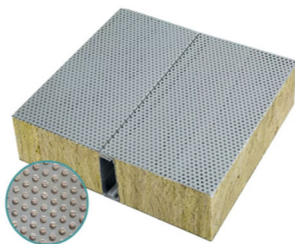
It is important to recognise the limitations of each method. Impedance tube measurements are useful for comparing material formulations, but they represent normal-incidence conditions and small-scale specimens. Outdoor applications involve inclined incidence, weathering, mounting systems, edge effects, and complex propagation paths.

#### Key takeaways:

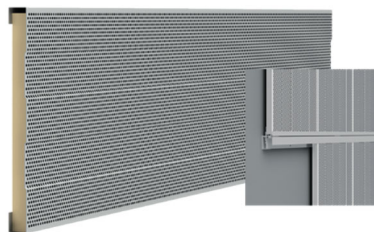
Outdoor noise mitigation should combine absorption, reflection, scattering, and diffusion rather than relying on absorption alone. The text explains that porous and biobased materials can absorb sound through interconnected fibres, pores, or granulates, while Helmholtz resonators can target specific frequencies through perforated cavity systems. Layering, surface texture, thickness, density, airflow resistivity, and pore structure all influence acoustic performance. However, outdoor acoustic products must also meet durability, fire safety, mechanical, cost, and sustainability requirements. A key challenge is balancing acoustic openness with strength and weather resistance, since more porous materials often absorb sound better but may be less durable.

## 2.3 Conventional Products & Systems

Commonly used materials for noise mitigation in urban settings are glass, transparent acrylic, (weather resistant) metal, concrete, brick, timber and perforated aluminium panels with an absorptive core. This core is usually made from glass wool or mineral wool. Most acoustic mitigation interventions are installed to reflect sound and protect residents or utility buildings behind them. As communicated previously in the research, the focus is on sound absorption to remove infrastructural, high urban stress levels. In figure 19 and 20, common perforated metal sheet products with an absorptive core are illustrated.



*Figure 19: Perforated aluminium sheet with mineral wool core product (source: [Hot Item] Acoustic Perforated Rock Wool Sound Insulation Sandwich Panel, n.d.)*



*Figure 20: Aluminium highway absorptive barrier (source: Perforated Aluminium Acoustic Sheet for Highway Noise Barrier and Buildings, n.d.)*



*Figure 21: Perforations on an industrial scale with the (punch method) (source: IndiaMART, n.d.)*



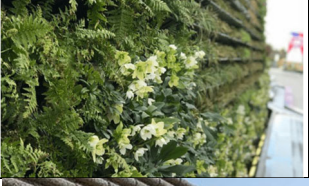


## 2.3.2 Conventional Outdoor Systems

Common systems for noise mitigation, are traffic noise barriers. They reduce exposure primarily by blocking the direct propagation path between source and receiver. The effectiveness of these systems depends on height, length, placement, mass, edge design, and the presence or absence of absorptive surfaces (Rijkswaterstaat, n.d.-a, Rijksoverheid, n.d.).

Rigid barriers usually provide shielding but may also reflect sound toward the opposite side of the road or into surrounding façades. Absorptive barrier systems typically include mineral wool, glass wool, perforated metal facings, wood wool cement boards, or porous concrete. An example of the perforation fabrication process is illustrated in figure 21. These products are usually encased in HEA or IPE profiles. Comparison on absorptive outdoor sound mitigation products is elaborated further.

From a sustainability point of view, many conventional barriers have a large carbon footprint. Concrete, metals, mineral wool, synthetic polymers, and glass can involve high embodied energy, fossil-based inputs, or limited recyclability depending on the system. This motivates research into biobased or circular alternatives that can provide acoustic mitigation while reducing environmental impact (Ahmad et al., 2025; Carruthers, 2012; Röck et al., 2020; UNEP & Yale Center for Ecosystems + Architecture, 2023).

Table 1: Comparison common noise mitigation products in highway and urban settings:

Product	Image	NRC (250,500,1000, 2000 Hz)	$\alpha_w$	CO <sub>2</sub> (kgCO <sub>2</sub> e/m <sup>2</sup> ) (per mm thickness)	Price (EUR/m <sup>2</sup> ) (lowest)	Lifespan (Years)
<b>Perforated Aluminium</b> sheet with absorptive core - Forster FF Products e.g. Solosar MAGNUM AL12- type		0.85 <sup>b</sup>	0.90 <sup>b</sup>	60	150	40 <sup>f</sup>
<b>Perforated (galvanised Steel)</b> perforated galvanized steel acoustic panel with rock wool, e.g. Ornitolink / SteelProfil type		0.80 <sup>b</sup>	0.80 <sup>b</sup>	35	65	35 <sup>g</sup>
<b>Modular Green Wall</b> Substrate base		0.60 – 0.75 <sup>b</sup>	0.60 – 0.75 <sup>b</sup>	20 – 60	150 – 300	15 – 30
<b>Wood Concrete</b> PHONOBLOC®		0.75 – 0.95 <sup>b</sup>	0.80 – 0.95 <sup>b</sup>	20 – 45	120 – 250	50
<b>Glass</b> performs similar to PMMA/acrylic transparent barrier		0.05 <sup>b</sup>	0.05 <sup>b</sup>	36	175	40 <sup>d</sup>


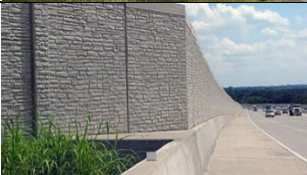

<b>Brick/ stone</b> single-leaf natural brick masonry wall		0.05 <sup>b</sup>	0.05 <sup>b</sup>	35	280	75 - 90
<b>Concrete</b> 150 mm precast / prestressed concrete barrier panel		0.05 <sup>b</sup>	0.05 <sup>b</sup>	45	120	75
<b>Timber</b> Jakoustic® Absorptive Acoustic Fencing		0.05 <sup>b</sup>	0.05 <sup>b</sup>	15	80	20 <sup>c</sup>

Table 1: (sources: a: Jacksons Fencing, n.d., b: Acoustic Supplies, n.d.; c: First Fence, n.d.; d: GlasBoertje, n.d.; e: Ornitolink, n.d.; f: Solosar, n.d.; g: SteelProfil, n.d.; h: Lacasta et al., 2016)

#### Key takeaways:

Perforated aluminium is the least sustainable in terms of carbon emissions and has the best sound absorption coefficient (0.90). Measurements for this product in the frequency bands for the NRC are also performing well (0.85). Stone barriers have the longest lifespan (up to 90 years). Perforated steel is the most affordable option (not considering installation speed and ease).

### 2.3.3 Low-Noise Road Surfaces & Porous Asphalt

Sound mitigation directly at the source is commonly considered the most effective strategy. Sound can be absorbed by the surface traffic drives on. Low-noise road surfaces are gaining attraction over the years. This is important because source control is generally more effective than treating sound after it has propagated. Figure 16 illustrates how tyre to road noise is especially important at medium and higher speeds. Porous asphalt and other low-noise pavements can reduce noise by modifying this interaction (Sandberg & Ejsmont, 2002).

Porous asphalt can be effective because its open structure reduces air-pumping effects and provides acoustic absorption. However, its performance may decrease over time due to clogging, ageing, dirt accumulation, and maintenance conditions. Low-noise road surfaces are useful but not sufficient as a stand-alone strategy. They need to be combined with barriers, façade strategies, absorptive surfaces, and traffic-management measures.

### 2.3.4 Conventional Sound Absorption Systems

The best sound absorbing materials are mineral wool, glass fibre, melamine foam, PET fibre panels, Open cell polyurethane foam, (micro) perforated wood, and other synthetic absorbers. These are widely used because their acoustic performance is predictable and well documented. These materials can achieve high sound absorption, especially at mid and high frequencies. They are often used behind perforated facings or inside acoustic barrier systems. Data on supplier websites indicate that for mineral wool, fiberglass, and melamine foam often high NRC values are reported, especially for thicker panels or systems with air cavities (Cellyx, 2025; Knauf Insulation, n.d.; Sound Acoustic Solutions, 2018). Not all these materials are necessarily used in outdoor systems. It is important to research these and obtain a thorough understand of why these materials perform well for sound absorption.

Table 2: Comparison best performing sound absorption materials:







Product	Image	NRC (250,500,1000,2000 Hz)	$\alpha_w$	CO <sub>2</sub> (kgCO <sub>2</sub> e/m <sup>2</sup> )	Price (EUR/m <sup>2</sup> ) (minimum)	Lifespan (Years) (indoor)
<b>Mineral Wool/ Stone Wool</b> Rockfon Sonar acoustic		0.85 - 0.95	0.75 - 1.00	4.15	53 - 69	50
<b>Glass Fibre</b> Ecophon Focus A Carbon Low		0.80	0.80	1.17	34 - 76	50 <sup>a</sup>
<b>Melamine Foam</b> Basotect G+ / 50 mm absorber		0.80 - 0.90	0.75 - 0.85	2.4 - 2.9	50 - 94	Prod. specific
<b>PET Fibre Panels</b> 9-24 mm recycled PET felt/polyester fibre wall panels		0.3 - 0.8	0.45 - 1.00	6.45	75 - 160	50
<b>Open-cell Polyurethane Foam</b> 50 mm PU acoustic foam panel		0.85	0.80	4.3 - 5.7	15 - 31	5 - 10
<b>(Micro) Perforated Wood &amp; MDF</b> Topakustik-type perforated		0.70 - 0.95	0.60-0.90	4.6	60 - 200+	30 <sup>j</sup>

Table 2: (sources: a: Saint-Gobain Ecophon, 2023; b: CertainTeed, n.d.; c: Rockfon, 2025a, 2025b; d: PlafondPlaza, n.d.; BASF SE, 2025; e: Post Acoustics, n.d.; f: Plastocell Kunststoff, n.d.; g: Yamamah Smart, n.d.; h: EUROPUR, 2025; i: ABM Trade, n.d.; Fibers & Foams, n.d.; j: Topakustik AG, 2025; SCS Global Services, 2024; k: Eckel Industries, n.d.; l: Acoustic Measurement, 2025; m: VTT Technical Research Centre of Finland, 2012; n: Vicoustic, n.d.; o: Thomann, n.d.; m: Yang & Sheng, 2023)

#### Key takeaways:

Mineral wool has the best sound absorption coefficient (up to 0.95). PET fibre panels are the least sustainable in terms of carbon emissions. Mineral and stone wool together with PET fibre panels have the highest durability (50 years). Open-cell polyurethane foam is the most affordable option.

### 2.3.5 Perforated Aluminium with Mineral Wool Core Production Process & EOL

Mineral wool production is a high-temperature materials-engineering process in which mineral raw materials are converted into a lightweight fibrous insulation product. The product has quality thermal, acoustic, fire-resistant, and mechanical properties, but also high carbon emissions during production and a waste problem at their EOL.

The first step in the process is the selection, crushing, screening, and blending of raw materials. These are commonly basalt, diabase, dolomite, limestone, metallurgical slag, (recycled glass).

The production of mineral wool requires high temperatures varying from around 1400 to 1600 centigrade. Different melting systems can be applied. This is either coke-fired cupola furnaces or electric melting systems to obtain a suitable viscosity to be able to fabricate the desired fibres. The molten material gets fibrised. This step is usually done with centrifugal spinning. Rotating wheels create fine fibres under high velocity. After, functional additives are applied to improve cohesion, durability, and moisture resistance.

The layered mats which are created are compressed to achieve the optimal density, thickness, fibre orientation and mechanical properties. The mat is then transferred through a curing oven. The binder hardens and stabilises the structure. After the curing process, the product is cooled and cut. Any final shape can be made. The main parameters are material composition, melting conditions, binder chemistry and the curing conditions. To complete the product (such as Solosar MAGNUM or FONOCON Type S), the aluminium sheets are industrially perforated in series. This is illustrated in figure 20. The complete production process is visible in figure 21. The acoustic random incidence sound absorption of Rockwool is illustrated in figure 22. Mineral wool and Rockwool perform very similarly.

At the end-of-life, perforated aluminium acoustic barriers with mineral wool are usually dismantled and separated into material fractions. The aluminium casing or perforated sheet is usually recovered as valuable scrap and recycled. Mineral wool is more difficult to recycle because it may be contaminated, bonded, wet, or hard to separate. Clean mineral wool can sometimes be taken back by the manufacturer or specialist recycling schemes. In many cases, however, it is still sent to landfills. Therefore, the main EOL benefit comes from aluminium recycling. The mineral wool remains the key circularity challenge.

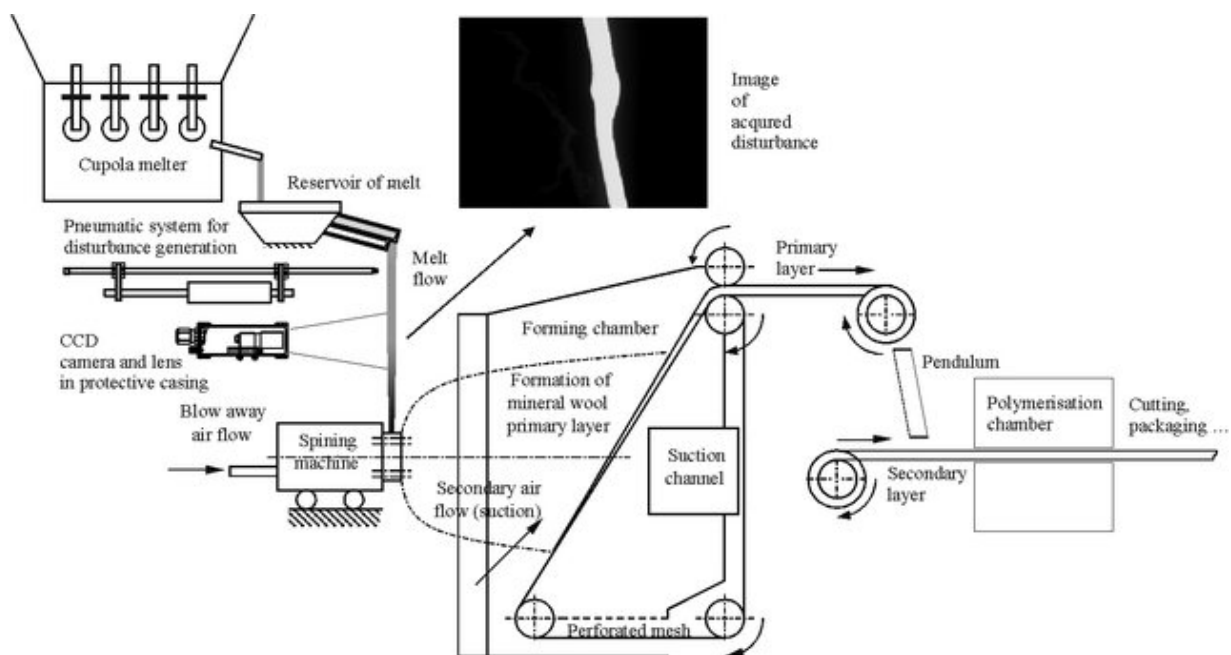


Figure 22: Production process mineral wool (source: Chen et al., 2011)

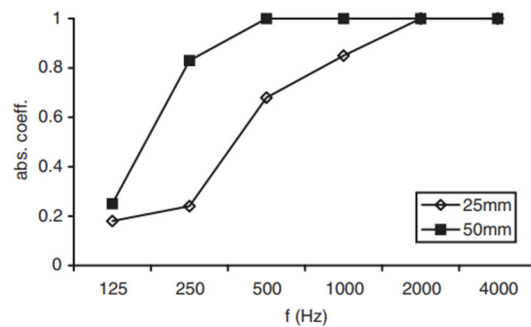


Figure 23: Random incidence absorption coefficient for Rockwool of two different thicknesses on a rigid backing (source: Cox & D'Antonio, 2004)

## Conclusions

Even if the fibrous, porous materials perform well acoustically and sometimes thermally, these materials also have limitations.

Mineral and synthetic absorbers may involve energy-intensive production, fossil-based components, irritation risks during handling, recyclability challenges, or performance degradation if exposed to moisture without protection. These limitations do not make them acoustically ineffective, but they do create motivation for alternative materials with improved environmental profiles.

Wood wool cement boards and porous concrete systems represent more mineral-based or hybrid alternatives. Wood wool cement boards combine wood fibres with a mineral binder, creating a relatively open structure that can provide sound absorption while maintaining durability and mechanical stability. These boards are often used in acoustic ceiling systems, barriers, and architectural applications. Their acoustic performance can be improved when combined with mineral wool backing or air cavities.

Porous concrete is another relevant material category. Reviews of sound-absorbing acoustic concretes indicate that porous concrete can provide moderate absorption while maintaining structural robustness (Amran et al., 2021). Kapicová et al. (2024) also show that pervious concrete can be developed for sound-absorbing applications. However, porous concrete is typically heavier and more mineral-intensive than biobased alternatives. Its sustainability performance therefore depends on binder content, aggregate type, service life, and end-of-life pathway.

### Key takeaways:

Mineral wool is produced by melting mineral raw materials at high temperatures. The fibres are created out of the melting process. Binders are added and the fibre mat is cured into insulation products. Although mineral and synthetic absorbers offer good acoustic and thermal performance, they can require high energy consumption and are hard to recycle. Also, they contain fossil-based components, which can cause handling irritation, and face recyclability or moisture-related issues. These drawbacks encourage the development of more sustainable alternatives, such as wood wool cement boards and porous concrete, which provide sound absorption and durability but depend on composition, binder use, service life, and end-of-life options, but ultimately also biocomposites and other low carbon alternatives.

## 2.4 Low Carbon Solutions

### 2.4.2 Natural-Fibre & Biobased Acoustic Materials

Natural-fibre materials gain attraction within acoustic research. Hemp, kenaf, coir, rice husk, sheep wool, bamboo, sunflower stem and other agricultural waste streams seem promising for sound absorption. See figure 24 with this overview. Asdrubali (2006) identified sustainable materials with promising acoustic properties. Chabriac et al. (2016) demonstrated the acoustic potential of agricultural by-products. Del Rey et al. (2017) investigated sheep wool as a sustainable acoustic material. Lekshmi et al. (2023) studied coir fibre and rice husk panels. Irvani et al. (2025) explored bamboo biocomposites as renewable sound absorbers.



Figure 24: An overview of natural fibrous materials (source: Author)

Recent reviews state the latest findings on natural-fibre reinforced composites for sound absorption applications. Mohammadi et al. (2024) emphasise the importance of fibre morphology and porosity. Namakka et al. (2025) identify natural waste biocomposites as a developing field with relevance for acoustic applications. Yang et al. (2020) provide a broader review of natural fibres and their sound absorption properties. Together, these studies show that biobased materials can achieve important acoustic performance when their structure is carefully engineered.

However, for outdoor applications, the literature is less developed and mature. Many natural-fibre acoustic materials are tested for indoor use only, where moisture, UV exposure, biological growth, and mechanical damage are less severe.

### 2.4.3 Natural Elements

Vegetation can influence outdoor sound through absorption, scattering, diffraction, and ground impedance effects. Green walls have been researched a lot in the past decade. Even if some research shows promising sound absorption, vegetation cannot be seen as a universal noise solution. Thin lines of trees or decorative vegetation usually provide limited physical attenuation. More meaningful effects require considerable depth, density, substrate absorption, and optimal placement.

Van Renterghem (2014) provides guidelines for optimising traffic-noise shielding using non-deep tree belts. Van Renterghem et al. (2015) discuss the use of natural means to reduce surface-transport noise during outdoor propagation. It is established that vegetation, soil, green roofs, and planted systems can contribute to mitigation when designed as part of a full acoustic system. Green walls and vegetated barriers are particularly relevant in dense urban environments because they introduce porous and irregular surfaces onto otherwise reflective façades or screens. The same effect could be researched in biocomposite development. As green walls are usually expensive. Commonly the price of green walls ranges from 150 till 300 euro per square meter (Lacasta et al., 2016).

In this research, vegetation systems are used as evidence that porous, biobased and irregular surfaces contribute to acoustic outdoor control. This elaborates on the design logic where acoustic function can be combined with sustainable design. The green walls are therefore used as an inspiration source.

## 2.4.4 Biocomposites

### Material Logic

Biocomposites is the term given to composite material made from a matrix and a reinforcement or filler, where at least one component is bio-based, naturally derived or renewable (Rudin & Choi, 2012).

A polymeric matrix, reinforcing fibre, fillers, additives and catalysts, all play a crucial role in biocomposite development. In figure 24, the needed components for biocomposite development are displayed.

The resin usually provides adhesion between the fibres and the matrix. Resins ensure stress transfer within the biocomposite. In biocomposite developed at NPSP, furan resin Biorez 14010 and Bio-polyester resins are used. These resins are UV resistant and durable. Façade panels from NPSP can achieve a lifespan of over 30 years. Fillers ensure improved density of the material and an affordable product. Fillers are responsible for fire resistance (besides fire retardants) and for the acoustic behaviour of the material, when treated as a porous filler. Examples of application of biocomposites at NPSP are façades, construction and mobility. Products like Nabasco 8010 contain natural fibres and fillers from waste streams. Nabasco 8010 is product which is largely biobased (over 97% biobased content).

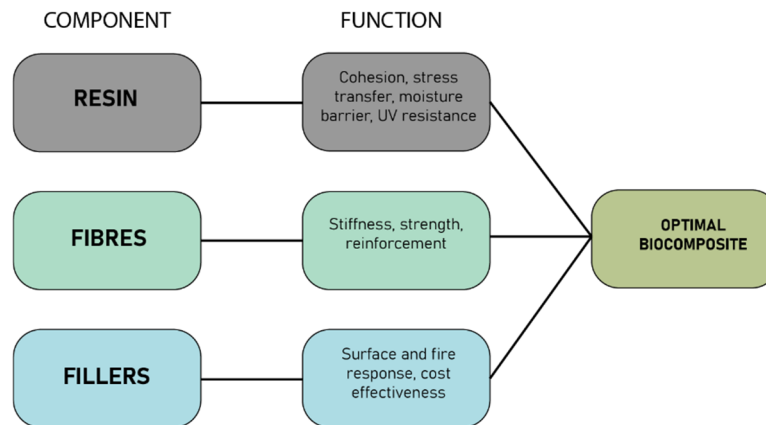


Figure 25: A three-part material diagram showing resin matrix + fibres + fillers, with indications of the functions of each constituent: "load transfer", "reinforcement", "volume/cost/fire/surface tuning", "durability", and "circularity" (source: Author)

### Circular Biocomposite Design

One of the key focusses of NPSP & Nabasco is the use of local and residual biological materials. Natural fibres such as flax and hemp are applied. Waste streams such as roadside grass and toilet paper are materials which are being explored. Biodiesel, sugar, paper and sewage-treatment processes are innovative material streams.

Materials at NPSP are produced using SMC and BMC production processes. BMC stands for Bulk Moulding Compound technology. Resin, lignocellulosic fillers and fibres are mixed to form a mouldable compound. Figure 23 illustrates how the production process at NPSP B.V. is conducted.

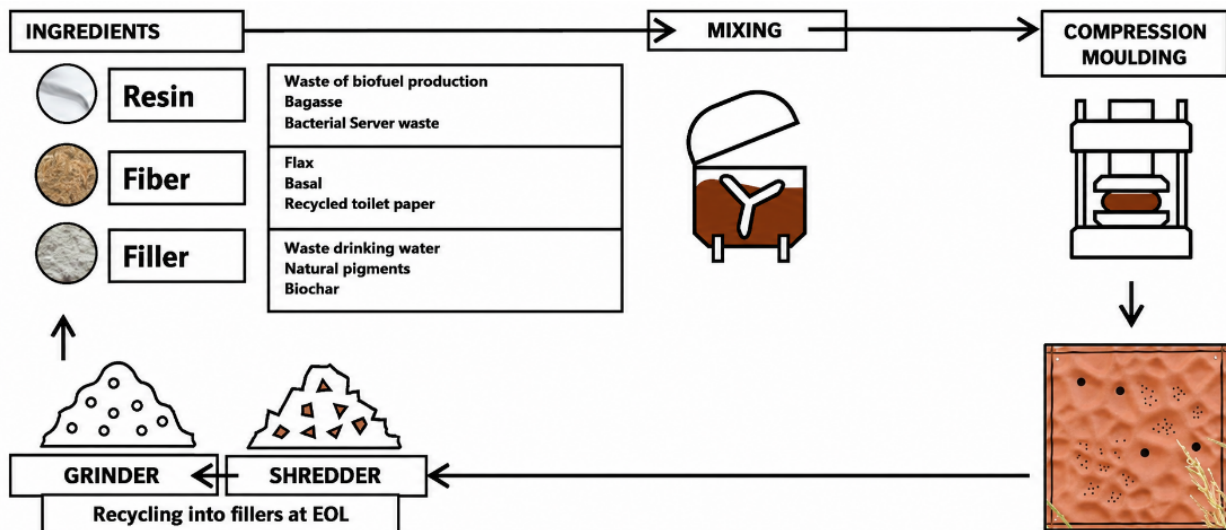


Figure 26: NPSP biocomposite production process (source: NPSP)

## Resin Systems in Biocomposites

Resins bind the components of the biocomposite together. Besides binding the fibres and fillers, the resin provides UV, water and thermal resistance.

Common resin types used in combination with natural fibres are unsaturated polyesters, vinyl esters, epoxy, phenolic, polyurethane, furan resin and thermoplastic matrices such as polypropylene, polyethylene, PLA and other biopolymers. Established thermosetting matrices are phenolic, epoxy and polyester. Common thermosets are vinyl esters (Li et al., 2007; Xie et al., 2010).

Thermosets cure irreversibly. The crosslinking process creates networks which cannot be changed after the curing stage. These materials are usually stable, heat resistant, stiff and durable in outdoor conditions. Thermoplastics on the other hand, can be remelted and reshaped. However, the fabrication process complicates fibre impregnation. This matters for natural fibres because lignocellulosic fibres are sensitive to thermal degradation, moisture and fibre-matrix incompatibility.

Table 3: Overview common resin types used for biocomposites and their main properties:

Resin	Biobased content	Processing details	Technical strengths	Limitations
Unsaturated (Bio)polyester	Medium	Fast curing, low cost	Established & good stiffness	Styrene exposure
Vinyl ester	Low to Medium	Similar to Bio polyester	Chemical resistance	Reactive dilutant and dependent on fossil fuels
Epoxy	Medium	Slower, precise curing	Low shrinkage, high mechanical properties	Costly
Phenolic	Low to Medium	Condensation curing	Bio derived	Brittleness & formaldehyde obstacles
Furan/ PFA	High	Acid-catalysed thermoset	Bio derived, heat and high chemical resistance	Brittleness, curing sensitive and dark colour
(Biobased) thermoplastics	Medium - High	Melt processing	Remelting potential	Thermally sensitive fibres

Table 3: Overview common resin types used for biocomposites and their main properties (source: Li et al., 2007; Mohammed et al., 2023; Odiyil et al., 2023)

## Furan resins

Furan resins are one of the most promising resin families for biocomposite development. It uses biomass conversion. The furan resins are based on furfuryl alcohol. The furfuryl alcohol can be synthesised from agricultural and forestry waste containing pentose. The use of waste streams is inherently different compared to polyester or epoxy systems. It is a common understanding that polyester and epoxy systems can be manufactured more easily, however, the carbon footprint of furan resins is significantly smaller. Even if furan-based composites tend to be more brittle, their sustainable argument is strong. Figure 27 demonstrates the low embodied energy of furan fibre composites compared to other composites, epoxies and plastics.

Furan resin is produced by hydrolysing and dehydrating pentosan-rich hemicellulose. The hydrolysis is acid catalysed. Lignocellulosic biomass forms the base component. By hydrogenating furfural, furfuryl alcohol is derived. This process is described further in the work of Odiyi et al. (2023) and illustrated in figure 26. Furfuryl alcohol is polymerised in acid conditions. In the polymerisation process, condensation, ring reactions, branching and cross-linkage reactions eventually form a thermoset. Lignin fragments and polyfurfuryl alcohol (PFA) chains can be crosslinked. Lignin is derived from pulp and biorefinery waste streams and is abundant. During the production, the resin will wet the fibres and create strong adhesion after the curing stage. The cure cycle, water content, catalyst choice and filler and fibre moisture should be chosen carefully.

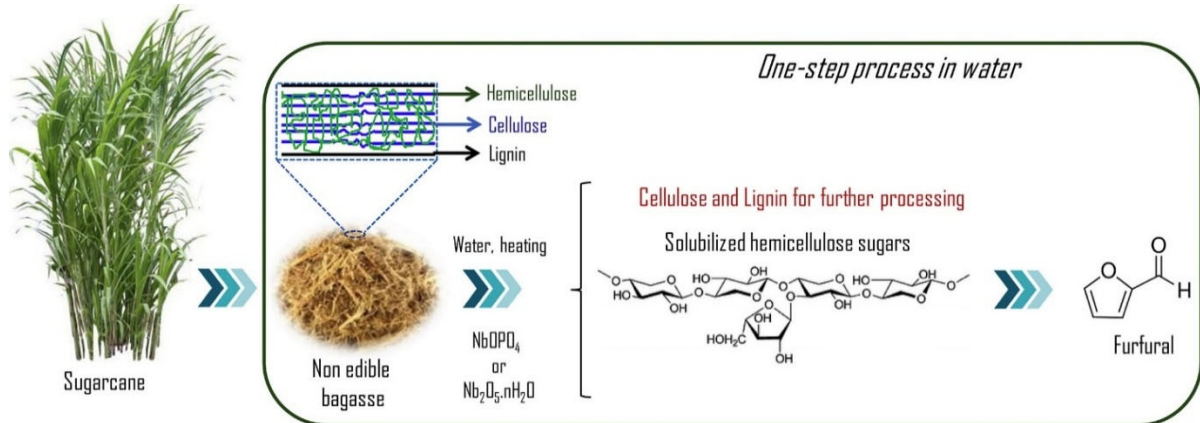


Figure 27: Production process furfural (source: Catrinck et al., 2020)

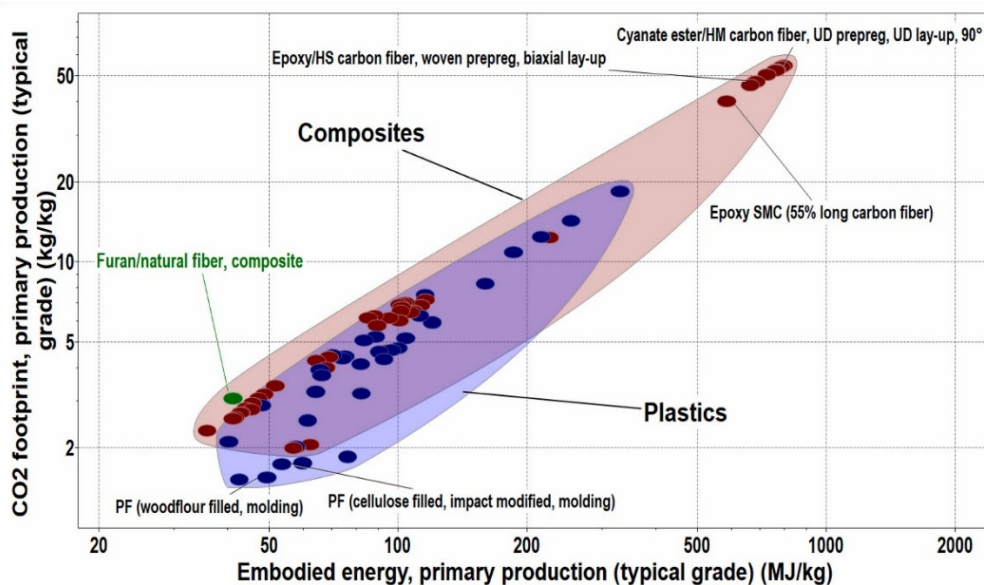


Figure 28: Placement of Furan Resin relative to plastics, and other composite materials (source: Odiyi et al., 2023)

## Fibres

Fibres are the primary load-bearing component in a fibre-reinforced composite. In a biocomposite, natural fibres such as flax, hemp, jute, sisal, reed, cane, cotton textile fibres and recycled cellulosic fibres may be used depending on availability, fibre geometry, cost, sustainability profile and target performance. Natural fibres are attractive because they are renewable, relatively low density and often lower in embodied energy than glass or carbon fibres. Their specific stiffness can be useful where lightweight design matters. However, they are not homogeneous industrial fibres in the same way as glass fibre. Their performance depends on plant species, growing conditions, harvest timing, retting, decortication, fibre extraction, drying, storage, fibre length and surface chemistry.

Common production of natural fibres involves harvesting of the plants, separation of the fibres, cleaning, drying and cutting. Plant fibres contain cellulose, hemicellulose, lignin, waxes and pectins. Cellulose provides stiffness. Plant based fibres can be hydrophilic due to hydroxyl groups. Surface treatments such as alkaline or silane treatments are used to improve the fibre-resin adhesion to reduce moisture sensitivity.

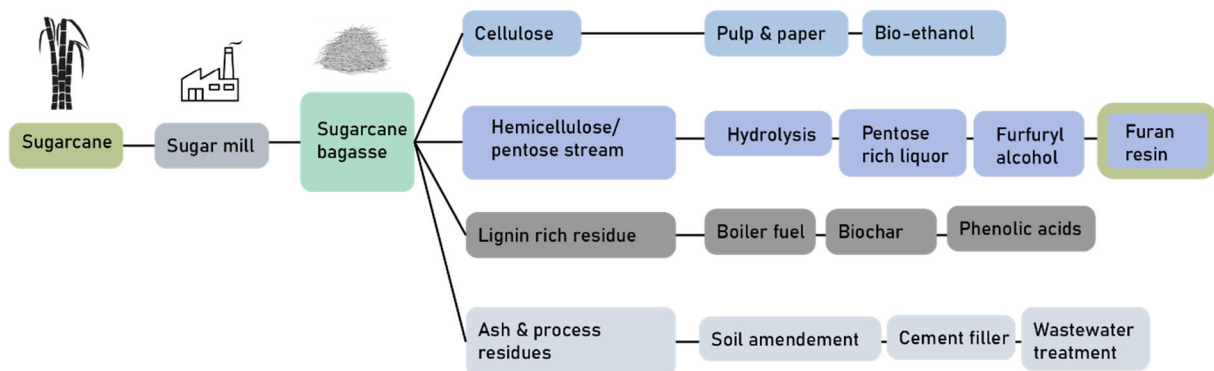


Figure 29: A scheme showing how sugarcane bagasse is processed and how furan resin is obtained (source: Author)

## Fillers

Fillers are not used just to bring the overall product price down. They function as design variables. Fillers control shrinkage, reduce resin content and increase stiffness. In this research porous fillers are explored to absorb sound. Cork fillers with different particle sizes are used. When these fillers are exposed to the external layer of façade panels, they can absorb high frequency sound.

In compression moulding or bulk moulding compounds, filler particle size and particle packing are important because they influence viscosity, flow, void content and resin consumption.

Filler production begins with material stream selection. Examples of biobased fillers include ground walnut shell, reed particles, recycled textile dust, paper sludge, ground roof tile, lignocellulosic powder and other locally available residual streams. The feedstock is then dried, milled, sieved, classified and sometimes thermally or chemically treated.

Recent work on food-waste fillers in furan-matrix biocomposites found that filler type, particle size and volume ratio strongly affect performance.

## Integrated Production for Biocomposite Products

NPSP's recent lignin-based BMC work is an example of this integrated logic: resin, lignocellulosic fillers and fibres are combined into a mouldable compound, then pressed under heat and pressure to form panels. This approach is especially suitable for scalable product families because it allows relatively consistent dosing, mould filling, surface replication and integration of inserts or product-specific features.

The most advanced biocomposite development does not optimise mechanical properties in isolation. It optimises a performance–processing–sustainability triangle. A material with excellent bio-based content but poor durability may be environmentally inferior to a slightly less bio-based material that lasts three times longer. Conversely, a mechanically impressive composite that cannot be recycled, repaired, remanufactured or safely processed may fail the broader circularity objective. NPSP’s ongoing work on recycling and biodegradation illustrates this complexity: MNEXT notes that furan resin and polyester/styrene Nabasco systems contain diverse components, making end-of-life treatment challenging, and describes biodegradation as a potential future route.

Table 4: Biogenic content in Nabasco Façade Panels, per FU (1 m<sup>2</sup>):

Biogenic Carbon	Share Biogenic Carbon per FU
	Nabasco 8040 (furan-based product)
Biogenic Carbon in the product	5.42 kg C
Biogenic Carbon in packaging	0.20 kg C

Table 4: Biogenic content in Nabasco Façade Panels, per FU (1 m<sup>2</sup>) (source: Nabasco EPD). The kg C/FU is taking the entire lifetime of the product into account

### 2.4.5 Emerging Acoustic Metamaterials & Structured Systems

Recent research also points toward bio-inspired and structured acoustic systems. Lu et al. (2025) discuss bio-inspired acoustic metamaterials for traffic-noise control and show how machine learning can support the design of structures targeting specific frequency ranges. Acoustic metamaterials are typically designed through geometry rather than only through material composition. They may include resonant cavities, periodic structures, locally resonant elements, or topology-optimised surfaces.

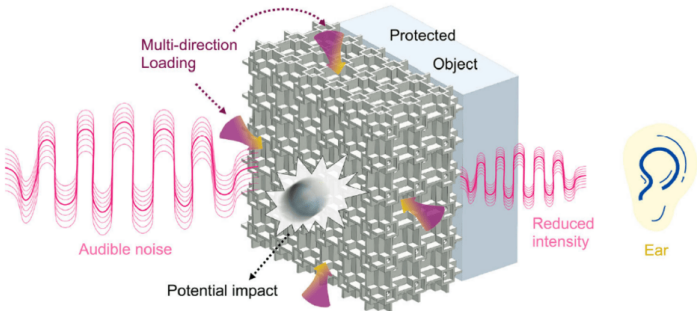


Figure 30: Lattice structure for sound absorption (source: Lattice Structures for Acoustics Applications – Zhai Group At NUS, n.d.)

While full metamaterial development may be beyond the scope of this project, the principle is relevant. It suggests that future biocomposite noise-mitigation products may benefit from combining material porosity with designed geometry. Surface patterning, cavities, graded layers, ribs, perforations, or bio-inspired structures could help extend performance beyond what is possible with a flat porous panel alone.

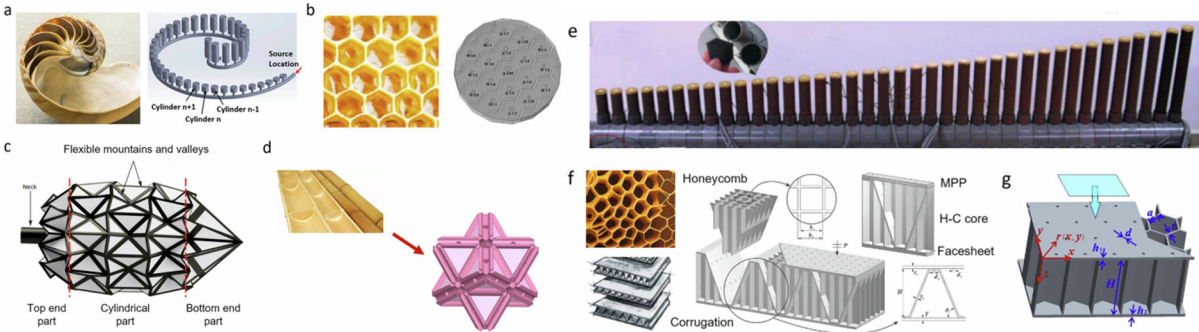


Figure 31: Metamaterial designs based on natural and bio inspired shapes (source: Lu et al., 2025)

Bio-inspired and metamaterial approaches may also provide useful design directions. Lu et al. (2025) discuss bio-inspired acoustic metamaterials for traffic-noise control and show that geometry, structural hierarchy, and computational optimisation can support acoustic performance. The research does not develop full metamaterials but provide relevant principles. Acoustic sound absorption can be designed through structural design besides material development.



*Figure 32: Fractals inspired acoustic sound absorption design (source: Wan et al., 2020)*

In France, research has been conducted regarding mathematics inspired fractal shapes for outdoor infrastructural acoustic mitigation. Irregular shaped objects have long been recognised as poor resonators. This was confirmed by Bernard Sapoval in the 1980s. His work led to the development of fractal-inspired acoustic barriers, later realised in collaboration with Marcel Filoche and Colas® as the patented Fractal wall®. Incorporation of different lengths and pores, the structure achieves broadband acoustic absorption. Measurements showcase 98% absorption of incident traffic-noise energy for specific frequency bands. This example illustrates how fractal geometry can enhance sound dissipation and the potential of collaboration between mathematical analysis, physics, and acoustic engineering.

#### 2.4.6 Nature Inclusivity

The proposed acoustic biocomposite system also offers potential for nature-inclusive design, meaning that the noise-mitigation element could support biodiversity while maintaining its primary acoustic function. This is relevant because acoustic barriers, façade panels, and urban screens often occupy large surface areas in infrastructural and urban environments. If designed carefully, these surfaces can combine sound absorption, low-carbon material use, and habitat creation.

Within the NPSP context, nature-inclusive concepts have already been developed through nesting chamber designs. These box-like chambers measure approximately  $120 \times 120 \times 260$  mm, although other dimensions are possible depending on the target species. The entrance perforations vary according to species requirements, commonly within a diameter range of approximately 30–40 mm for several cavity-nesting birds. Relevant species include small birds and bats. Insect habitat could be integrated through reed or bamboo strips with varying internal diameters, especially for cavity-nesting insects such as solitary bees.

However, nature-inclusive additions must be designed as part of the acoustic system rather than added afterwards. Large openings, nesting boxes, or dense habitat modules may alter perforation ratio, airflow resistance, cavity depth, and therefore acoustic performance. A modular strategy is therefore

most appropriate: standard acoustic panels can be combined with selected biodiversity modules where ecological conditions are suitable. This allows bird, insect, bat, or small-mammal features to be integrated without compromising the acoustic continuity of the full system.

Nature inclusive design moves from a single function of nature inclusivity into a multifunctional infrastructure component by performing well for sound absorption in the desired frequency band width. The approach remains exploratory within this research and would require ecological validation in later field applications, nevertheless it demonstrates clear potential for combining acoustic performance, circular material development, and biodiversity support in outdoor urban environments.

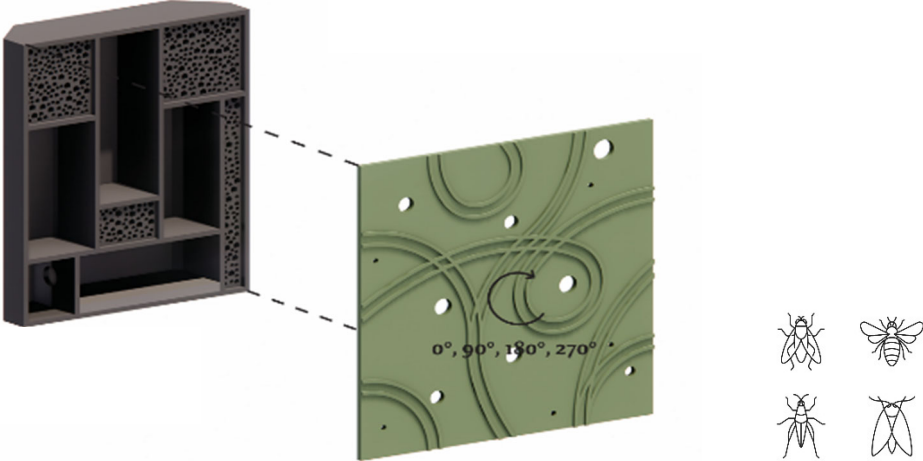


Figure 33: Nature Inclusive design system (source: Studio Marco Vermeulen)

### 2.4.7 Positioning of this Research within Existing Products

The existing product landscape shows that no single solution addresses all requirements. Conventional barriers provide shielding but may be materially intensive and reflective. Low-noise road surfaces reduce noise at the source but degrade over time and cannot fully address propagation. Mineral wool and synthetic absorbers perform well acoustically but raise sustainability and recyclability concerns. Porous concrete and wood wool cement boards provide durable alternatives but may remain mineral-intensive. Natural-fibre materials and biobased resins are promising. Their potential is investigated in the next chapters.

## 2.5 Strategic KPI's

To assess how newly created materials compare and compete with the most important conventional products and materials, benchmark factors are created. This is illustrated in table 5. After researching existing noise mitigation products for outdoor infrastructural environments and demonstrating the best performing established sound absorbing materials, the newly created materials can be assessed. New materials are assessed on their Alpha absorption coefficient, Noise Reduction Coefficient (NRC), Emissions in kg CO<sub>2</sub>, their biobased content, price per square meter and the lifespan estimation. The values for the expected lifespan of products are based on NPSP degradability data on 8040 Fire Hemp (furan resin-based material). In table 5, the final product is displayed as an example.

Table 5: Grading tool to assess the innovative materials:

Created Products	
αw	0.7
NRC	0.8
Emissions (kg CO <sub>2</sub> e/m <sup>2</sup> )	20 - 70
Biobased content (%)	97.5
€/m <sup>2</sup> (EUR)	150 - 250
Lifespan (y)	30




Table 5: Grading tool (source: Author)

03

EXPERIMENTAL  
INVESTIGATIONS

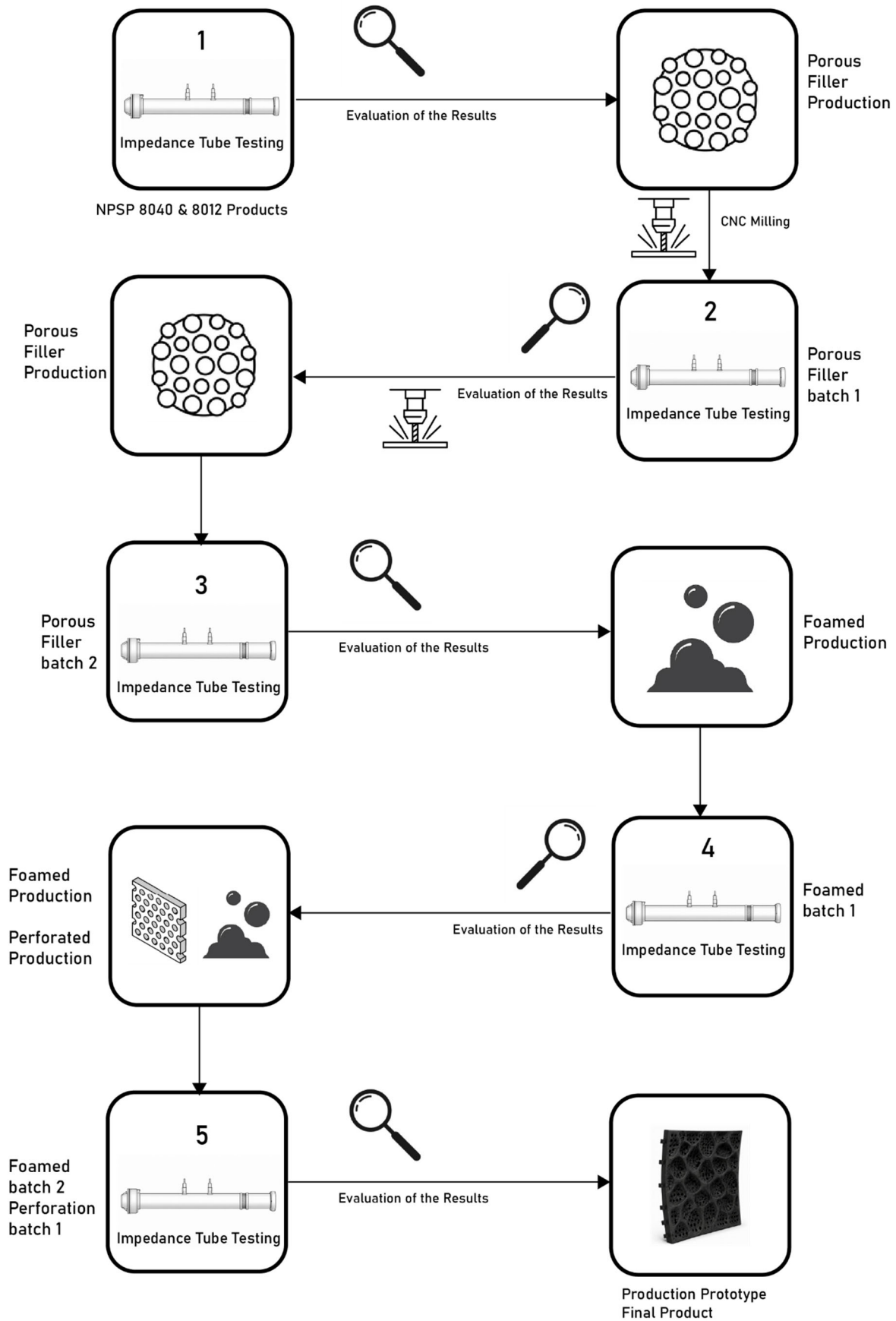


Figure 34: Flowchart production, testing & evaluation of material development (source: Author)

### 3.1 Materials & Methods

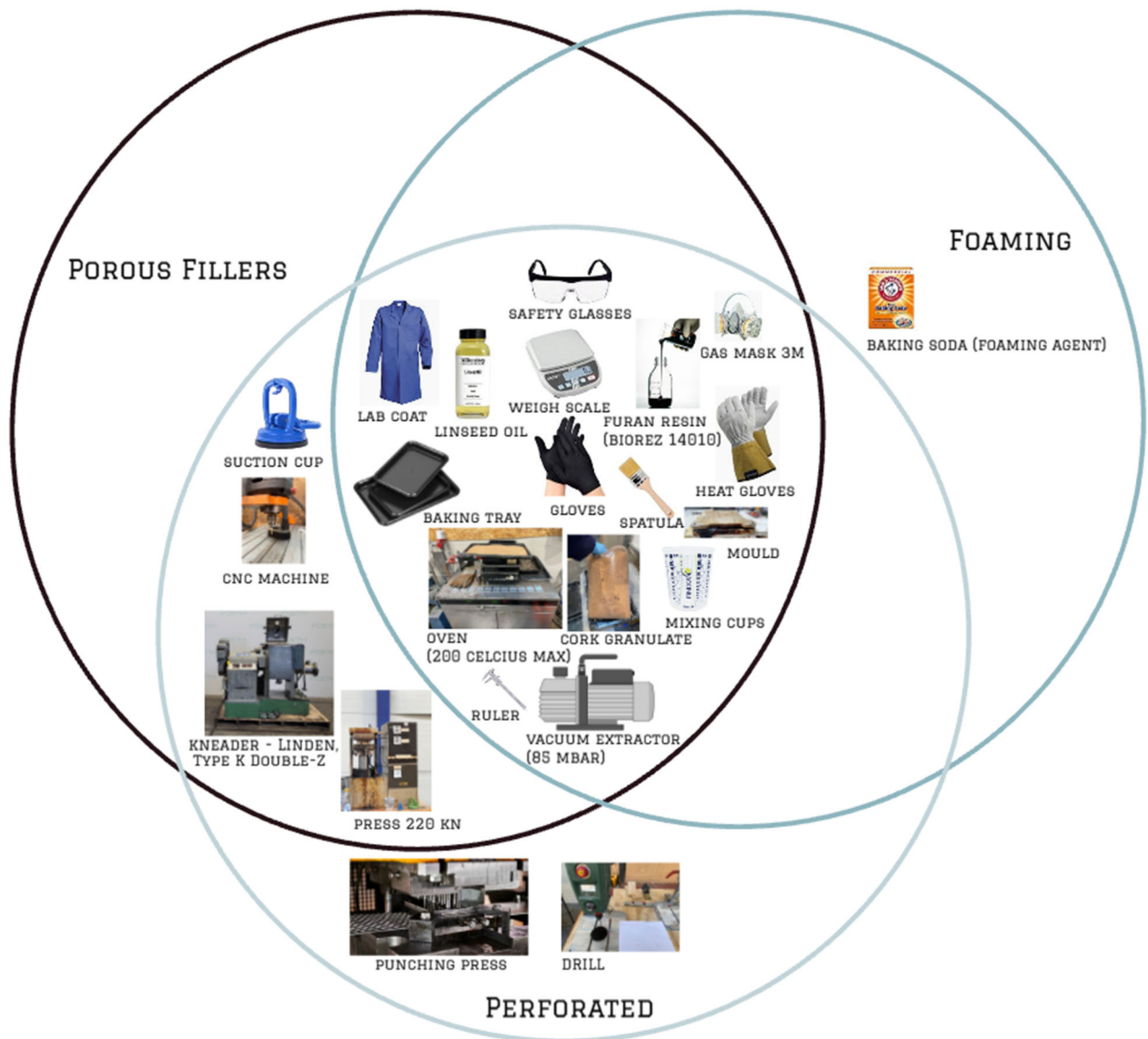


Figure 35: Equipment needed in the lab for different produced materials (porous fillers, foamed materials and perforated materials) (source: Author)

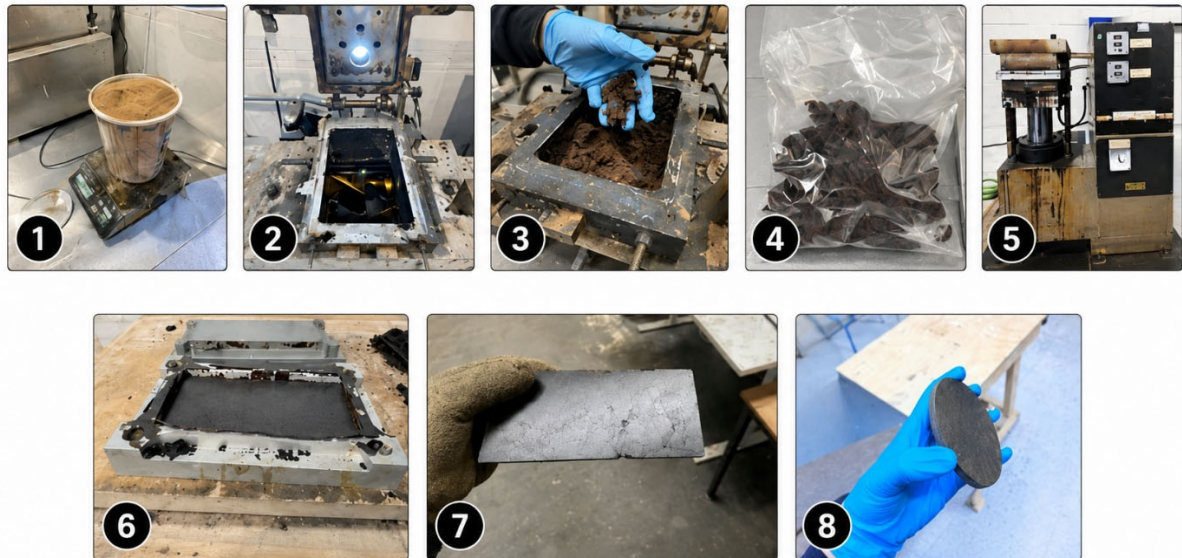
#### Introduction

The applied fabrication and test strategy is illustrated in figure 34. The first impedance tube test identified the absorption coefficient of established products at NPSP. These showed mainly reflection. The second and third impedance tube test used porous fillers-based materials. These had similar results and confirmed that porous fillers with a surface layer which is resin, do not absorb sound significantly. The fourth and fifth impedance tube test demonstrate that some foamed materials are promising. Perforated materials with absorbing materials behind them can perform even better.

In figure 35, the needed equipment is illustrated for each of the applied production techniques. Equipment and machine in the centre of the figure are used in all three production methods. Facilities at NPSP are used as well as knowledge on how the production works best. The following pages demonstrate which steps must be conducted to create the porous filler, perforated and foamed materials.

## 3.2 Production Process & Observations

### Production Porous Fillers & Perforated Materials



*Figure 36: Porous Filler Production Process (source: Author)*

#### The manufacturing process:

- 1. Mixture preparation:**  
Weigh and mix the raw materials to achieve the desired blend.
- 2. Mixing in the kneader:**  
The rotation blades mix the 'dough'. Make sure the Kneader stays around 85 centigrade to prevent the crosslinking process to start at this stage.
- 3. Filling:**  
Check if the viscosity is correct. Add the fillers. Conduct research based on weight fraction or volume fraction. The mixture should be 'thick' enough and still bind together. If this is true, the 'dough' can be taken out of the kneader.
- 4. Material storage:**  
Store prepared materials in sealed bags to maintain the quality.
- 5. Compression:**  
The 'dough' can be compressed under temperatures ranging from 140 to 145 degrees for furan resin. The applied pressure is usually 100 bar. Lower pressure can be applied as well, for sound absorption properties this is especially an important performance indicator. By applying a layer of linseed oil or olive oil first, the dough is prevented from staying attached to the mould when being removed.
- 6. Demoulding:**  
Carefully open the mould and use the heavy-duty suction cup to get the plate out of the mould.
- 7. Inspection:**  
Sheet thickness check and surface quality assessment.
- 8. Testing specimen:**  
Cut the material with the CNC machine for the preparation of the samples for the impedance tube acoustic testing (100mm & 29mm samples) as stated in ISO 10534.

## Production Foamed Materials



Figure 37: Foamed Material Production Process (source: Author)

### The manufacturing process:

1. Mixture preparation:  
The particle (=granulate) size is largely affecting the foaming process and size of the pores. In this research cork granulate of 0.5 mm is selected.
2. Checking the moisture content:  
Check this with a moisture meter.
3. Selection of fibres:  
The fibre selection is an important step. Cork and bamboo fibres are lightweight, so a small share in weight is used in the produced materials.
4. Extracting moisture from the Biorez furan resin:  
The resin will become stiffer once it is moisture less and cools down.
5. Mixing (in the kneader/ by hand):  
The low moisture resin can then be taken out of the kneader and be mixed in mixing cups with the fillers or fibres desired. A catalyst is added first, to ensure the dough will cure later under 140 centigrade.
6. Filling:  
Mixing the fibres, resin and potentially fillers is an important process. The quantities of fillers and fibres can be added in batches for optimal mixing properties. As stated before, it is important to mix in time when the resin is still warm (above 70 centigrade)
7. Baking tray preparation:  
A layer of olive oil or linseed oil is applied to the baking tray. This layer prevents the material from attaching to the tray.
8. Mixture placement in the tray:  
The mixture should be placed in the baking tray evenly.
9. Testing specimen:  
Cutting out the testing sample can be done using the CNC machine. For thicker samples. Other cutting methods should be applied. A saw or waterjet cutting are effective alternatives.

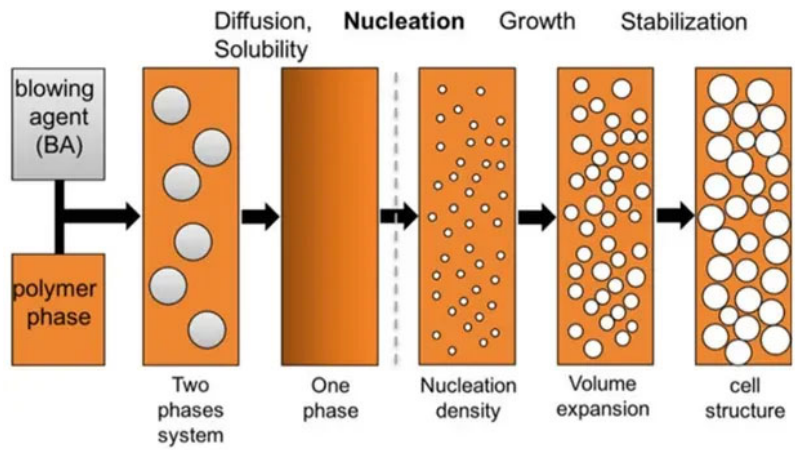


Figure 38: Foaming process using a BA (source: Karger-Kocsis, József; Bárány, Tamás (2019). Polypropylene Handbook (Morphology, Blends and Composites) // Foams., 10.1007/978-3-030-12903-3(Chapter 10), 579–641)

### Foaming Process

To obtain pores which oscillate sound in the most optimal way, different parameters can be adjusted. The created foamed materials demonstrate 5 significant factors influencing pore size creation. These are illustrated in table 6 and are the following: Moisture content, volume fraction, mass fraction, particle size, curing temperature and ultimately the density.

Table 6: Controlling the Material Properties:

Governing Factors	Remarks
Moisture content (%)	Low moisture quantities create smaller pores
Volume Fraction (%)	
Mass Fraction (%)	Light fillers get a bigger share in the total composite
Particle Size (mm)	A particle size smaller than 1 mm face mixing difficulties in the kneader
Curing Temperature (Centigrade)	Curing on 140°C is optimal (100 °C is also possible, but takes 3x more time)

Table 6: Controlling Parameters Material Development (source: Author)

Foamed materials can be obtained by adding foaming agents (=blowing agent) to the material mixture. Common foaming agents in baking processes are baking soda e.g. Baking soda ( $\text{NaHCO}_3$ ) also known as sodium bicarbonate, reacts when it gets in contact with acids with moisture and forms carbon dioxide gas. This agent has been added to the material mixture in S12 (Baking Soda). Dicalcium phosphate, manganese dioxide and sodium bicarbonate are products which can create foamed materials and could be explored within biocomposite development. Sodium bicarbonate releases carbon dioxide gas when heated or brought in contact with an acid. Dicalcium phosphate can act as a reactive component. Manganese dioxide can act as a catalyst and create gas when combined with a gas-forming compound.



Figure 39: Potential foaming agents (source: left to right: American Society of Baking, n.d.; Cereals & Grains Association, n.d.; MIT OpenCourseWare, 2012; Lehmann & Voss & Co. KG, 2024; Reglero Ruiz et al., 2015)

## Observations Material Production

This section describes the observations during the experimental investigation production phase of the biocomposites. It is elaborated how different material compositions and parameters influence the formation, workability and internal structures of the developed materials. The fibre type, filler quantity, cork granulate size, viscosity, curing temperature, and baking time are considered.

### Porous Biocomposite Materials

The porous filler materials are based on cork granulate, glass bubbles and rice husk. The objective is the creation of internal porous structures while maintaining sufficient mechanical stability.

During the production, it can be concluded that the addition of fillers is necessary to improve structural performance. Samples consisting of mainly furan resin were brittle and could fracture easily. Already with 10 wt% filler (e.g. cork), mechanical properties significantly improved after curing. Materials containing fibres (e.g. S10: bamboo fibre), had much better mechanical properties.

Cork granulate is selected as it has a low density, is nature based, and has promising sound absorbing properties. However, the quantity of cork filler has a significant influence on the production process. A cork filler content of 20% by weight was too high to create the desired pore structure and size. Due to the low density of the cork and the fact that the cork seems to absorb a part of the resin, large cork filler quantities were difficult to process. After multiple trials, a cork content of around 10% by weight is optimal. This ratio ensures good internal structures and workability.

Cork granulate size is a major factor in processing. Cork of 1 mm absorbed much of the resin and blocked the kneader blades eventually. Very fine particles could not be pressed well. The material flow was so high, the plates were not thick enough. An optimal granulate size of 0.5 mm was discovered for processability, filler distribution and pore formation.



*Figure 40: Foamed material production S9 (source: Author)*

### Foamed Biocomposites

The foamed biocomposites were produced by allowing gas formation and expansion within the furan resin matrix during curing. The process was highly sensitive to moisture content. Moisture was observed to play a crucial role in the development of the internal pore structure. A default moisture content of 13% led to the formation of extremely large bubbles during curing. Especially when the materials were cured under 140 degrees. The bubbles were too large for practical use. The top layer was fragile and could easily break. This happened in multiple cases. Later trials with lower moisture content had promising results. An overview of the pore sizes of well performing materials is illustrated in table 7. Figure 40 illustrates an example of a foamed material (S9 Almond Shell).

Table 7: Porosity Analysis:


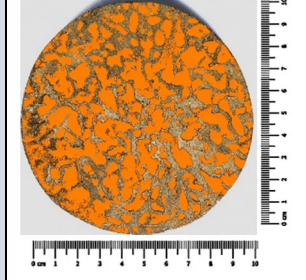

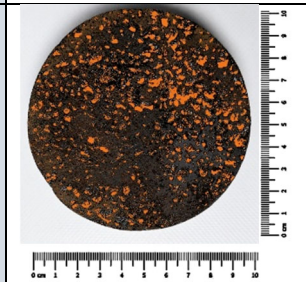

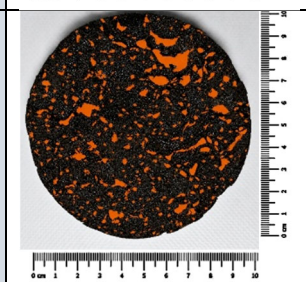
	<p><b>Bamboo Fibre (S10)</b> Pore sizes visual observation: medium (0.7mm)</p>	
	<p><b>Foamed Cork 3 (S11)</b> Pore sizes visual observation: small (0.2mm)</p>	
	<p><b>Foamed Cork 1 (S3)</b> Pore sizes visual observation: small-medium (0.4mm)</p>	

Table 7: Porosity Analysis S10, S11 & S3 (source: Author)

Moisture contents of below 2% were optimal for pore formation. The results indicate that reducing moisture content before production is essential for producing stable foamed biocomposites. Stable examples of foamed materials with a low moisture content are illustrated in figure 41 and 42.

Baking time has a large effect on pore formation. A curing time of 30 minutes at 140 °C was found to be optimal for the production process. At higher temperatures or during faster baking, the bubbles had less time to escape from the material mixture. This results in larger pores and irregular pore structures. Curing time significantly increases with lower temperatures. Temperatures of 100 centigrade were used where curing time increased from 30 minutes to 2 hours. The catalyst performs best for temperatures around 140 centigrade.

The viscosity of the mixture was another important processing factor. A low viscosity was preferred because it facilitates the mixing of the material and ensures good flow into the mould and around filler particles. As the viscosity increased, the mixture became harder to distribute evenly. This affects the quality of the final material. It is therefore important to complete the mixing and moulding steps before the resin became too viscous.



*Figure 41: S9 foamed material (source: Author)*



*Figure 42: S13 foamed material (source: Author)*



*Figure 43: Perforated biocomposite 8040 Hemp Fire (20% perforation rate)*

## Perforated Biocomposite Materials

In addition to porous and foamed materials, perforated biocomposites were produced to investigate how controlled perforation rates (open area), could influence the material structure and potential acoustic behaviour. Controlled perforations ensure absorption can be tuned more easily. Based on literature, perforation rates of 10%, 20% and 30% were applied. Simulations on Whealy and Acoustic Modelling formed additional guidance into this optimal perforation rate (*Helmholtz Calculator*, n.d.-b; *Porous Absorber Calculator*, n.d.). An example of a perforated material with a perforation rate of 20% is illustrated in figure 43.

Another reason to develop perforated materials is the fact that externally used biocomposite facades should be strong enough to withstand wind, and impact loads. Fillers and fibres improve stability and reduce the risk of cracking behaviour.

The perforated materials were perforated using a drill with a 6 mm head. It is a common understanding that hole diameter is acoustically optimal when it matches the material sheet thickness. Based on simulations mentioned above, a perforation rate of 20 to 25 % seems most promising.


### Key takeaways:











Moisture content was one of the most important factors in the foaming process. High moisture levels caused large bubble formation. Moisture levels below 0.5% resulted in smaller and more stable pore creation.

The use of natural fillers and fibres improved the strength of the materials. Cork granulate was found to be most effective for the processing and later the acoustic performance. More elaboration on the acoustic behaviour of the newly created materials can be read in the next chapter. A 10 wt% and a particle size of approximately 0.5 mm is optimal. Larger cork particles absorbed too much resin and reduced workability. A baking process of 30 minutes at 140 °C provided the best result in curing efficiency and pore formation. Low viscosity during mixing ensured good workability and an even material distribution.

To conclude, the scientific investigations showcase that porous filler-based materials, foamed materials, and perforated biocomposites can be successfully produced from the biobased furan resin, natural fillers and fibres. Moisture content, filler size, filler quantity, viscosity, and curing conditions were controlled to create optimal materials.

Table 8: Selection Production Overview:

	S3	<b>Foamed Cork 3</b> Furan Resin (90wt%) Cork 0.5mm (10wt%) T: 140 centigrade Time: 30 min Thickness: 15 mm Weight: 31.12 g (moisture less) Density: 0.264 g/cm <sup>3</sup> Low Moisture (less than 2%)	-
---	----	--	---

	<b>S8</b>	<b>Foamed Cork 8</b> Furan Resin (87.5wt%) Cork 0.5mm (12.5wt%) T: 140 centigrade Time: 30 min Thickness: 11-13 mm Weight: 19 g Density: 0.202 g/cm <sup>3</sup> Low Moisture (less than 2%) With Mould	
	<b>S9</b>	<b>Almond Shell</b> Furan Resin (82.5wt%) Almond Shell (17.5wt%) T: 100 centigrade Time: 120 min Thickness: 20 mm Weight: 53.9 g (moisture less) Density: 0.343 g/cm <sup>3</sup>	
	<b>S10</b>	<b>Bamboo Fibre</b> Furan Resin (90wt%) Bamboo Fibre (10wt%) T: 100 centigrade Time: 120 min Thickness: 20 mm Weight: 101.9 g (moisture less) Density: 0.648 g/cm <sup>3</sup>	
	<b>S11</b>	<b>Foamed Cork 9</b> Furan Resin (90wt%) Cork 0.5 mm (10wt%) T: 120 centigrade Time: 120 min Thickness: 20 mm Weight: 73.0 g (moisture less) Density: 0.464 g/cm <sup>3</sup>	
	<b>S13</b>	<b>Foamed Cork 10</b> Furan Resin (90wt%) Cork 0.5 mm (10wt%) T: 120 centigrade Time: 120 min Thickness: 70 mm Weight: 69,1 g (moisture less) Density: 0.126 g/cm <sup>3</sup> Low Moisture (less than 0.5%)	

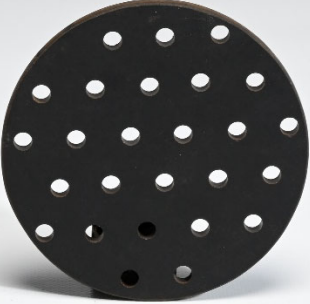






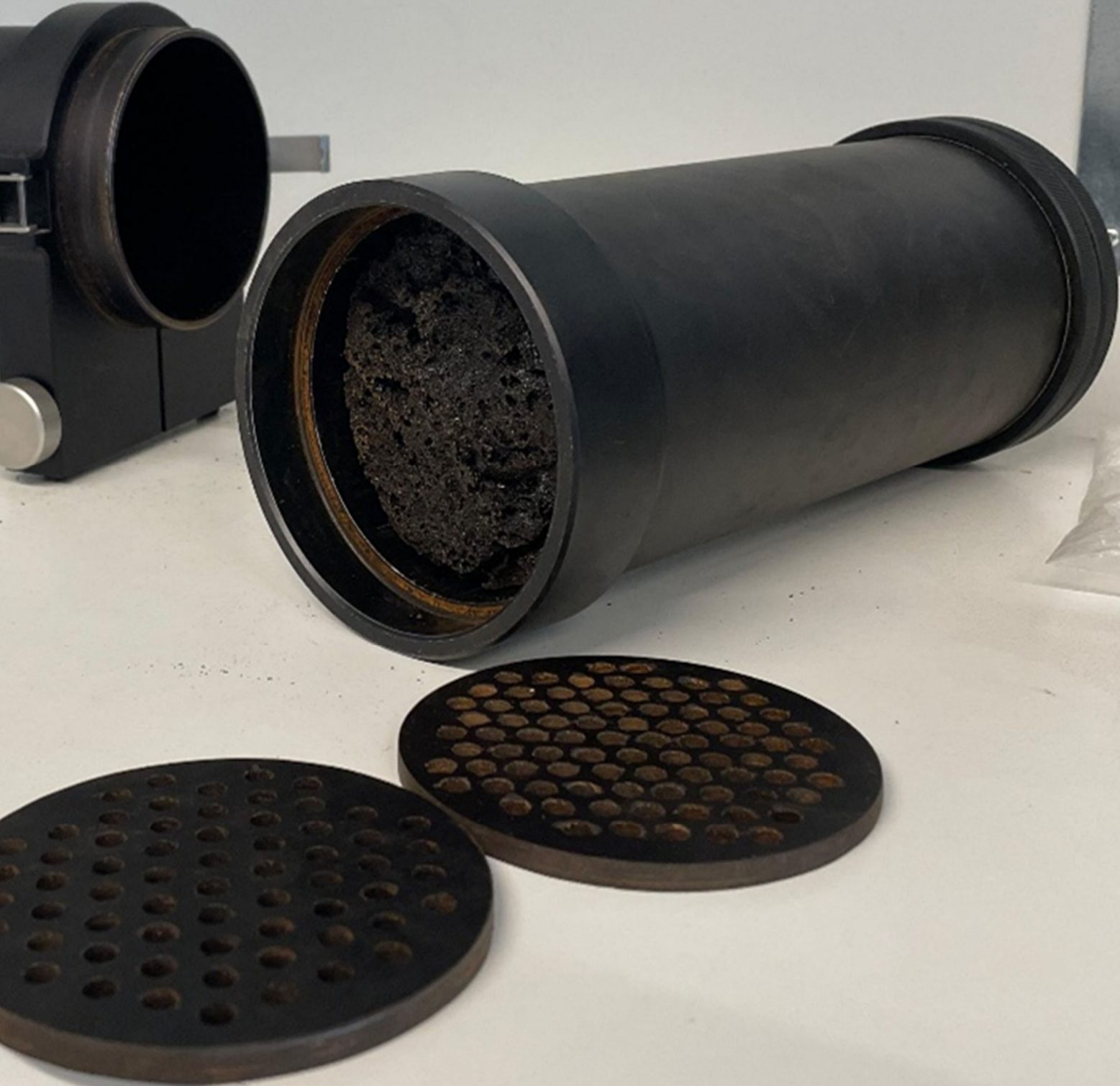
	C1	<b>8040 Hemp Fire</b> 10% open area Hole diameter: 6 mm Thickness: 6 mm Weight: 62 g	-
	C2	<b>8040 Hemp Fire</b> 20% open area Hole diameter: 6 mm Thickness: 6 mm Weight: 50 g	-
	C3	<b>8040 Hemp Fire</b> 30% open area Hole diameter: 6 mm Thickness: 6 mm Weight: 46 g	-
	D	<b>Cork 0.5mm</b> - Sandblasted Thickness: 6 mm Weight: 65 g Density: 1.379 g/cm <sup>3</sup>	
	E	<b>Reed (100mm)</b> Hole diameter: varying Thickness: 100 mm Weight: 115 g Density: 0.146 g/cm <sup>3</sup>	

Table 8: Production Overview Material Development (source: Author)

3.3 Test Results



### 3.3.2 Porous Fillers

The developed porous fillers-based materials are discussed in this section. The absorption coefficient of four materials is illustrated in figure 44. These materials are part of porous filler batch 1. All these materials do not absorb sound significantly. Absorption coefficients of higher than 0.1 are not achieved within the focus range. Generally, sound absorption is higher on higher frequencies. Porous filler batch 2 materials are illustrated in figure 45. Glass bubbles of 0.5 mm are mixed with bio-polyester resin. Glass bubbles are porous materials. Different pressure levels are applied to see if lower pressure leads to higher absorption. Therefore, cork samples are pressed under 10 bar pressure. Literature in the SOTA (state-of-the-art) section show research where this is the case. Absorption is still low due to an external layer which is still sealed due to the dense resin surface.

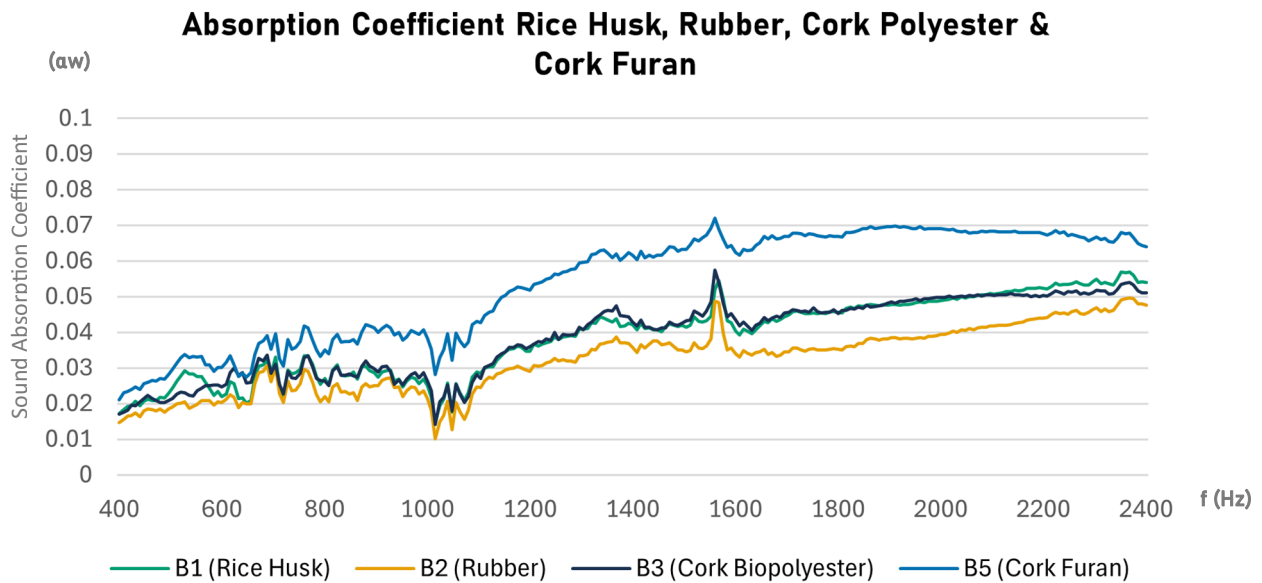


Figure 44: Impedance Tube test – Absorption Coefficient Rice Husk, Rubber, Cork Bio-polyester & Cork Furan (source: Author)

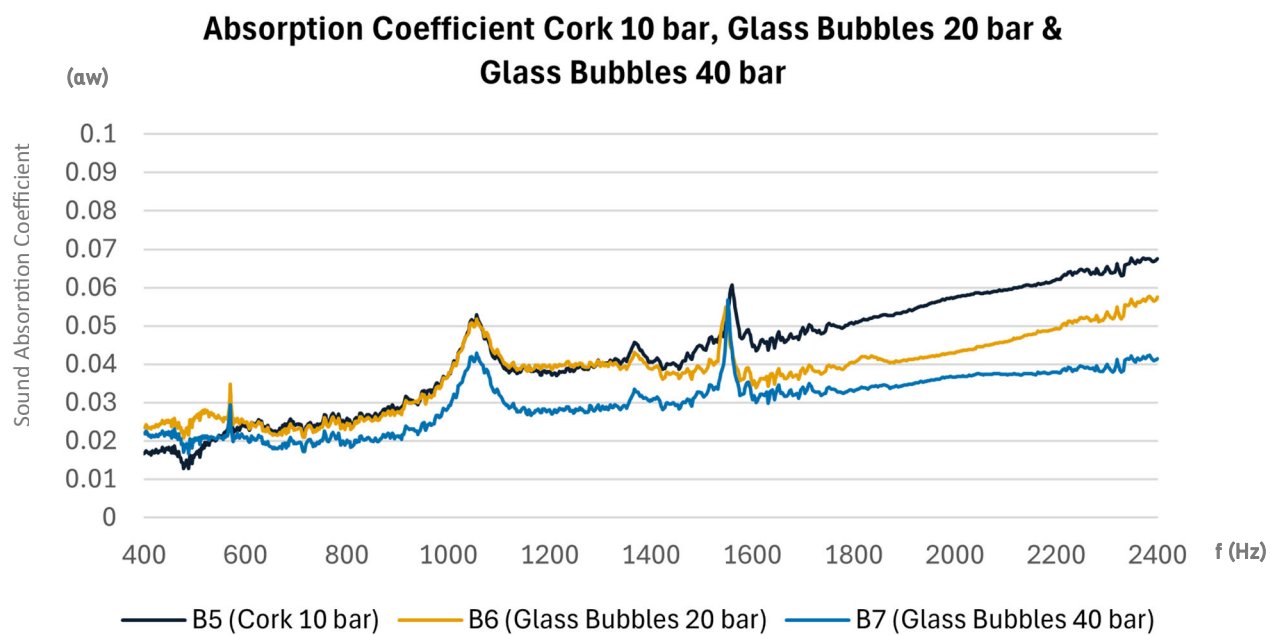


Figure 45: Impedance Tube test – Absorption Coefficient Glass Bubbles on different pressures & Cork Furan on low pressure (source: Author)

### Influence of Sanded Surface

Surface finishing influence sound absorption on high frequencies. In sanded samples, the top resin layer was partially removed, exposing the cork particles directly to the surface. See figure 47 for details on the surface texture of the sanded material.

Cork granulate absorbs sound especially in higher frequencies. When cork is exposed at the surface, sound waves can interact with the cork structure. The sanded cork sample D is illustrated in figure 46. At frequencies around 5200 Hz, absorption is significant. A similar effect may occur inside the pores of the foamed materials. In digital microscope modelling, this cork granulate exposure to the outer layer is visible.

The observation suggests that the combination of cork filler and porous structure may be beneficial for acoustic applications. However, further testing would be required to quantify this effect and determine the relationship between pore size, filler exposure and ultimately sound absorption.

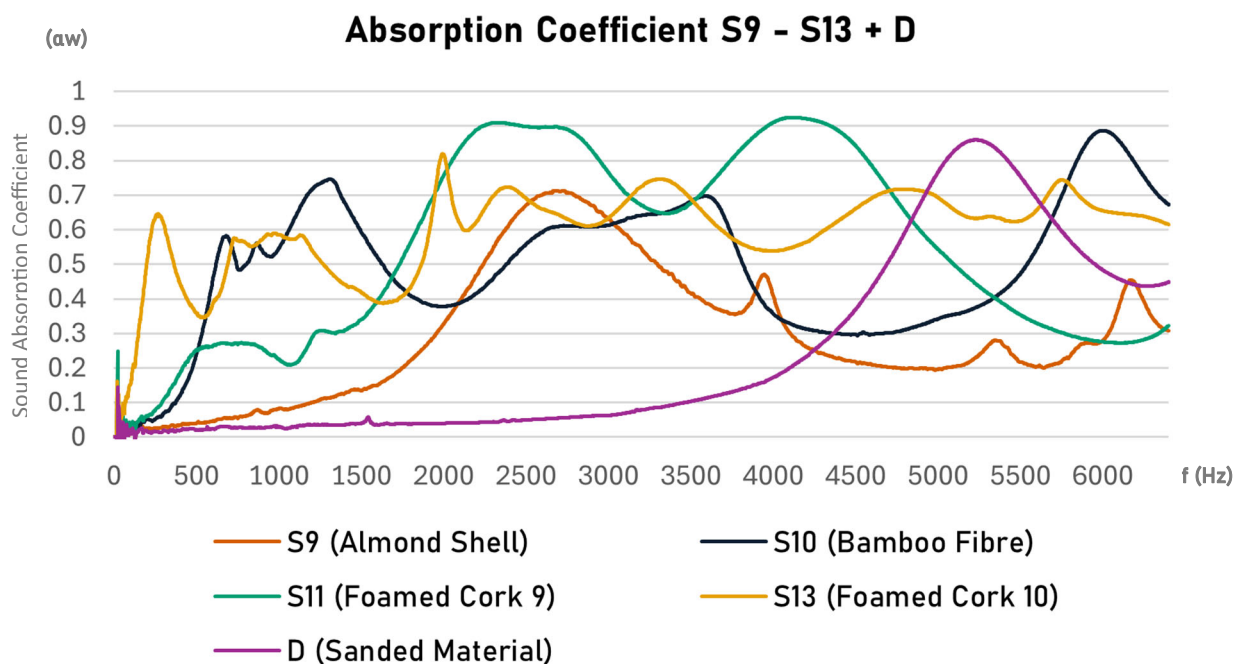


Figure 46: Impedance Tube test - Absorption Coefficient S9-S13 & Sanded Material full spectrum 0-6400 Hz (source: Author)



Figure 47: Sanded Cork Furan Material D (source: Author)

### 3.3.2.2 Mechanical Testing

At NPSP a 3-point bending test has been conducted to measure the effect of the porous fillers on the mechanical properties of the created materials. 6 porous filler-based materials have been tested on FS (flexural strength) and strain. Figure 48 illustrates the setup at NPSP. In figure 49, the effect of the cork filler on mechanical performance, is visible. Flexural strength decreases by 50% compared to conventional almond shell filler-based materials. Material B2 contains rubber granulate (180 mu) and almond shell. Flexural strength decreases from 70 MPa to 35 MPa on average. If a perforated biocomposite sheet is cork filler-based (and sandblasted), for high frequency and low frequency sound absorption, this decrease in mechanical performance should be considered. Specific values are elaborated in table 25 in the appendix.

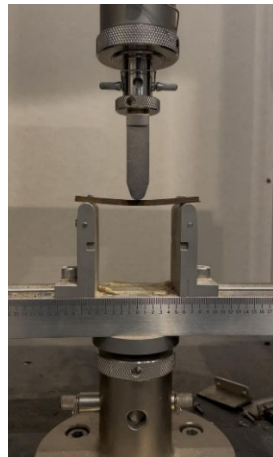


Figure 48: **B3** Cork & Bio-Polyester 3-point bending test (source: Author)

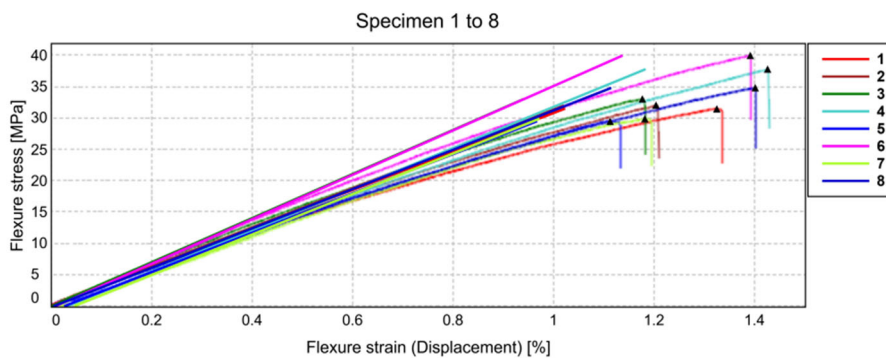


Figure 49: **B3** (Cork filler-based material) (source: Author)

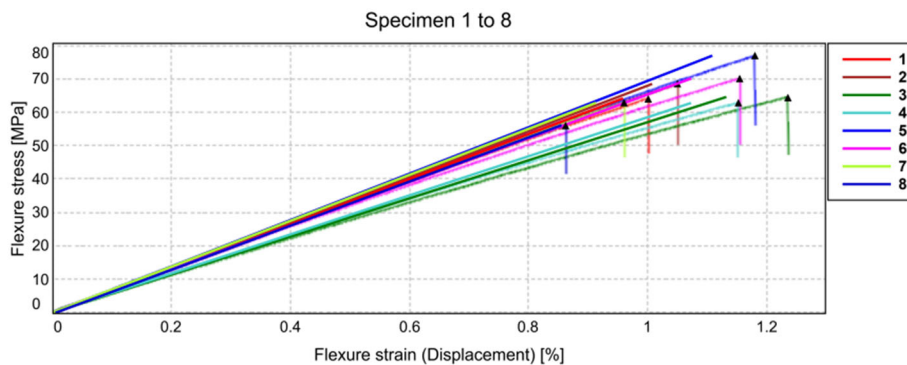
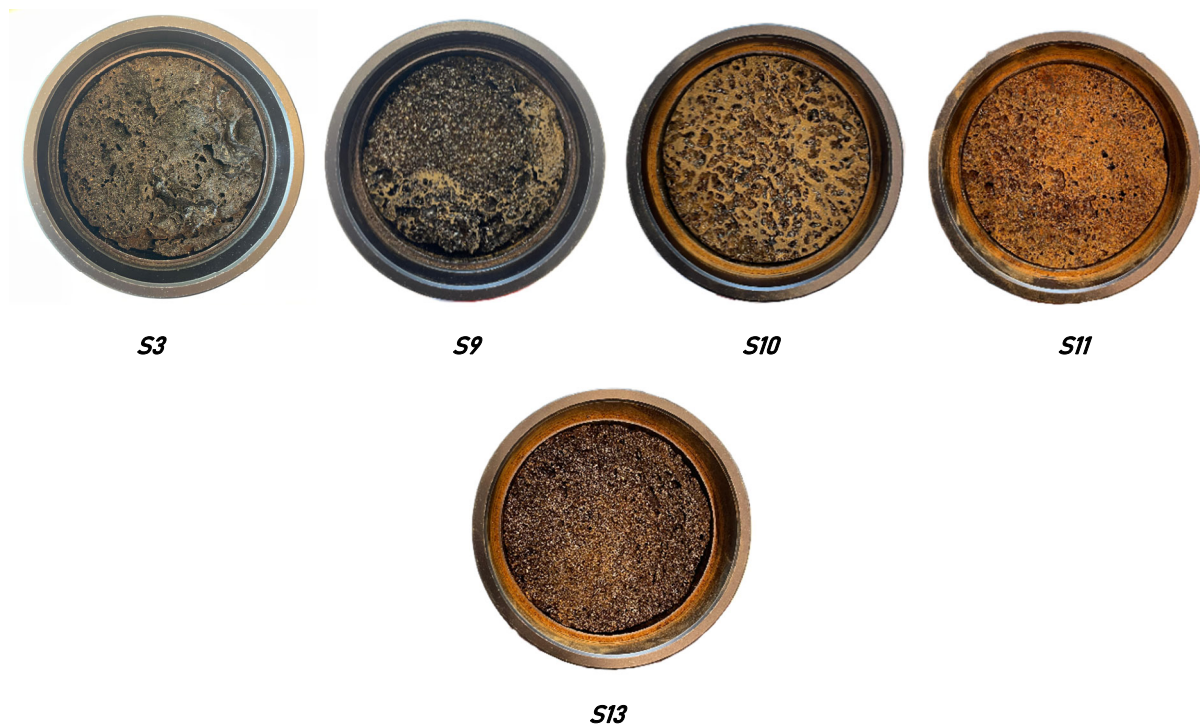


Figure 50: **B2** (Cork filler-based material) (source: Author)

### 3.3.3 Foamed Materials

One established method to absorb sound, is to make sure the noise waves created in urban environments can penetrate the absorbing material. Different pore sizes provide sound waves to penetrate the material and dissipate. Soundwaves are transferred into heat. This process is further improved by the flow resistivity and interpore connections.

As stated in the literature in previous sections, the foaming procedure of materials, is usually done by a heating process where gasses are released. These gasses are e.g. H<sub>2</sub>O or CO<sub>2</sub>. The overview of the best performing porous materials for sound absorption between 400 and 2500 Hz is illustrated in figure 50.



*Figure 51: Overview of the best performing foamed materials (S3, S9, S10, S11 & S13) (source: Author)*

Material S3 (Foamed Cork 3), has an absorption coefficient of above 0.8 from 1450 Hz onwards. The absorption is illustrated in figure 52. The sample is 15 mm thick. Generally, a thicker, porous material leads to lower frequency absorption. A 30 mm thick or 45 mm thick foamed furan resin-based material with the same material specifications as S3 would be a promising discovery.

Material S5 (Foamed Cork 5), demonstrates the potential foamed furfuryl alcohol-based materials can have for sound absorption. The absorption curve is illustrated in figure 53. Maximum absorption is achieved around 4400 Hz and remains significant for higher frequencies.

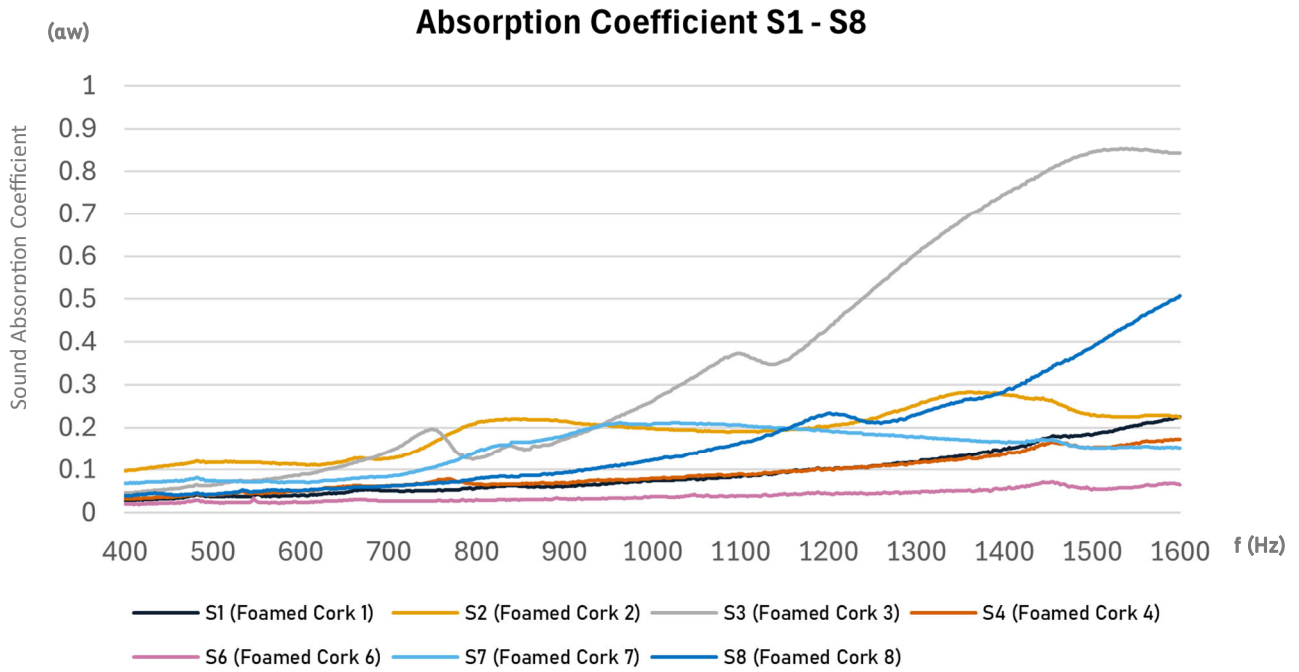


Figure 52: Impedance Tube test – Absorption Coefficient **S1-S8 Large Samples (100 mm)** (source: Author)

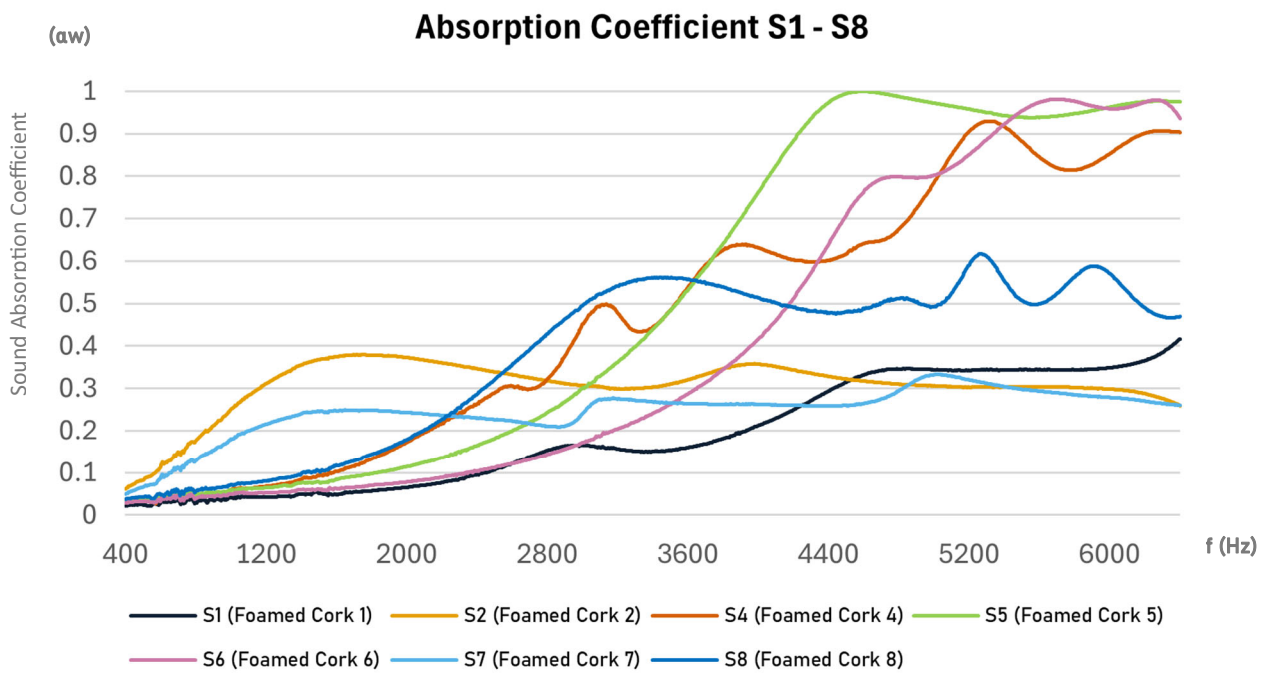


Figure 53: Impedance Tube test – Absorption Coefficient **S1-S8 Small Samples (29 mm)** (source: Author)

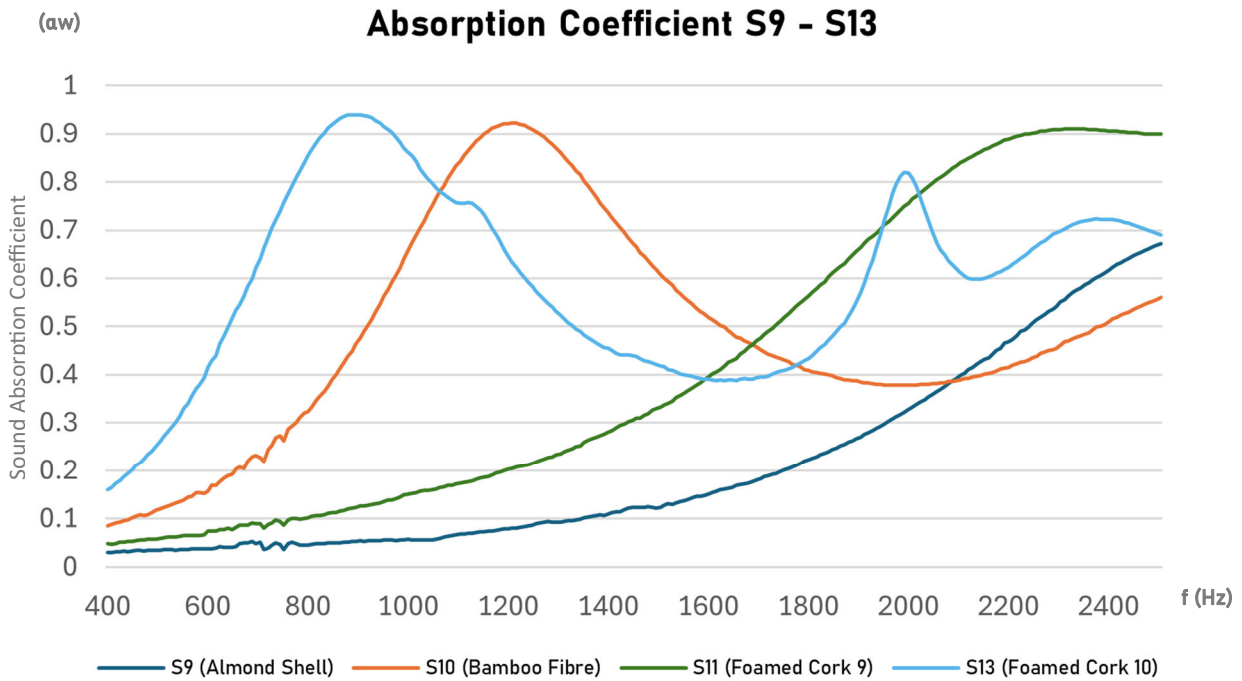


Figure 54: Impedance Tube test – Absorption Coefficient **S9-S13** (source: Author)

Figure 54 demonstrates the absorption curves of the created S9, S10, S11 & S13 materials. Comparison between the created materials can be done using the NRC,  $\alpha_w$  and surface area under the sound absorption coefficient graph. For the following comparison, the surface under the graph for the specific frequency range has been taken. For the comparison between the materials, samples S9 to S13 are compared as they have the most promising sound absorption based on the visual result from the graphs.

Table 9: Comparison for the materials S9-S13 on Sound Absorption:

Material	Surface Area under SAC curve ( $\alpha \cdot \text{Hz}$ )	NRC (500, 1000 & 2000 Hz)
S9	432	0.15
S10	1018	0.40
S11	872	0.30
S13	1243	0.65

Table 9: S9-S13 (source: Author)

Material S13 performs best for the total sound absorption. However, this material is 70 mm thick. A good choice would be to move forward with S10 (Bamboo Fibre), as this material is stronger due to the bamboo fibres and has a promising sound absorption. The SAC of S10 demonstrates a steep curve. Ensuring multiple sized pores would enlarge this graph and the SAC band width.

### 3.3.3.2 Digital Microscope Imaging

Comparison between the best performing materials is assessed on their pore dimensions using the digital microscope at BK. The following sub chapter demonstrates differences in pore dimensions for the most promising materials based on sound absorption.

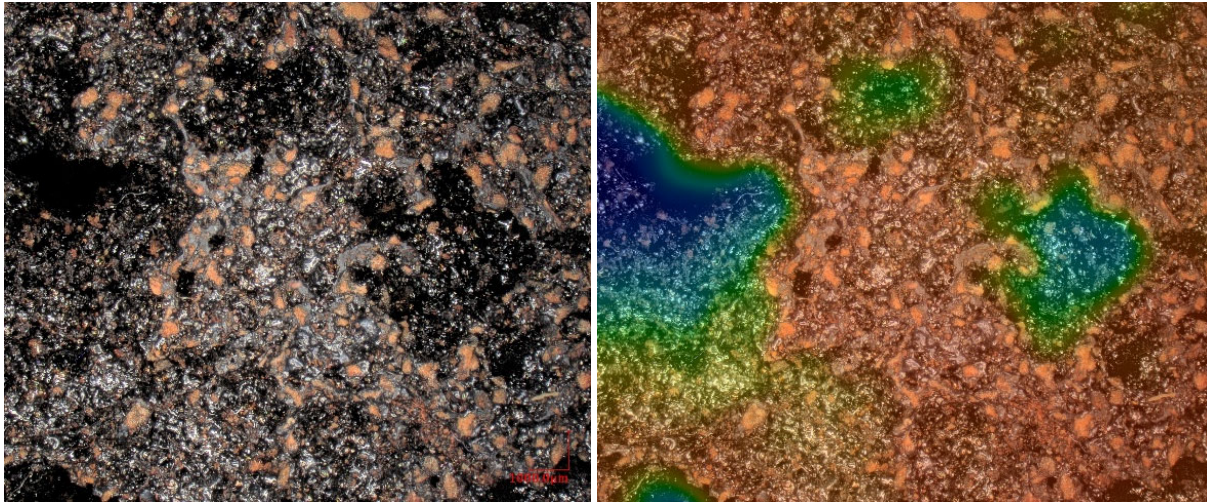


Figure 55: **S3** Porosity Assessment (source: Author)    Figure 56: **S3** Depth Assessment Colour (source: Author)

Figure 55 illustrates a close-up image of the cork granulate exposed to the exterior in the S3 (Foamed Cork 3) material. On the right image (figure 56), the depth is assessed for this frame.

Figure 57 demonstrates a close-up of S10. More even pores are visible compared to S3.

Figure 59 demonstrates a similar surface texture compared to S3 with less extremes.

Figures 61 and 62 illustrate a 3D analysis of the surface texture for optimal comparison. Pores on the surface of S11 are more extreme. Even if the pore size is more significant, acoustic performance of S13 is better. This is likely to the considerable difference in thickness (20 mm compared to 70 mm).

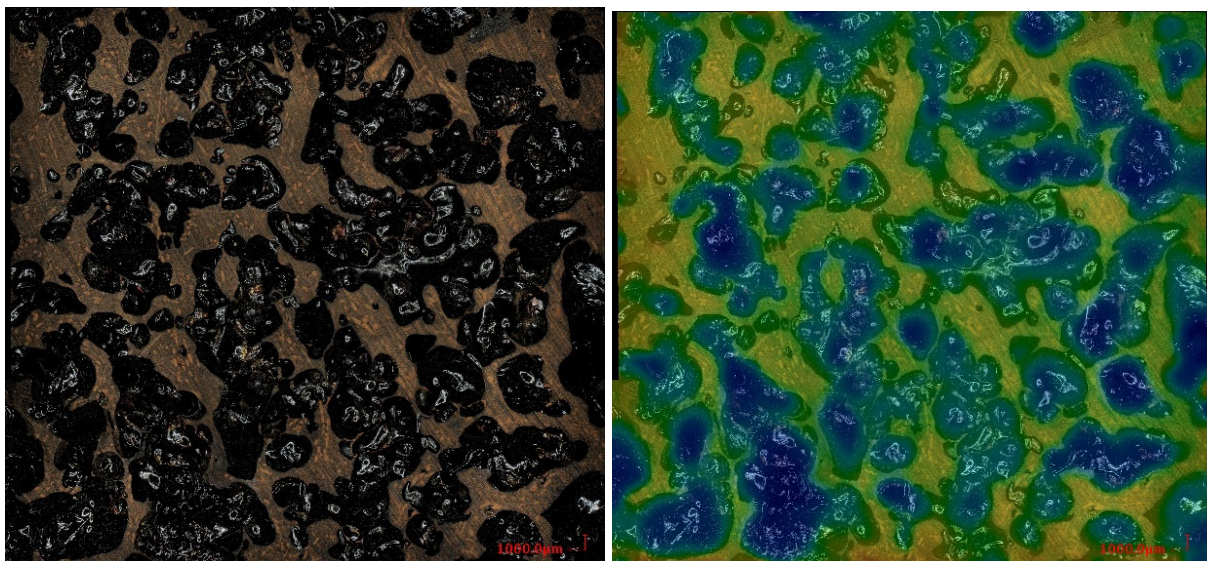


Figure 57: **S10** Porosity Assessment (source: Author)    Figure 58: **S10** Depth Assessment Colour (source: Author)



Figure 59: **S11** Porosity Assessment (source: Author)

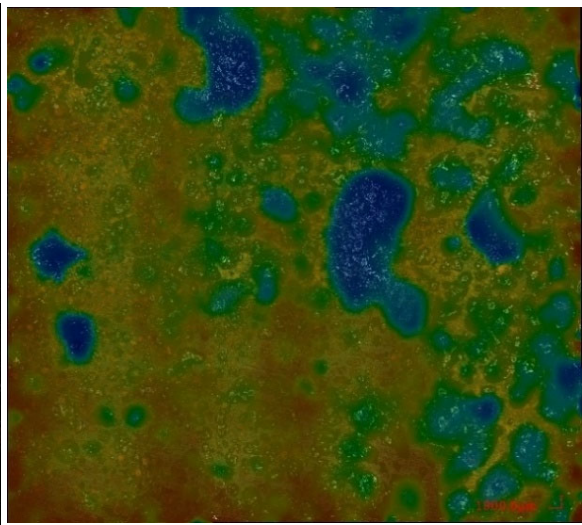


Figure 60: **S11** Depth Assessment Colour (source: Author)

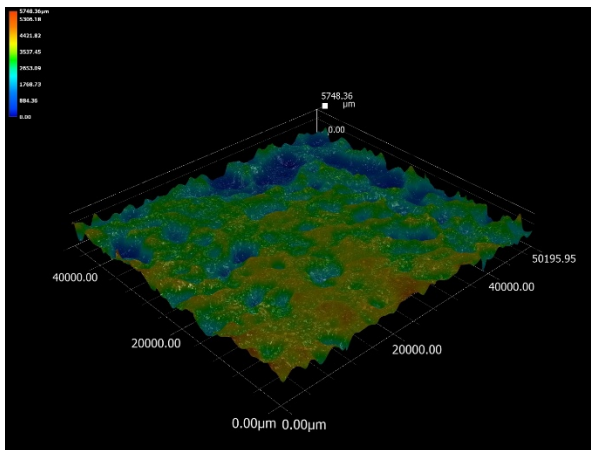


Figure 61: **S13** Depth Assessment 3D (source: Author)

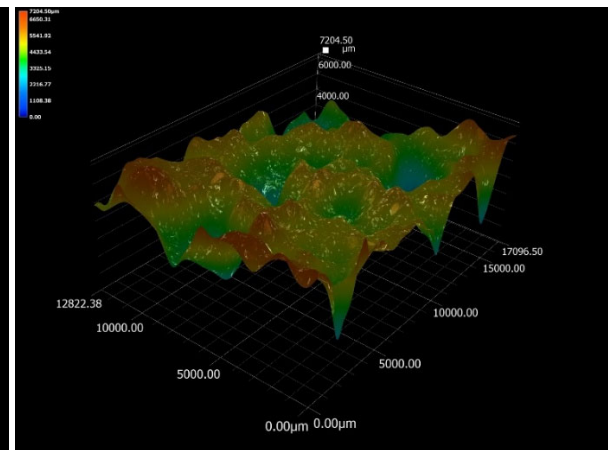


Figure 62: **S11** Depth Assessment 3D (source: Author)

### 3.3.3.3 Capillary Water Absorption

A capillary water absorption test has been conducted in the Heritage & Technology lab at BK. According to NEN EN 1925, specific water uptake intervals are conducted. Total testing time is 8h. The set-up is illustrated in figure 63 and 64.

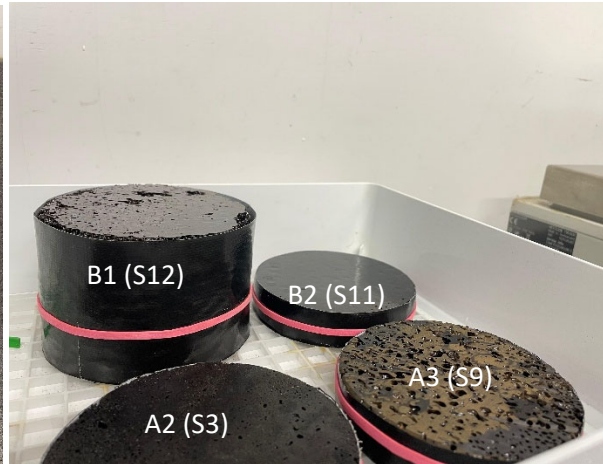
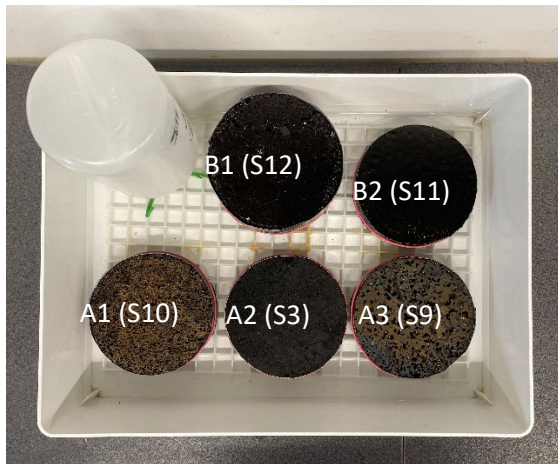


Figure 63: Capillary water absorption of 5 samples      Figure 64: Close-up of samples with tape wrapped around the materials (source: Author)

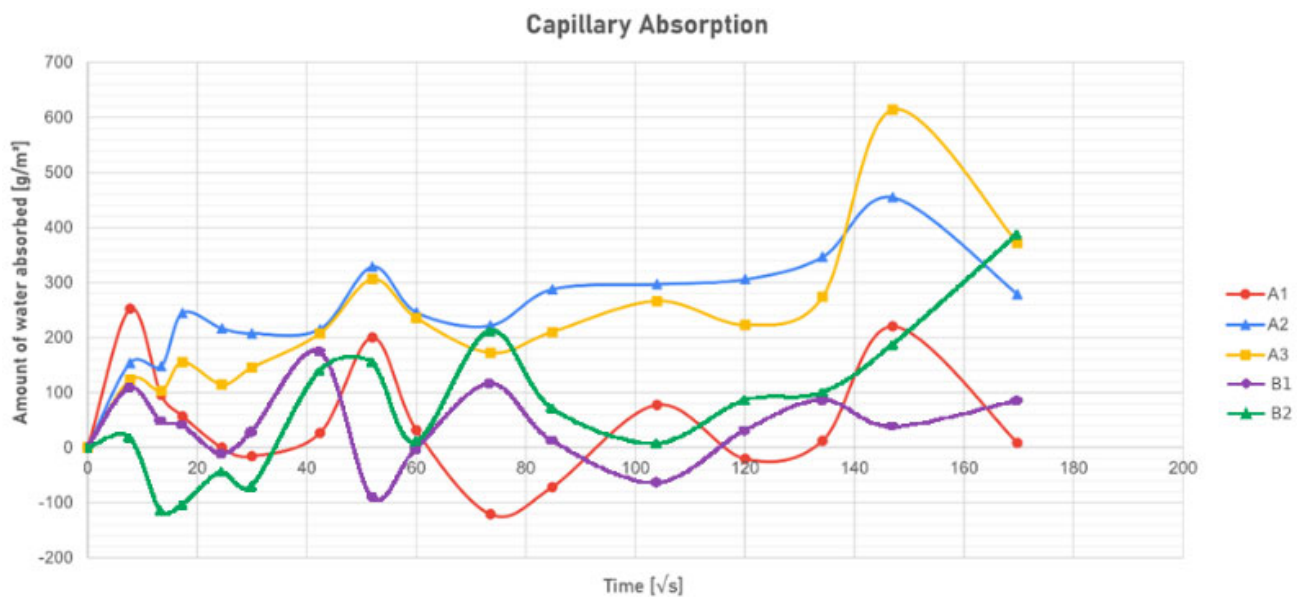
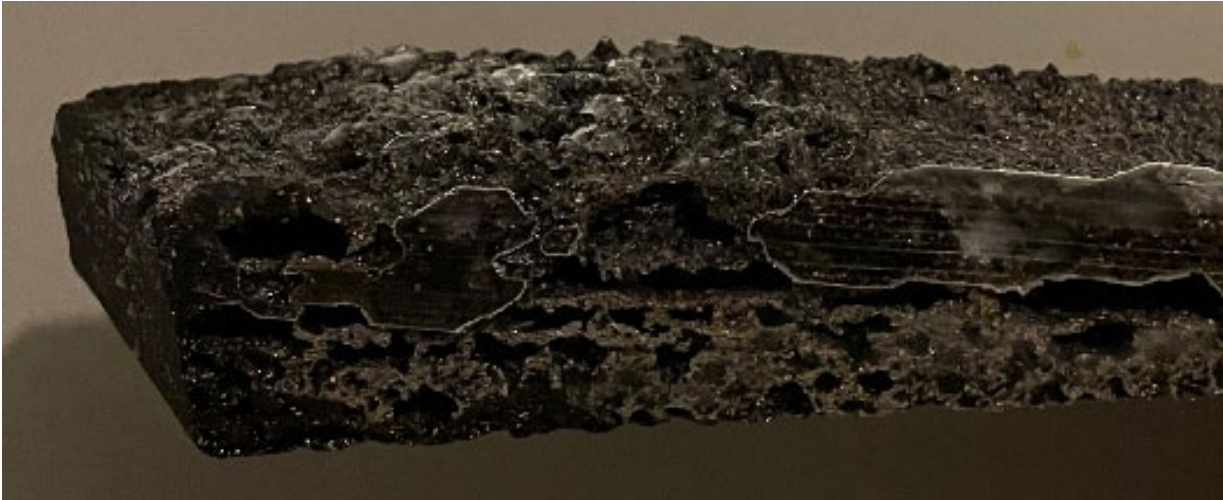


Figure 65: Amount of water (capillary) absorbed for each sample after 8h (A1=S10, A2=S3, A3=S9, B1=S12, B2=S11) (source: Author)

Total capillary absorption for all 5 materials is visible in figure 65. Common absorption patterns are a consistent increase and flattening of the curve after complete or near complete saturation of the material. This graph shows inconsistent increase in capillary absorption. A possible explanation for this phenomenon can be that the weighing scale cord attached to the device had contact with the table the scale was placed on. Therefore, drawing conclusions on the absorption over time is difficult. However, it can be concluded that furan resin does not absorb water in a significant pace. Even if the materials are porous, the surface texture and/or pore sizes are likely to prevent significant water uptake.

### 3.3.3.4 Freeze-Thaw

Material S11 has been saturated with water. A preliminary freeze thaw test demonstrates that porous, cork-based samples can withstand a freeze cycle of 24h under -21 centigrade. There were no cracks visible to the human eye. More elaborate freeze-thaw cycles should be conducted to draw complete conclusions on the performance of the created materials over time.



*Figure 66: Early-stage freeze-thaw assessment S11 (source: Author)*

### 3.3.4 Perforated Materials

This section of the report demonstrates the results for the perforated materials. As introduced in the State-of-the-Art overview, the Helmholtz resonance principle is applied. Different cavity configurations are visible in figure 67. Figure 68 provides an overview of the produced perforated materials. It is expected that a perforation rate of 20 percent should be optimal. This is confirmed by simulations using Acoustic Modelling and Whealy. These simulation tools are elaborated in section 3.4. Behind the perforated front sheet, reed of 100 mm is placed as the absorptive material.

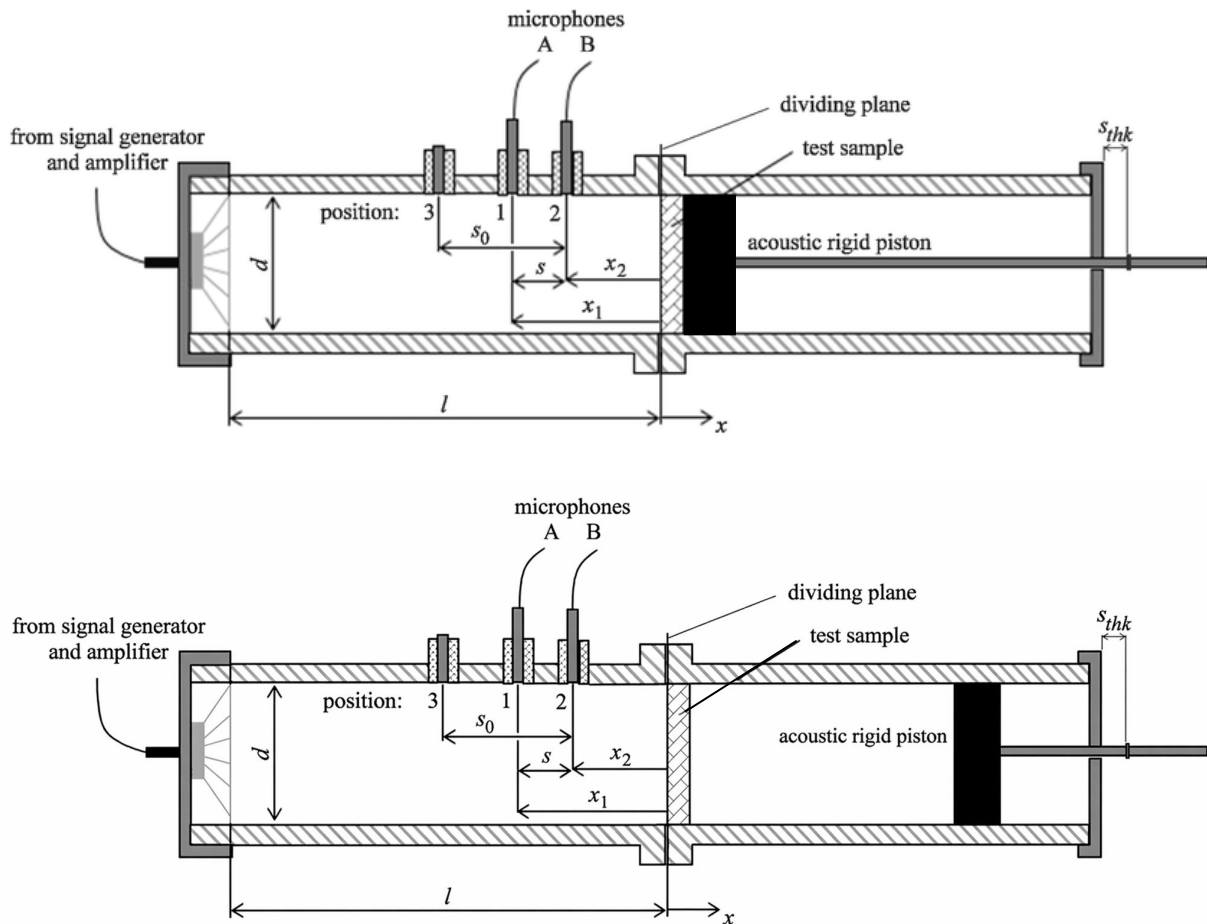


Figure 67: Impedance Tube with and without a cavity (source: Adjusted from Ďuriš & Labašová, 2021)

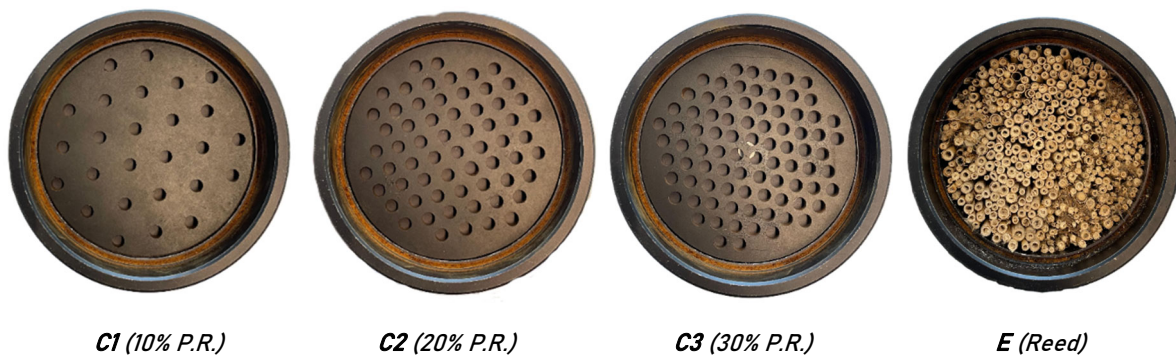


Figure 68: different perforated materials C1, C2, C3 & Reed

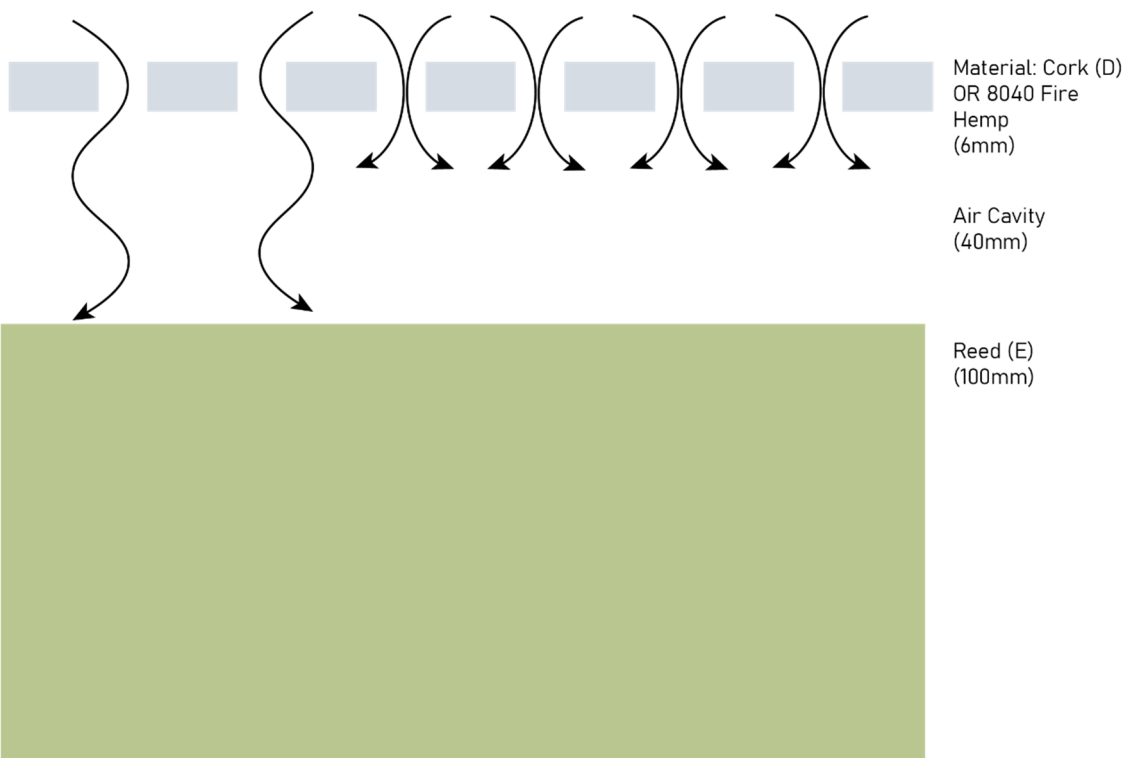
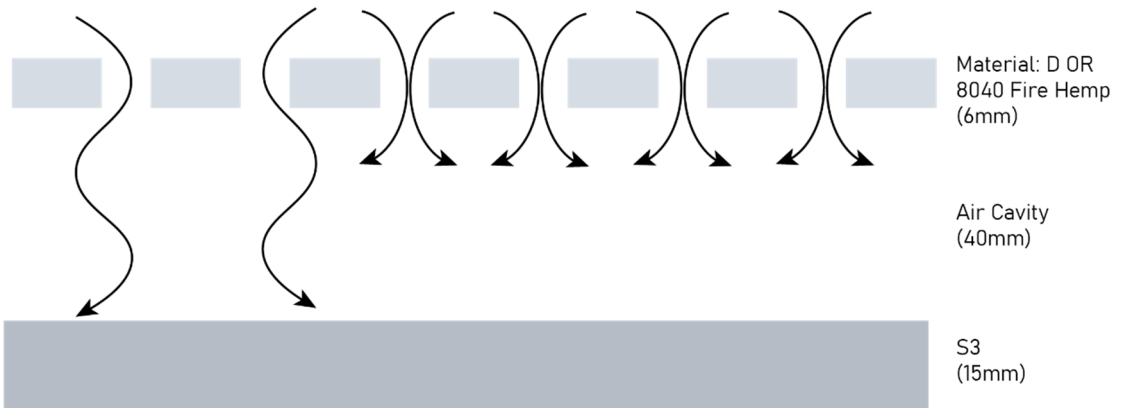


Figure 69: Illustration on different setups tested with the impedance tube. The behaviour of the soundwaves and Helmholtz resonance is visible (source: Author)

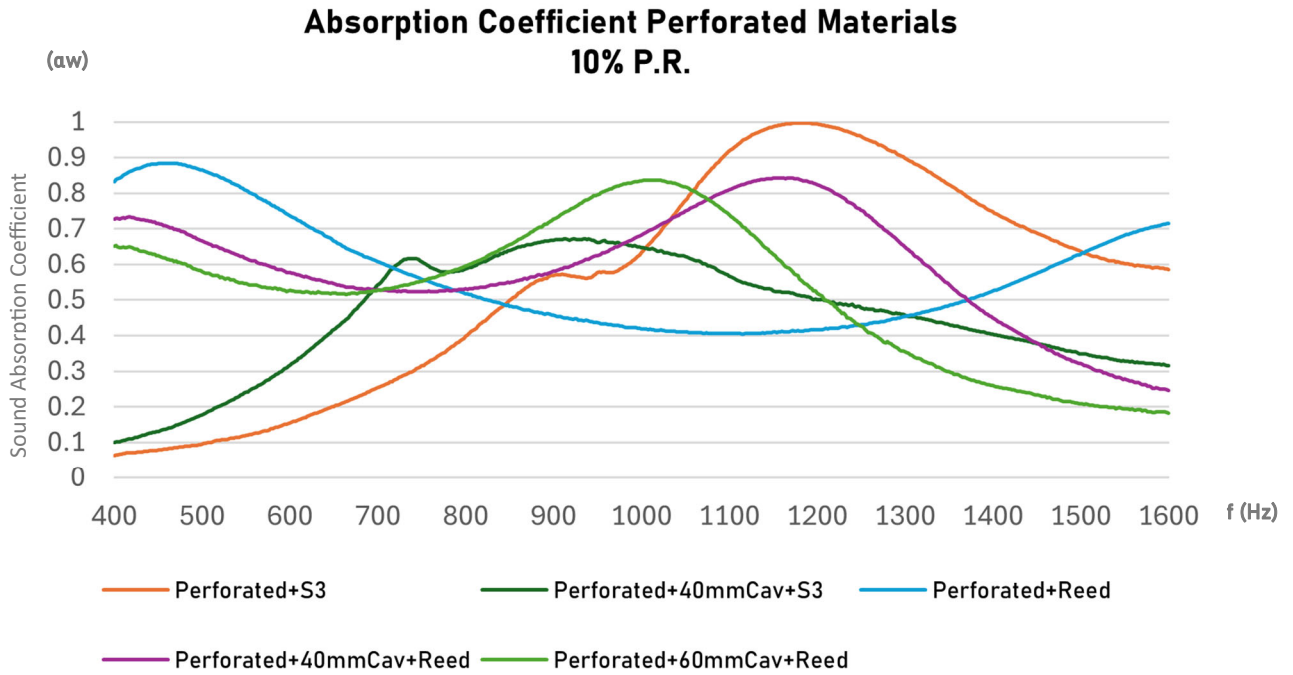


Figure 70: Impedance Tube Test Result: Sound Absorption Coefficient perforated samples 10% open area. (Cav stands for Cavity) (source: Author)

Figure 70 illustrates the absorption coefficient of the 10% open area 8040 Hemp Fire material. The following conclusions can be drawn:

- Adding reed leads to higher absorption, especially for lower frequencies
- Increase of the cavity from 40 to 60 mm has a negligible effect
- A cavity is needed to also absorb higher frequencies

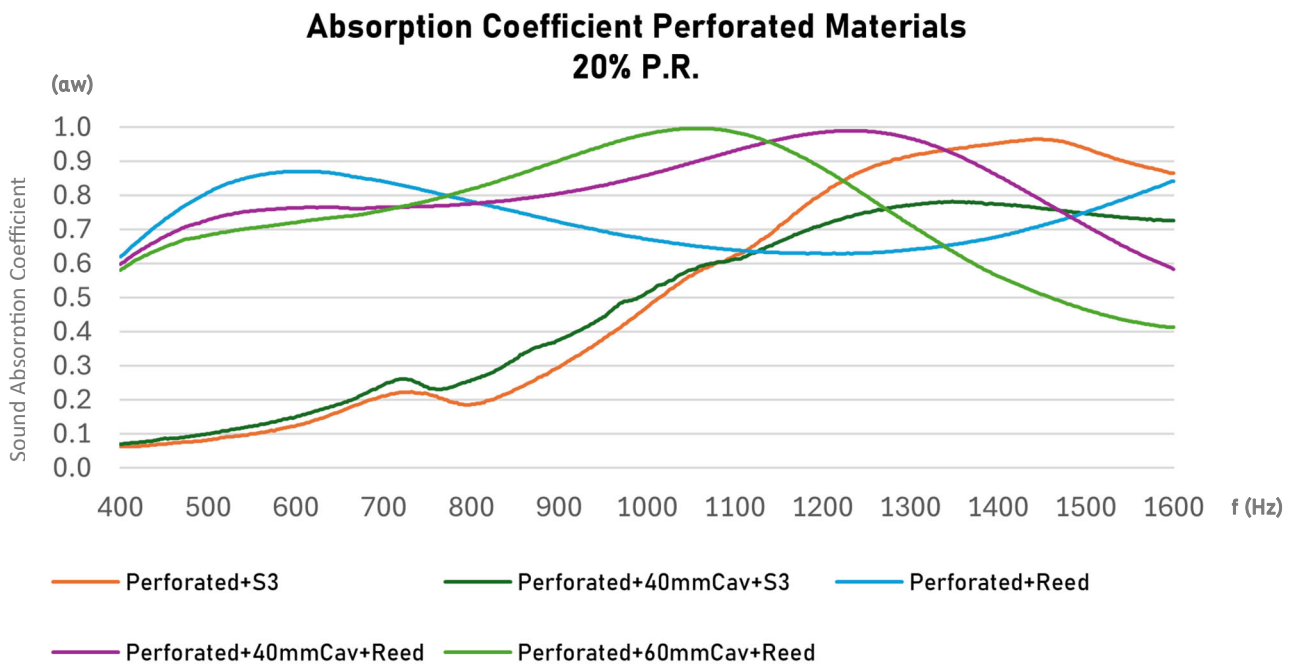


Figure 71: Impedance Tube Test Result: Sound Absorption Coefficient perforated samples 20% open area. (Cav stands for Cavity) (source: Author)

Figure 71 illustrates the absorption coefficient of the 20% open area 8040 Hemp Fire material. The following conclusions can be drawn:

- Reed absorbs well on lower frequencies
- S3 performs well for higher frequencies (with and without the perforated front sheet)
- A cavity has an impact on higher frequencies (a change from 40 to 60 mm has a small effect)

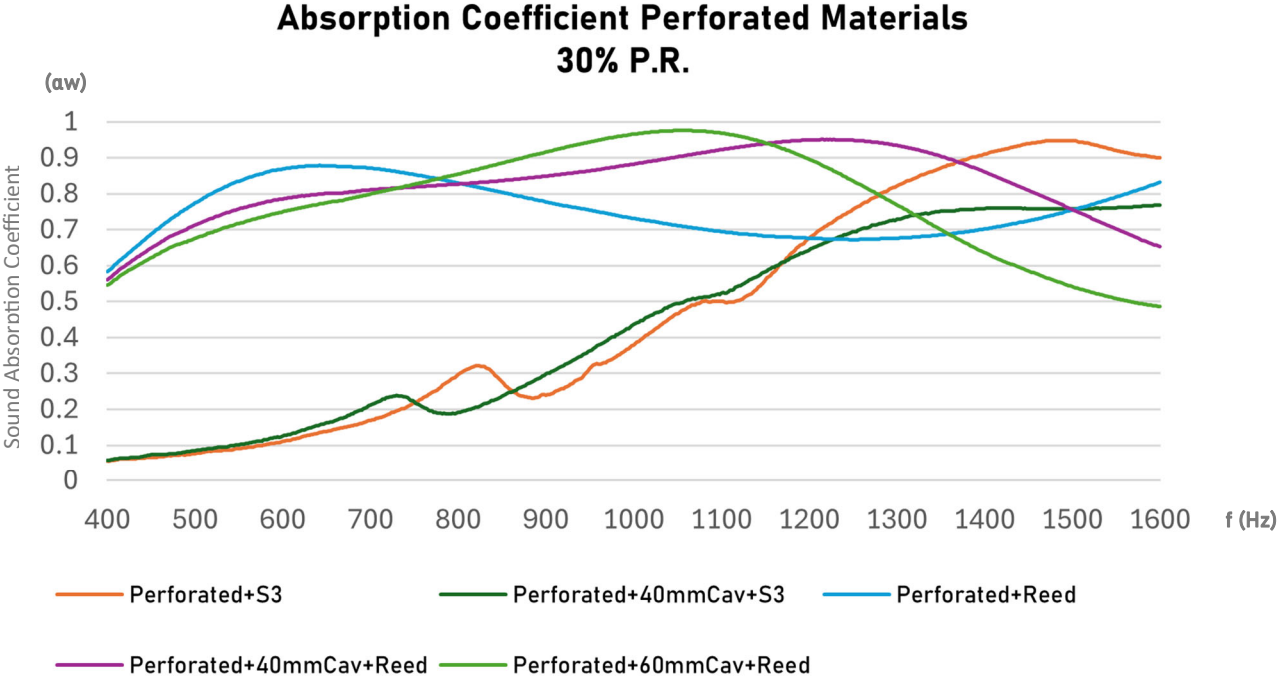


Figure 72: Impedance Tube Test Result: Sound Absorption Coefficient perforated samples 30% open area. (Cav stands for Cavity) (source: Author)

Figure 72 illustrates the absorption coefficient of the 30% open area 8040 Hemp Fire material. The following conclusions can be drawn:

- A cavity with a reed back structure does not influence the absorption much compared to a reed back structure without a cavity. Only from 850 Hz onwards a cavity has a positive effect
- A 40 mm cavity is better compared to 60 mm
- The S3 absorption curve is very similar with and without a cavity

### 3.3.4.2 Geometry Research

For an outdoor acoustic panel backed by an absorbing cavity and back structure, the perforated facing should be made of circular perforations. Circular perforations are structurally optimal as they transfer the loads optimally within the structure. Elongated slots, square openings or hexagonal patterns are more sensitive to thermal expansion and eventually cracks. Sharp corners tend to work as stress concentrators. Different perforation designs are illustrated in figure 73.

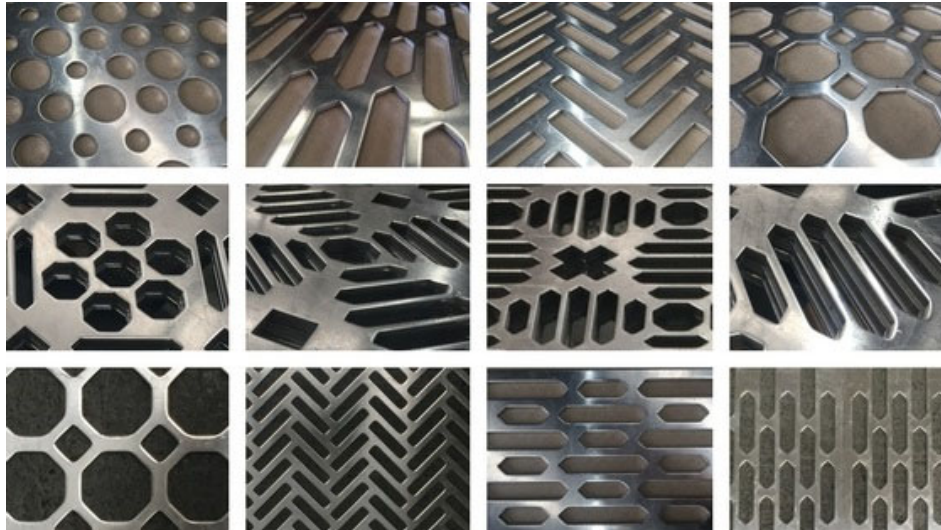


Figure 73: Different steel perforated geometries (source: Okhrimenko, 2022)



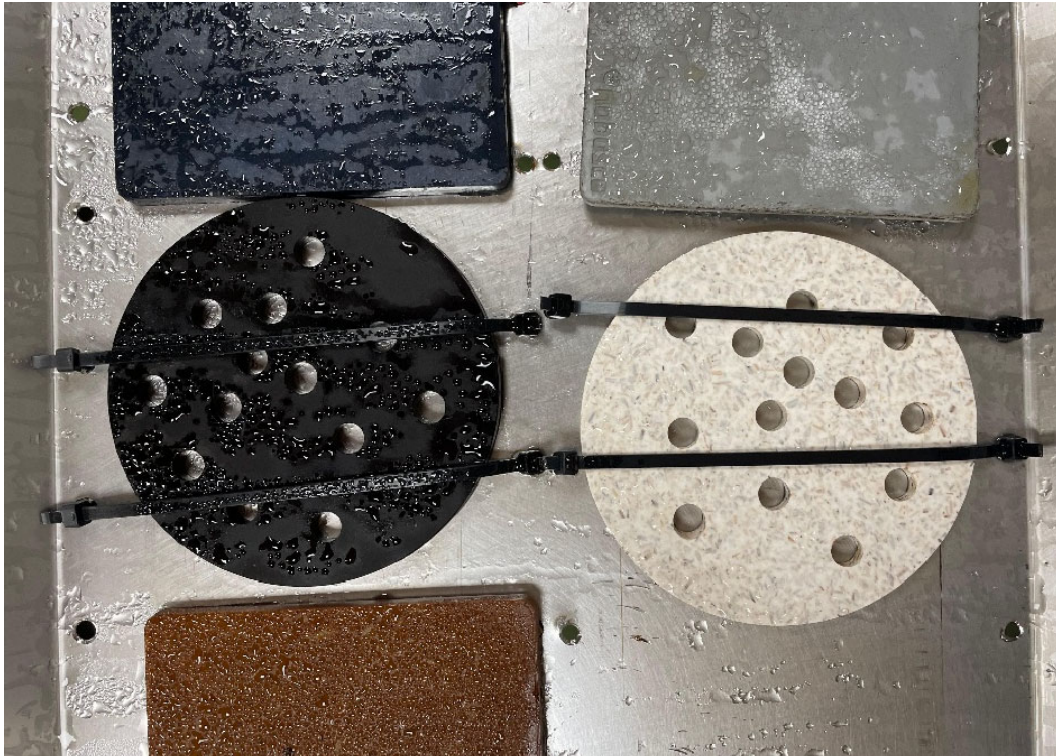
Figure 74: Different set-up configurations for the perforated external material (20%) and **S3** (left), 100mm **reed** (middle) & 100mm **mineral wool** (right) (source: Author)

Figure 74 demonstrates different set-up configurations for optimal sound absorption. The top sheet should have a perforation rate of 20% based on findings in this research. A cavity of 40 mm is optimal for sound absorption in the targeted frequency range, as concluded with impedance tube testing and acoustic simulations. Reed has the highest performance competing with conventional mineral wool. However, reed is combustible. Therefore, S3 could be a solution for buildings with higher fire safety standards such as high-rise buildings.

The performance of the complete system depends heavily on the backing absorber and cavity design. A hydrophobic or well-protected porous absorber should be used to prevent water saturation, since moisture can significantly reduce acoustic performance and accelerate deterioration. The assembly should include drainage and ventilation options, together with a protective veil, scrim, or fine mesh to limit fibre loss. This also improves insect ingress, and particulate contamination.

### 3.3.4.3 QUV-testing

QUV-testing is a worldwide testing method to assess the ageing of materials. By imitating weather cycles and UV exposure, samples can be tested on durability. Figure 75 illustrates two tested materials. These are 8040 Hemp Fire and 8012 Bio-polyester-based materials. A perforation rate of 14% is chosen for early-stage testing.



*Figure 75: Perforated Hemp Fire 8040 material (A2) & 8012 Bio-polyester (A1) QUV-testing (source: Author)*

The correlation between accelerated ageing by QUV exposure and actual outdoor ageing is not governed by a universal conversion factor. Depending on the polymer type, 1,000 hours of QUV exposure may correspond approximately to six months to two years of outdoor exposure. For conventional plastics, QUV testing is therefore most reliable as a comparative method: materials that perform better under accelerated ageing generally also show superior performance under outdoor conditions.

For biocomposites, however, this relationship is less straightforward. Their degradation involves additional mechanisms that are not fully represented in ASTM G154 Cycle 1, particularly water uptake, rain exposure, swelling, fibre-matrix interactions, and possible biological degradation. As a result, 1,000 hours of QUV exposure may represent only around three months of outdoor ageing for certain biocomposites. Moreover, the ranking of different biocomposite formulations under accelerated conditions may not necessarily match their ranking after real-world exposure, since the outcome depends strongly on the matrix, fibre type, additives, and environmental interactions.

Consequently, real-world ageing data remain essential for assessing long-term material performance. Accelerated QUV testing is valuable for identifying relative trends, but its predictive accuracy improves only after it has been calibrated against outdoor exposure results for the specific material system under investigation.

Within this research QUV testing has been conducted for 5 weeks. There was no significant damage to the samples visible. Neither on the surface, nor in the perforated areas. Figure 75 illustrates 4 weeklong rain cycles and UV exposure.

### 3.4 Simulations Acoustic Modelling

Acoustic simulations can be conducted on different websites. Within this research, Whealy (Porous Absorber Calculator, n.d.), and Acoustic Modelling (*Helmholtz Calculator*, n.d.-c) are applied to predict and compare results with real-world impedance tube testing. The parameters used for these simulations are illustrated in table 10. Table 11 uses a Flow Resistivity of 40,000 rays/m which is derived from advice from M. Tenpierik. The airgap parameter is changed for different simulations.

Simulations conducted with Whealy:

Table 10: Perforated Panel Properties:

Perforated Panel	Panel Thickness (mm)	Holes Centred Every (mm)	Hole Radius (mm)	Porosity
Values:	6	9 (3+6+3)	6	0.785

Table 10: Perforated panel (source: Porous Absorber Calculator, n.d.-b)

Table 11: Absorber Properties:

Perforated Panel	Absorber Flow Resistivity (rays/m)	Absorber Thickness (mm)	Air Gap (=cavity) (mm)
Values:	40,000 <sup>a</sup>	20	60

Table 11: a: flow resistivity taken on 40,000 with M. Tenpierik (source: Porous Absorber Calculator, n.d.-b)

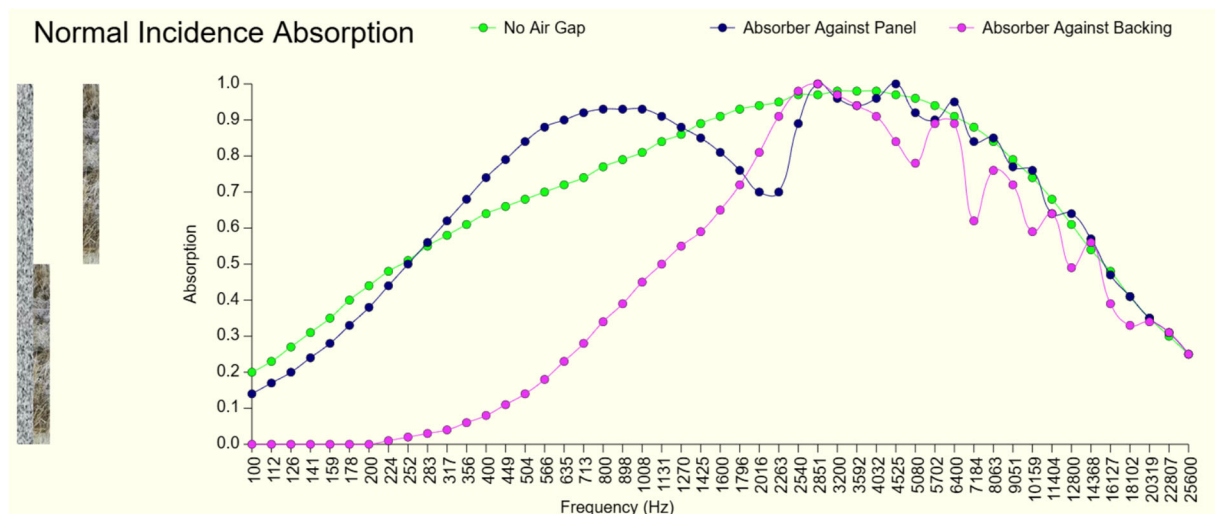


Figure 76: Simulation of the expected sound absorption curve on whole octave subdivisions based on the values in table 10 and table 11 (source: Porous Absorber Calculator, n.d.-b)

Table 12: Absorber Properties:

Perforated Panel	Absorber Flow Resistivity (rays/m)	Absorber Thickness (mm)	Air Gap (=cavity) (mm)
Values:	40,000 <sup>a</sup>	20	40

Table 12: a: flow resistivity taken on 40,000 with M. Tenpierik (source: Porous Absorber Calculator, n.d.-b)

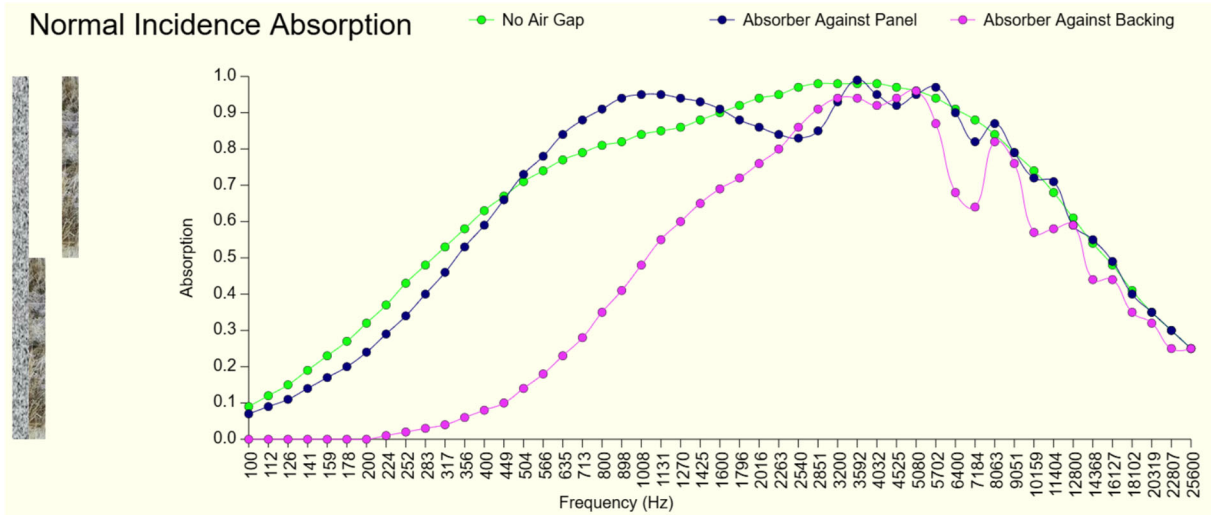


Figure 77: Simulation of the expected sound absorption curve on whole octave subdivisions based on the values in table 10 and table 12 (source: Porous Absorber Calculator, n.d.-b)

Table 13: Absorber Properties:

Perforated Panel	Absorber Flow Resistivity (rays/m)	Absorber Thickness (mm)	Air Gap (=cavity) (mm)
Values:	40,000 <sup>a</sup>	100	40

Table 13: a: flow resistivity taken on 40,000 with M. Tenpierik (source: Porous Absorber Calculator, n.d.-b)

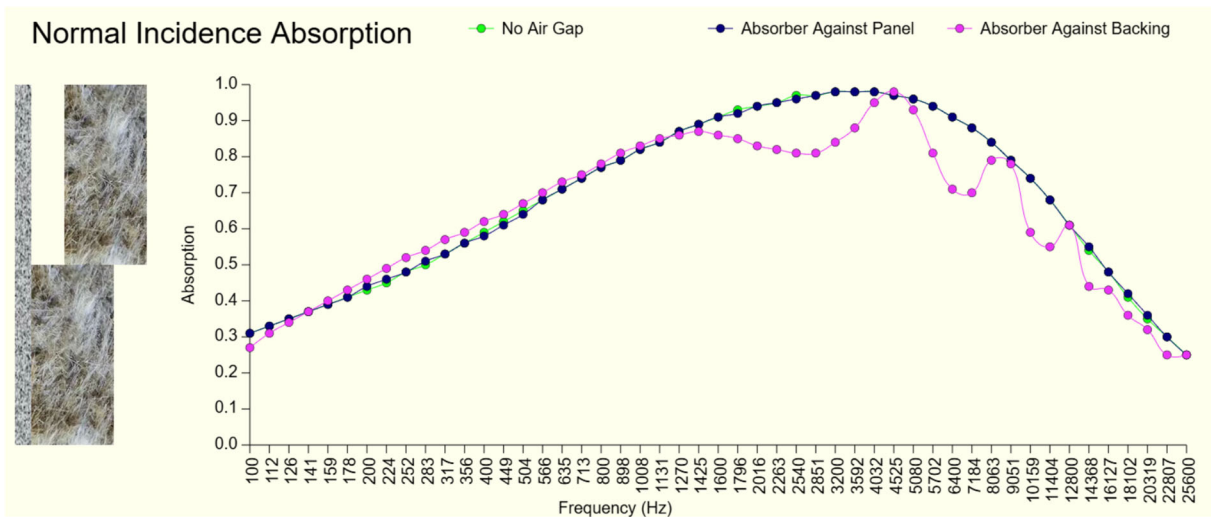


Figure 78: Simulation of the expected sound absorption curve on whole octave subdivisions based on the values in table 10 and table 13 (source: Porous Absorber Calculator, n.d.-b)

### Conclusions Whealy:

One key conclusion which comes forward from comparing the graphs is that a thicker absorptive layer decreases the difference in sound absorption between the configuration where the absorptive layer is placed right behind the perforated sheet or against the back layer. Data from the KU Leuven (appendix) confirms this negligible difference.

A cavity of 60 mm compared to 40 mm, result in a small change in sound absorption. Increasing the thickness of the absorbing layer has a significant impact.

The absorbing layer against the perforated sheet seems better compared to placement against the back structure.

Figures 76 and 77 confirm the data retrieved from the impedance tube testing.

### Simulations conducted with Acoustic Modelling:

Table 14: Perforated Panel Properties:

Perforated Panel	Panel Thickness (mm)	Holes Centred Every (mm)	Hole Radius (mm)
Values:	6	9 (3+6+3)	6

Table 14: Perforated panel (source: Helmholtz Calculator, n.d.-c)

Table 15: Absorber Properties:

Perforated Panel	Absorber Flow Resistivity (rayls/m)	Absorber Thickness (mm)	Air Gap (=cavity) (mm)
Values:	40,000 <sup>a</sup>	20	60

Table 15: a: flow resistivity taken on 40,000 with M. Tenpierik (source: Helmholtz Calculator, n.d.-c)

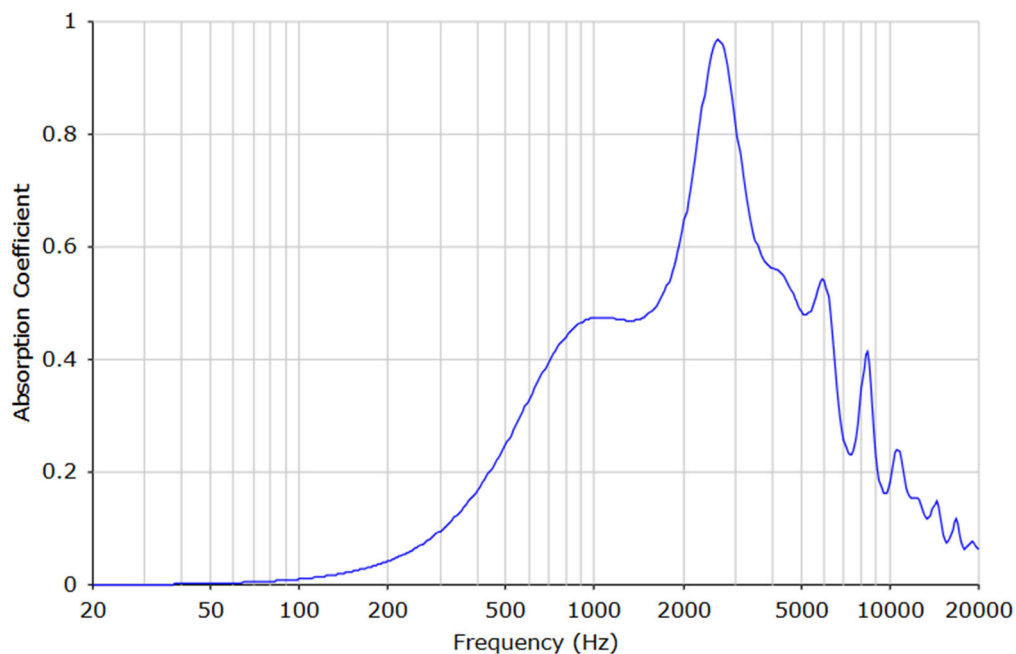


Figure 79: Absorption Coefficient simulation Acoustic Modelling using Table 14 and 15 (source: Helmholtz Calculator, n.d.-c)

Table 16: Absorber Properties:

Perforated Panel	Absorber Flow Resistivity (rayls/m)	Absorber Thickness (mm)	Air Gap (=cavity) (mm)
Values:	40,000 <sup>a</sup>	20	40

Table 16: a: flow resistivity taken on 40,000 with M. Tenpierik (source: Helmholtz Calculator, n.d.-c)

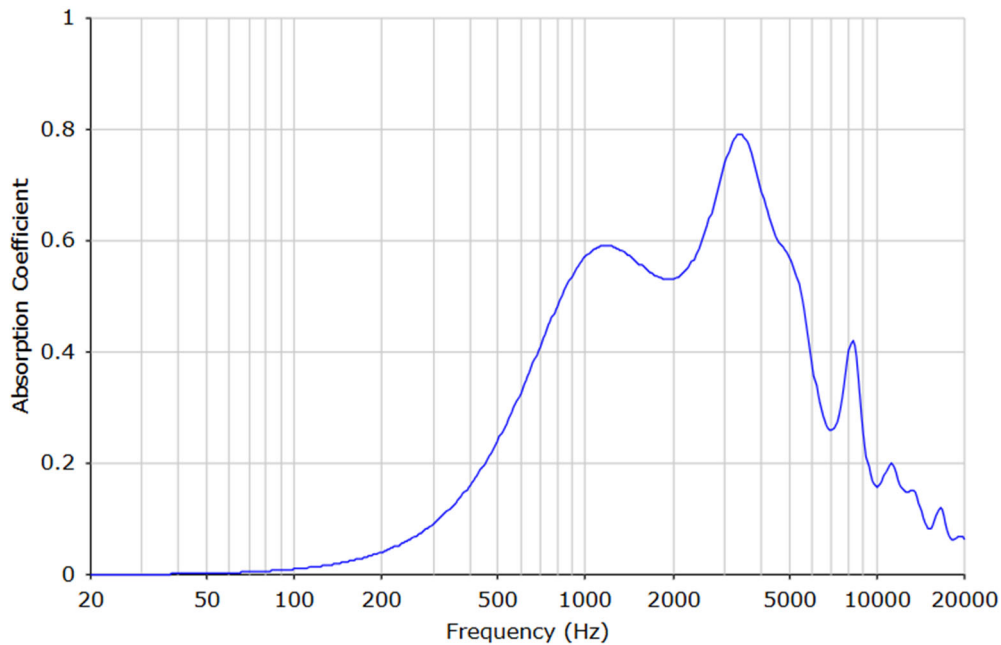


Figure 80: Absorption Coefficient simulation Acoustic Modelling using Table 14 and 15 (source: Helmholtz Calculator, n.d.-c)

#### Conclusions Acoustic Modelling:

It can be concluded from figures 79 and 80 that a cavity for sound absorption on frequencies around 500-1000 Hz, is beneficial for sound absorption. The absorption peak, however, is smaller with a cavity of 40 mm compared to 60 mm and is placed around 3000 Hz.

The simulations are limited by a general absorptive material. This is purely an indication what cavity dimensions and absorber thicknesses can achieve when optimally designed.

*The simulation from Acoustic Modelling is based on the work of Trevor J. Cox and Peter D'Antonio (2009) from Acoustic Absorbers and Diffusers: Theory, design and application, 2<sup>nd</sup> Edition and work from J. F. Allard and N. Atallia (2009).*

### 3.5 Discussion

The findings of the impedance tube testing are elaborated further in this section.

The impedance tube testing confirms that increase in thickness has a large effect on sound absorption. Thinner samples mainly absorb higher frequencies. Thicker, porous materials provide better absorption for lower frequencies. This confirms why S13 (Foamed Cork 10), has the highest overall absorption.

S3 (Foamed Cork 3), showed promising acoustic behaviour despite its limited thickness of 15 mm. Its performance suggests that the material has a suitable porous structure. Low frequency absorption remains a challenge. However, increase of the material thickness to 30 or 45 mm would have a significant increase in sound absorption. S5 also confirmed the potential of foamed furfuryl alcohol-based materials, showing strong absorption at higher frequencies. With a maximum around 4400 Hz.

The perforation rate strongly influences the absorption curve. With a perforation rate of 20-30% being the optimal perforation, while still ensuring mechanical strength of the sheet.

The perforation rate, cavity depth, and backing absorber all contribute to the final acoustic response. The cavity improved absorption in certain frequency ranges. However, an increase of the cavity from 40 mm to 60 mm, produced limited additional benefit based on real-world impedance tube testing. A cavity of 40 mm is most efficient and cost effective. The simulation of Whealy in figure 77 indicates that an absorber behind the facing sheet has better sound absorption compared to placing the layer to the back structure. To ensure nature inclusivity, and based on real-world testing, a cavity of 40 mm is selected.

Reed performed very well acoustically, especially at lower frequencies and can compete with conventional absorbers.

Nevertheless, S3 remains a relevant alternative. In locations where fire safety is important, foamed furan-based materials could be an alternative as they are less combustible compared to reed. Highrise buildings could be an example where foamed biobased materials are relevant and a thick façade with a reed backing structure, is not.

#### Key takeaway:

The results show that acoustic performance depends on the complete system rather than the absorber alone. The advised direction is to combine a perforated front sheet with an open-area of 20%, a 40 mm cavity, and a thicker version of a promising foamed furan resin-based absorber such as S3.

An aerial, black and white photograph of a multi-lane highway. The highway is filled with cars and trucks, moving away from the viewer. On the left side, there are several tall, multi-story apartment buildings with many windows. The highway is flanked by dense trees and greenery. In the foreground, there is a pedestrian bridge or overpass with a person walking across it. The overall scene is a busy urban highway environment.

04

CASE STUDY

## 4.1 Introduction

Within this research, the Amsterdam A10 highway is taken as a case study. This highway is known for its environmental noise stress. As stated in the introduction of this research by Park & Lee, et al. (2010), the A10 highway is a main source of environmental noise pollution. Neighbourhoods like Surinameplein, Overtoomse Veld or parts of the Zuidas experience regularly SPL (Sound Pressure Levels) of over 70 dB, which is above the legal limit. This is especially the case since a part of the A10 noise barriers was removed due to storm caused damage (*Parool*, 2023). The Zuidas has recent plans (since 2016), to install more sound barrier systems (Zuidasdok & Zuidasdok, 2026).

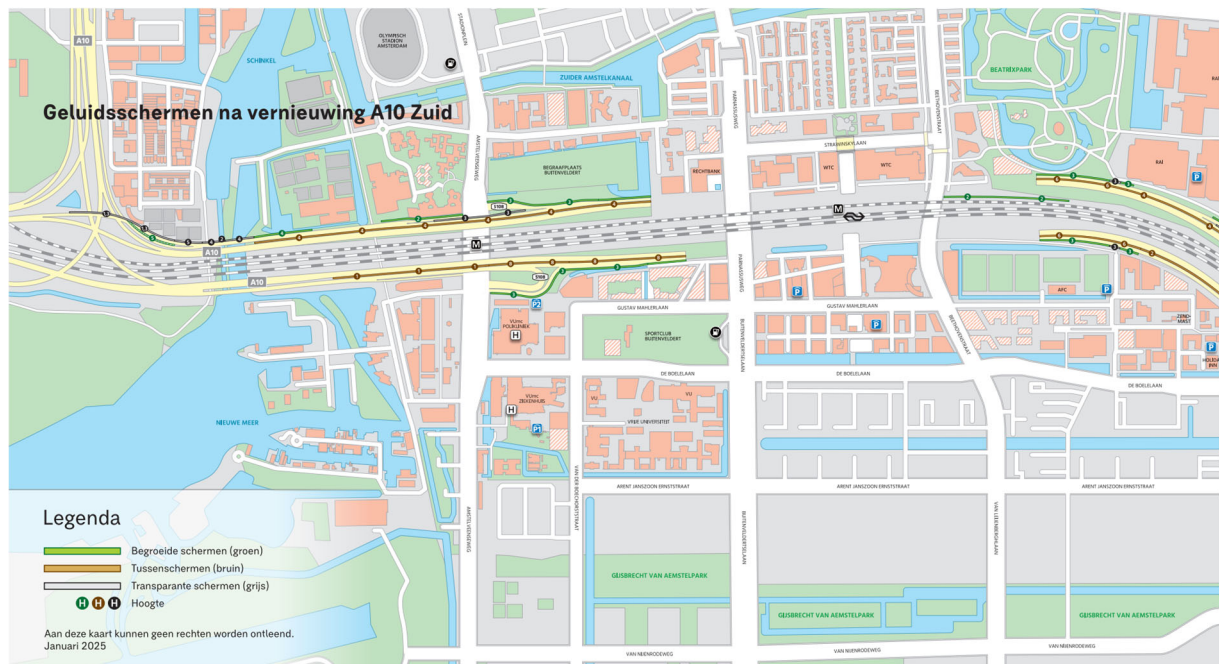


Figure 81: Noise barrier system installation locations A10 Zuidas (source: Zuidasdok & Zuidasdok, 2026)

In this part of the report, the optimal geometry and allocation of the absorptive versus reflective panels is explored. Grasshopper Aeolus allows for visualisations on the sound direction and behaviour for different geometries. The focus is on the sound barrier design. To be able to translate this to product level development. It is important to find the optimal geometry, which includes the noise norms and available budget, following statements from Hans de Haan (sound advisor expert) (Zuidasdok & Zuidasdok, 2026).

## 4.2 Acoustic Analysis of Existing Situation

The specifically chosen site for the acoustic macro scale modelling, is the Surinameplein in Amsterdam West on both sides of the A10 highway. See figure 82 for an impression of this location. This location has a slightly lower noise pollution quantity, but as there are more houses and people living in this area, it is the most important location to consider.

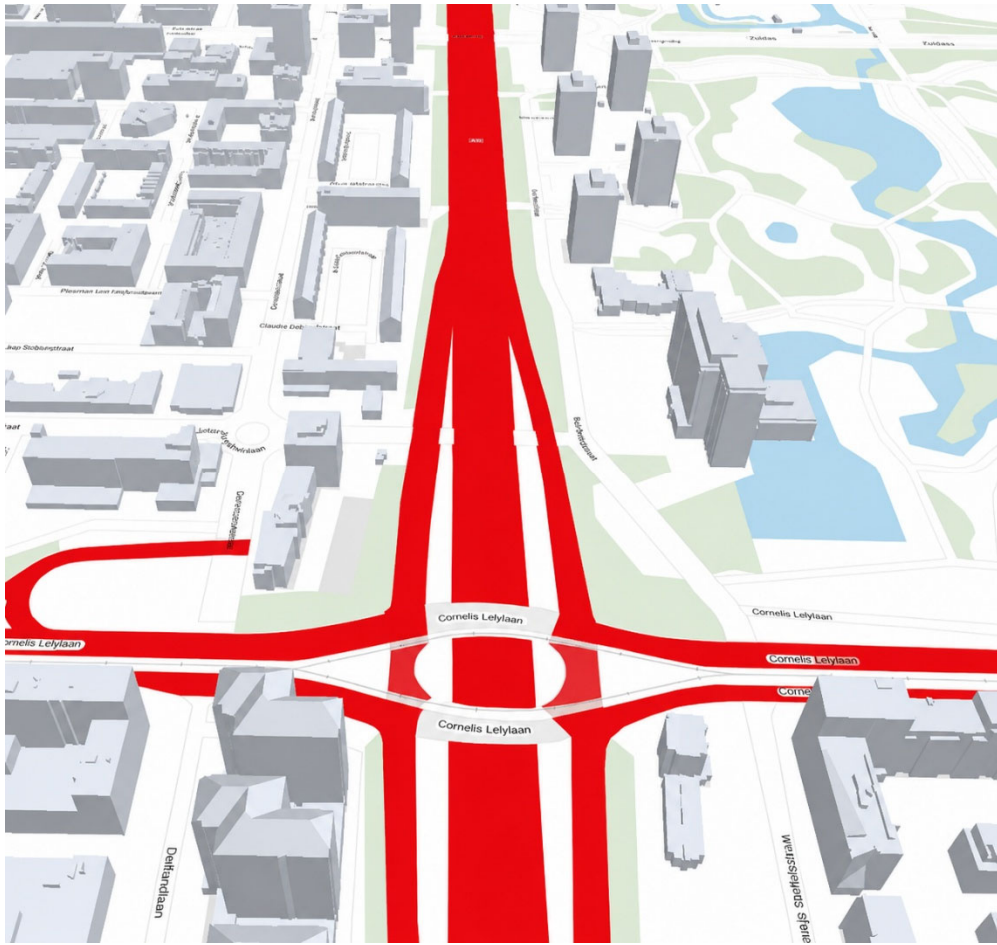


Figure 82: A10 highway Amsterdam West Surinameplein (source: 3DBAG Viewer, n.d.)

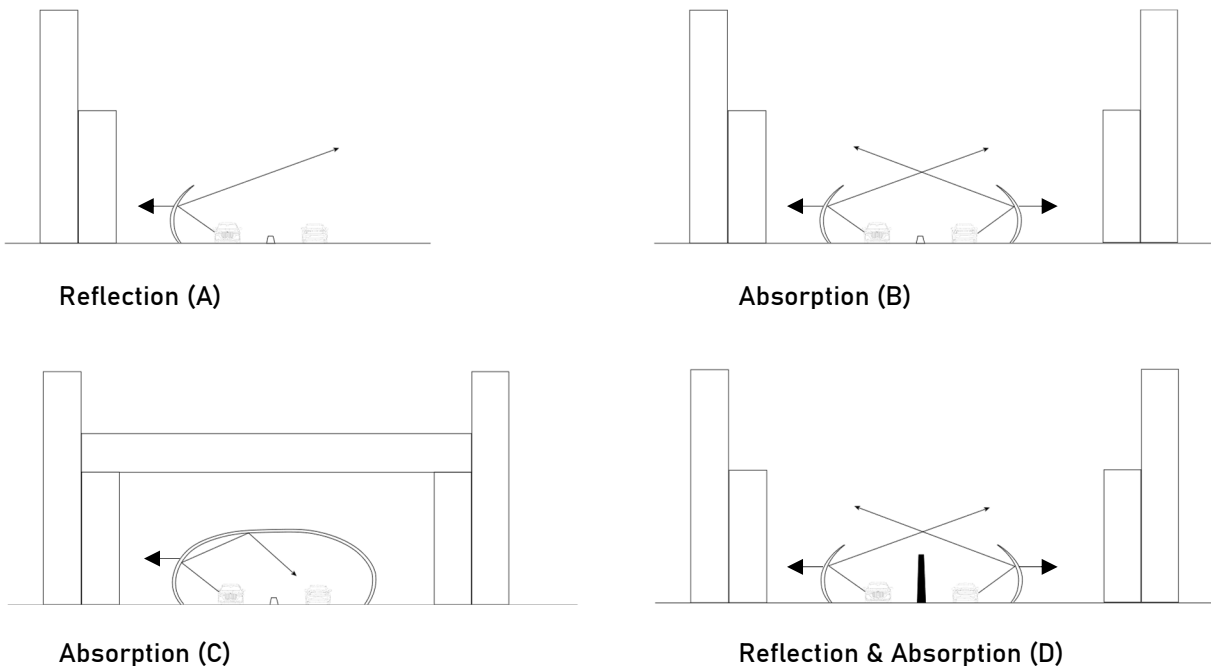


Figure 83: Urban situation diagrams (source: Author)

## 4.3 Parametric Model with Shape Variations

This section elaborates on design exploration on the total design of the product. A step-by-step introduction on how the model is made, is illustrated underneath. Figures 84 and 85 illustrate the urban situation with the parametric model. The first step in simulations is to set a performance indicator.

A performance indicator, often called a KPI (Key Performance Indicator), is a quantifiable measurement used to evaluate success in achieving specific objectives. It turns broad strategic goals into concrete numbers to assess the result. In this part, maximising SPL exposure on specific internal areas on the target surface is the aim. As a balance for absorptive and reflective panels could be found by proceeding with this method.

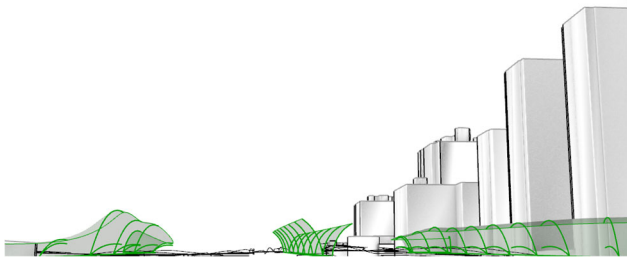


Figure 84: An impression of acoustic barriers on the chosen location (source: own)

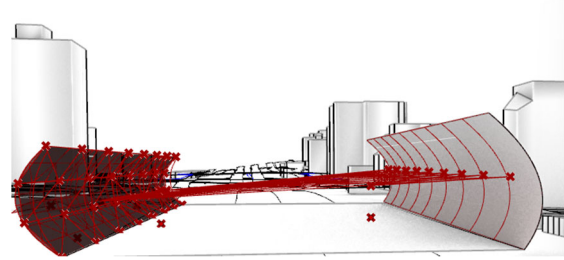


Figure 85: Close-up impression of reflecting sound in the parametric model (source: Author)

### 1. The first step is to setup an acoustic scene:

- The reflector surfaces are chosen. These will reflect sound to the receiver points. These are seen as people driving their car on the highway at Surinameplein. Two sound sources are chosen, representing two lanes of traffic.
- A duplication factor can enhance the number of cells (UV)
- The sound sources are referenced (order is important -> list will order these depending on that)
- Create a surface using plane surface
- Construct a domain (square e.g.)
- Set the domain
- Now that the first steps are done, place a geometric container
- Reference the geometry for the reflecting surface
- The next step is to define the sounds source object
- SD and ROT data define the sound source type
- In this situation, omnidirectional sound source can be selected
- Specific octave bands can be selected

### 2. The second step is acoustic analysis:

- Analysis components like direct sound and image source, are used
- The image source component will be populated with data
- Only one or two values are sufficient for the acoustic reflector assessment as most sound is dispersed in the first 100 milliseconds

### 3. SPLs visualisation

- The sound pressure levels can be visualised with Pathmapper, SPL sum, selection of the limit values and ultimately by connecting the geometry.

Figure 86 illustrates how the sound reflections are working in the urban scene. Two sound sources are chosen. These represent traffic, e.g. cars, in the chosen Surinameplein area of Amsterdam.

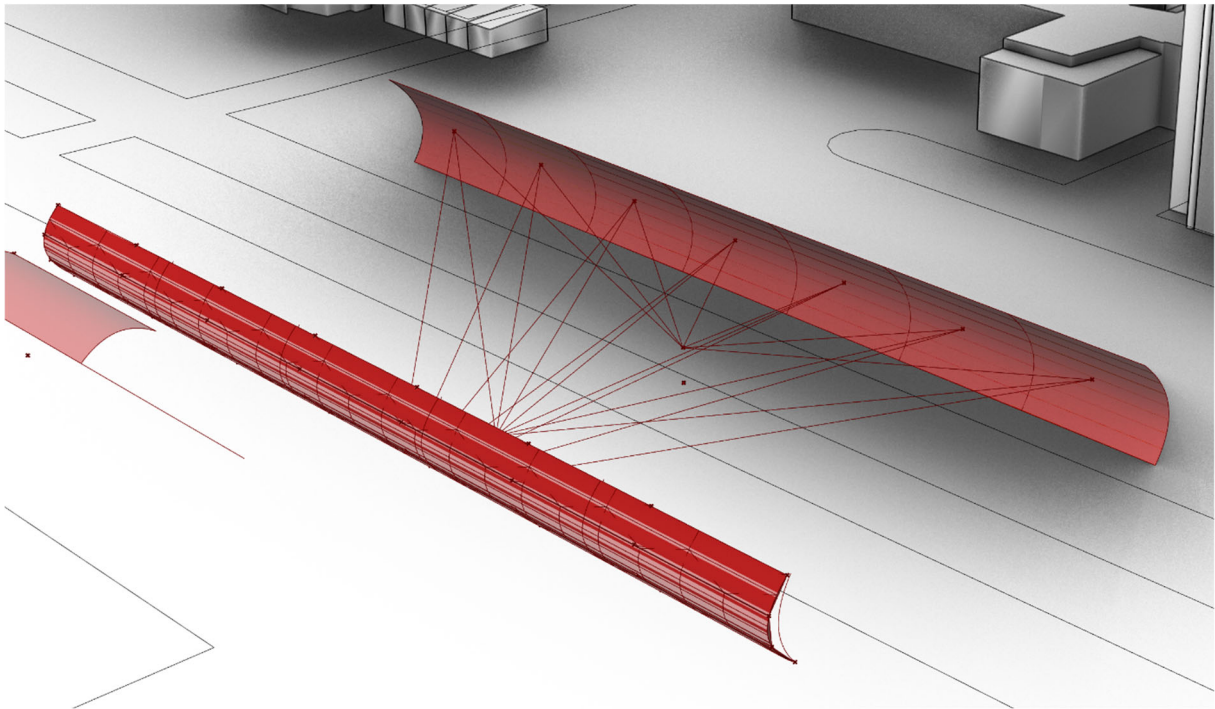


Figure 86: An impression of the sound reflections on the two chosen traffic lanes (source: Author)

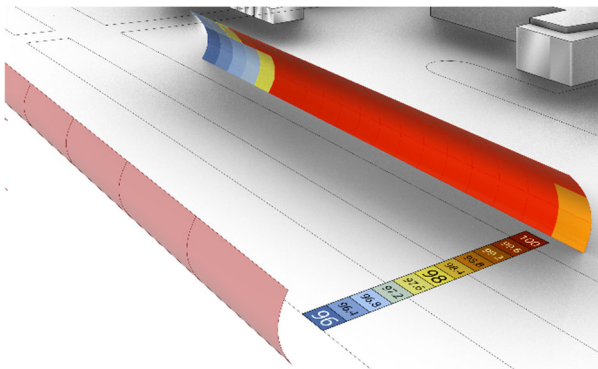


Figure 87: The evaluation of the SPL on the target surface (source: Author)

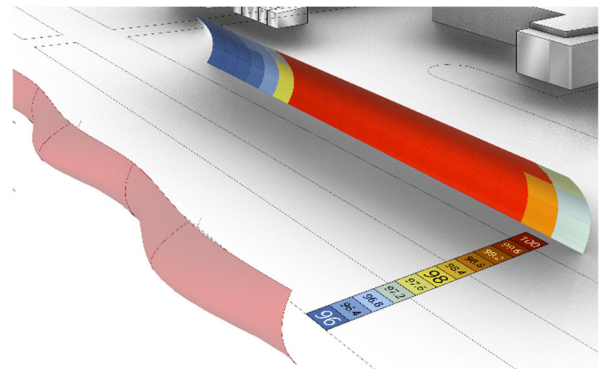


Figure 88: The evaluation of the SPL on the target surface (source: Author)

Figures 87 and 88 illustrate how shape variation influence the retrieved reflection on the target surface.

The Standard Deviation component can be recalled evaluating the SPL sum into a Quick Graph. Visualisation of the SPLs is necessary for thorough comparison. With a simple table, the numerical differences can be compared. It can be concluded that the double curved design variation, visible in figure 88, shows more extremes in SPL distribution on the targeted surface on the right.

Further steps would be to evaluate which areas show significant increase in exposed SPLs and which areas have less total exposure. Based on this distribution, reflective and absorptive panel placement can be designed. This ensures an economically optimal solution, as perforated or porous absorptive materials for outer façade systems, are usually more expensive. These arguments also apply to the prototype developed in this research.

## 4.4 Optimisation & Validation

There are multiple optimisation strategies and tools. In this section, the optimisation targets and the Galapagos tool are elaborated.

Preliminary optimisation does not require a large amount of reflection orders. However, in outdoor conditions two reflection orders should be taken as a minimum (*Acoustic Analysis - DigiPedia, 2025*).

The workflow for this research is illustrated in figure 89. First, the case study location is defined. Then performance is evaluated. Later, a sensitivity analysis should be conducted and ultimately, optimisation.

For the optimisation, the performance indicator of maximisation of sound in specific locations is chosen. As explanation in the previous section.

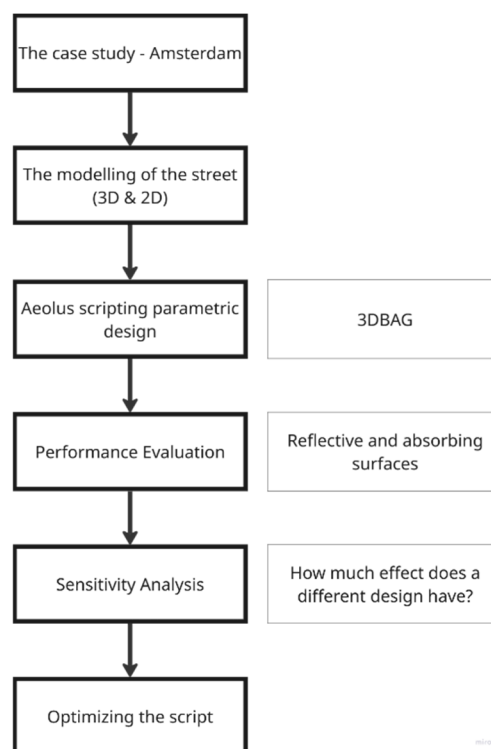


Figure 89: Workflow diagram digital simulation (source: Author)

### Galapagos optimisation

Identifying and maximizing local sound pressure level concentrations is the objective for the optimisation. Full optimisation has not been conducted in this research, however, based on the reflection paths of the sound waves, it can be concluded that some areas show higher concentrations of sound influenced by the surface on the left (in figure 90 and 91). In section 4.5, more elaboration on the design has been given.

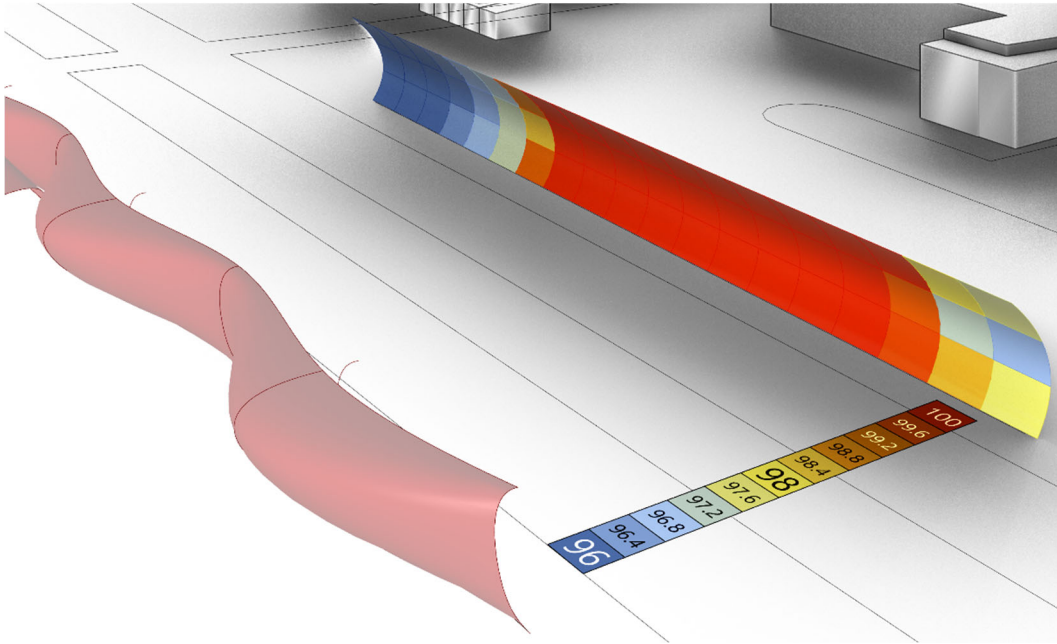


Figure 90: SPL visualisation with  $N=2$  (5715 dB total) (source: Author)

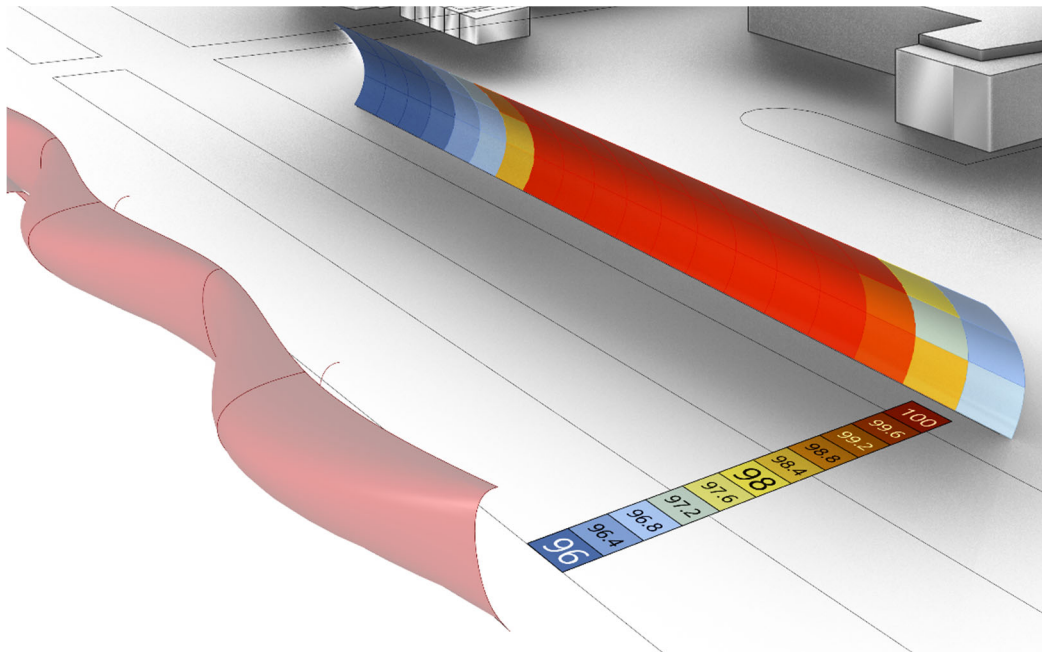


Figure 91: SPL visualisation with  $N=3$  (5710 dB total) (source: Author)

## 4.5 Grasshopper Components & Design Logic

This section elaborates on the most special and influential components used in the model.

### Components

**Galapagos:** The component is evaluating a local maximum. A graph is obtained with information on the local maximum.

**UV count:** The UV count changes the resolution of the simulation. It is advised to find a UV count which informs the designer enough clear distinguishment between results, without overcomplicating the density of the simulation.

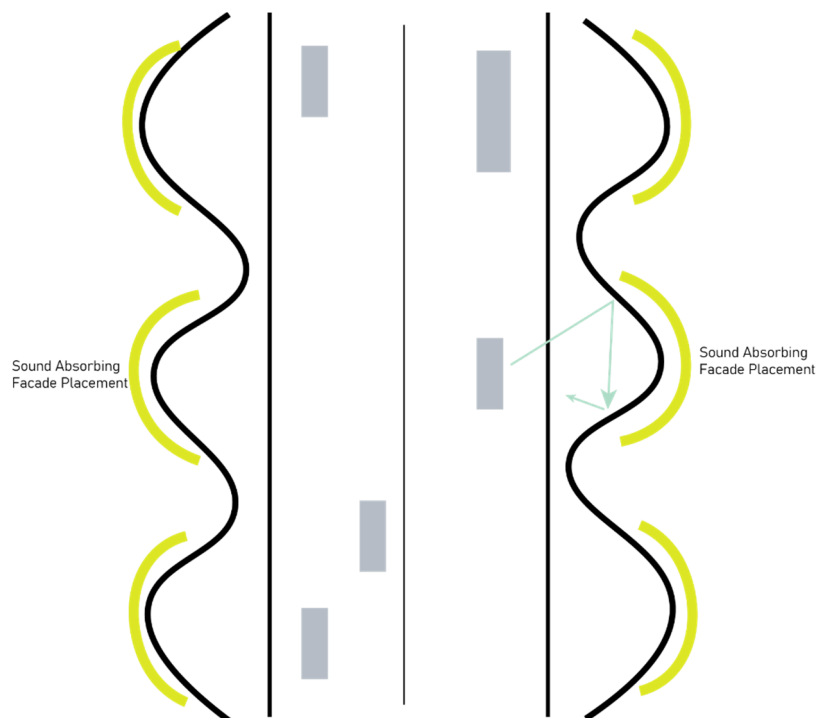
**Time:** Time has been set to 0.0076 s initially.

**n:** n in the Image Source component is set to 2. This indicates a double sound reflection. A simulation with n=3 has also been made for comparison.

**Mass Addition:** this component is used to compare the results for n=2 (5710) and n=3 (5715).

### Design Logic

Figure 92 illustrates how the allocation of absorptive façade elements could be made. The green areas could implement absorptive façade elements. This is further defended by figure 94 where the reflecting sound waves are visible. The design makes use of shape variations in the X and Y directions. This is done to ensure no further visual obstruction is made for residents. Also, the cost of higher noise barriers, which are commonly 3 to 5 meters high, is higher. Higher noise mitigation systems require e.g. additional structural elements.



*Figure 92: illustration on allocation of absorptive façade elements in top view (source: Author)*

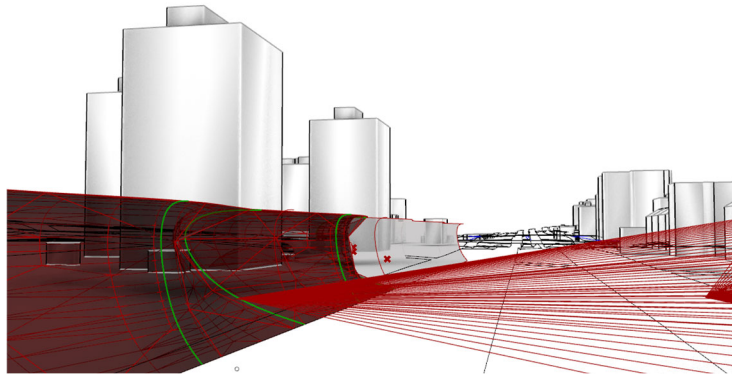
## 4.6 Reflection Simulations

The degree of simulation accuracy can be adjusted within Grasshopper Aeolus. The number of sound sources and the placement configuration can be altered. A limitation within the simulation with Aeolus is the fact that surfaces should be flat. A choice should be made between the simulated accuracy and time. Nevertheless, Aeolus can provide valuable insights and analysis for early-stage design exploration. A quality valuable in architectural design.

Acoustic scenes largely affect computational cost during simulation. The number of acoustic reflectors is a setting worth adjusting carefully. As this will influence simulation time. In highway barrier design, acoustic reflectors and absorbers are often curved. By tessellating the curves, straight curves can be obtained.

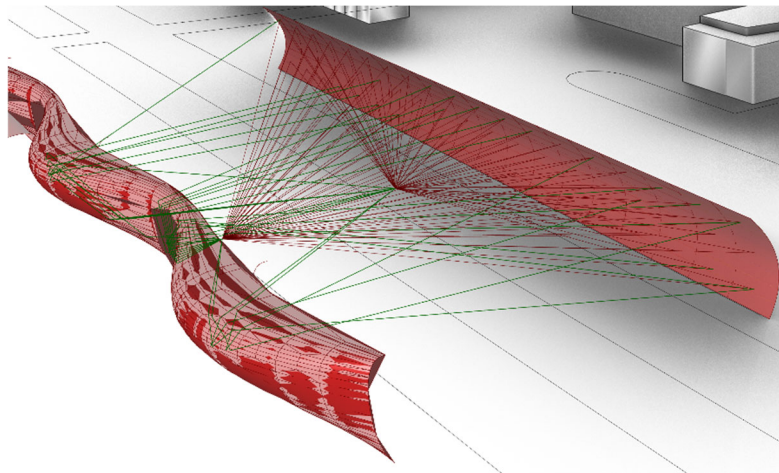
The Sound Pressure Map on the target area can be adjusted for more accurate result resolutions. Selection of subdivisions can be made and adjusted anytime.

In figure 93, an impression of the sound reflections in the urban landscape is provided.



*Figure 93: impression of sound waves and barrier geometry in the urban landscape (source: Author)*

In figure 94, secondary reflections are illustrated. It is important to emphasise on the computing time consideration for the simulations. Adjusting  $n$  (=the number of reflections) to a higher number, significantly complicates the reflection distribution and requires more computation time.

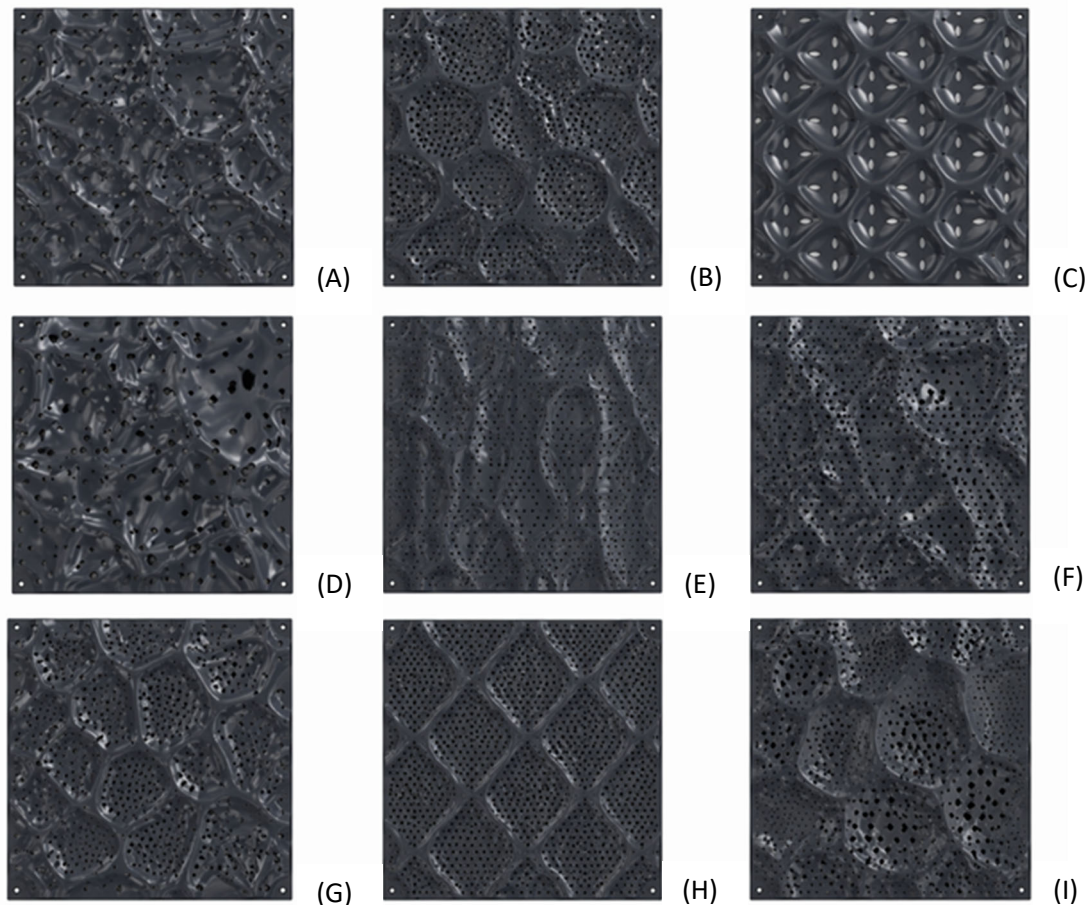


*Figure 94: impression of sound waves and barrier geometry in the urban landscape (source: Author)*

## 4.7 Design

Now that the total geometry is defined for different urban situations and the total geometry of the product, the panel design itself can be made. Different surface topologies are explored in this section.

A perforation rate of 20% should be translated to an optimal façade panel design. Perforations form a weaker area in the design. Figure X illustrates different configurations for the perforations. The protruded areas of the panels ensure mechanical stability. The main load on the surface of the panels is wind load. Systematic protruded area designs are showcased in C and H in figure 95.



*Figure 95: Design variations 600x600 panels (source: Author)*

Figure 96 demonstrates How a 20% perforation rate on an existing NPSP panel could look like. Perforations are only applied in the flatter surfaces of the panel. In figure 96, stress distribution in the panel is illustrated based on tensile forces on the top and bottom of the panel. Tools such as FreeCAD FEM allow for stress assessments. Thinner parts of the panel ultimately cause more stress concentrations and are more prone to fracture.

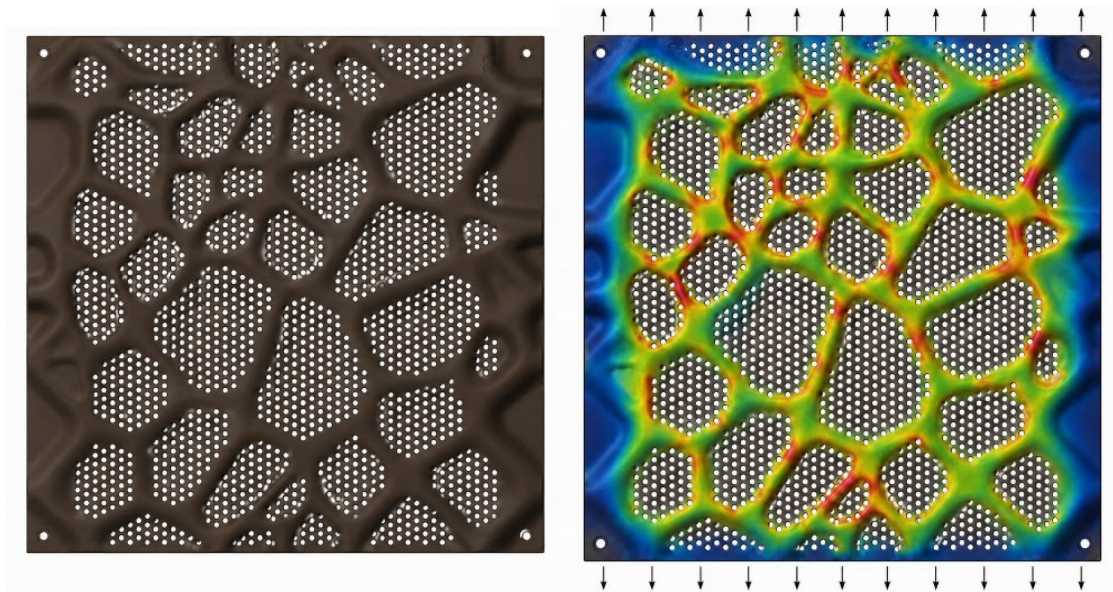


Figure 96: Quantitative 2D Stress Distribution (source: Author)

Figure 97 illustrates different façade configurations based on the previously conducted research. On the left, there is the perforated panel with a conventional mineral or rockwool absorbing layer and a 40 mm cavity. The second panel from the left demonstrates a 100 mm reed sub layer. The set-up in the middle uses foamed furan resin (based on S13), as the absorptive back structure. A thinner reed layer of 80 mm is proposed in the fourth set-up. The last design in the row illustrates how nature inclusivity could be integrated allowing bird species to enter and live in the façade, while still performing sufficient thermally by adding a mineral wool layer (this could be changed to reed or other natural/biobased materials).



Figure 97: Potential design variations with different back structures; from left to right: mineral wool, reed, foamed furan resin, reed higher density, nature inclusive (e.g. birds) (source: Author)



05

CONCLUSIONS

## 5.1 Scientific Findings

### Material Development and Acoustic Performance

The findings of the experimental investigations will be elaborated further in this section. This research showcased the potentials of furfuryl alcohol-based material development. Within the foamed material development, it can be concluded that sound absorption is strongly influenced by pore structure, material thickness, surface texture and the full design of a façade set-up. Perforation rates and cavity depth play crucial roles in total sound absorption.

Based on findings from the acoustic testing, it can be concluded that thickness plays a key role in porous material development. Material S3, with a thickness of 15 mm shows promising sound absorption. Especially when taking its thickness into account. It is generally known that increasing the thickness of the material, for example to 30 or 45 mm, would significantly increase absorption. This would be a logical next development step.

Material S5 achieved high sound absorption. Close to 1.0 around 4400 Hz. The absorption remains high for higher frequencies. Dissipation of sound is significant. However, the targeted frequency range is not largely included in the sound absorption graph. It is advised to proceed with another material or increase thickness.

S13 has the highest sound absorption in the desired frequency range. However, the thickness is 70 mm, and comparison can therefore not be made 1 on 1. Improved performance is likely caused by its thickness. The NRC of S13 is 0.64 and measured on 500, 1000 and 2000 Hz. Mineral wool performs better, but the biobased content of S13 is 99.5%. Details are illustrated in table 17.

Material S10 is mechanically most promising. Consisting of bamboo fibres, this material is stronger and heavier compared to other cork-based materials. S10 has a thickness of only 20 mm and an absorption coefficient of 0.49. This demonstrates that the created pores can absorb half of the normal incidence sound exposed to the surface.

Pore structure is not the only governing factor for sound absorption. S3 shows that exposed cork granulate at the surface can absorb sound well in combination with the right pore networks. In digital imaging, the cork granulate exposed at the surface can be observed. Material optimisation should include airflow resistivity, pore connectivity, tortuosity, density, and layer thickness.

### Acoustic System and Simulations

The tested configurations with perforated 8040 Hemp Fire front sheets demonstrate that the open area of the front sheet, the cavity depth, and the backing absorber all affect the resulting absorption curve.

The results indicate that a perforation rate of approximately 20% provides the most favourable balance for the system. A cavity design of 40 mm is optimal. This can be retrieved from measurement data and is illustrated in table 17.

S3 behind a perforated sheet and without, show very similar results, which is positive and could mean that a thin façade product could be made with a perforated front sheet of 6 mm thickness and an absorbing secondary structure of only 15 to 30 mm.

A cavity has important effects for sound absorption in between 500 and 1000 Hz. A cavity of 40 mm is optimal as there is no significant difference with a cavity of 60 mm and a larger façade system only costs more resources and financial means.

The position of the absorptive layer is relevant. The acoustic modelling indicates that placing the absorptive layer directly behind the perforated sheet generally performs better than placing it against the back structure. Nevertheless, this difference is smaller as the absorptive layer becomes thicker. Thin absorbers require correct placement. For thicker absorbers, the system becomes less sensitive to the absorber position.

The simulations confirm the experimental trend that increasing absorber thickness has a greater effect than increasing cavity depth. Increasing the cavity depth is not the key parameter for improved sound absorption. The simulations are nevertheless limited. They make use of general formulas and materials and are not tuned to the specific materials in this research. Future modelling should include measured values like airflow resistivity, porosity, tortuosity, and density to improve accuracy.

### Water Absorption and Durability

The capillary absorption tests show that the furan resin-based materials do not absorb water at a significant rate. The pores could be partly closed, poorly connected, or insufficiently hydrophilic to allow rapid water movement through the material.

The measured capillary absorption curves show an inconsistent increase over time. This reduces the reliability of detailed conclusions about absorption rate. A likely explanation is experimental interference caused by contact between the weighing scale cord and the table. Also, QUV testing does not degrade the perforated holes after 5 weeks, which confirms longevity.

This is a positive result for building applications. Acoustic materials are exposed to humidity, condensation and occasionally wetting in outdoor environments. Material which absorbs a lot of water can suffer from freeze-thaw damage or faster degradation.

### Total Product Evaluation

At product level, the research shows that a biobased acoustic panel using foamed furan resin-based materials is promising. A perforated material with an open area of 20% with a 40 mm cavity and an absorbing back material is optimal. The back material could be reed as the acoustic performance is significant and competes seriously with established materials such as mineral wool. Especially considering the carbon footprint. However, combustion dangers remain a challenge. S3 (Foamed Cork 3) does not outperform reed for absorption but could be more fire resistant and a good alternative. S3 could be implemented in areas where fire-safety plays a bigger role. Such as high-rise buildings where thick façade modules are even more expensive.

A successful final product must balance sound absorption, durability, sustainability, cost, ease of manufacturing and architectural integration.

The findings also show that future development should focus on increasing absorber thickness rather than only changing cavity depth.

To conclude: this research confirms that foamed furfuryl alcohol-based materials can be developed as sustainable acoustic products. Some produced materials show good sound absorption, limited water uptake, and preliminary resistance to freeze-thaw exposure. The simulations and impedance tube measurements further elaborate on optimal acoustic systems and design. Absorber thickness increase and pore optimisation form key next steps within furan resin-based material development. Reed and perforated panels are the real promising products.

Table 17: Assessment Best Performing New Materials Compared to Conventional Materials:

Sample Code	Explanation	Area (under Sound Absorption Coefficient curve) (400-2500 Hz)	NRC (sum of intervals within target freq.)	aw	CO <sub>2</sub> (kilotonnes) / CO <sub>2</sub> e/m <sup>2</sup>	Price (€/m <sup>2</sup> )	Lifespan (Y)	Biobased (%)
S3	Foamed Cork 3	1225 <sup>w</sup>	0.41	0.58	Around 5.62 (kg CO <sub>2</sub> e/m <sup>2</sup> ) <sup>y</sup>	Resin 2.95 €/kg	30	99.5
C2 + S3	20% P.R. + Foamed Cork 3	1263	0.41	0.58	Low	100-250 (exl. inst.)	30 (est)	90 & 99.5
S9	Almond Shell	432	0.14	-	Low	-	-	99.5
S10	Bamboo Fibre	1018	0.39	0.49	Low	-	-	99.5
S11	Foamed Cork 9	872	0.32	0.42	Low	-	-	99.5
S13	Foamed Cork 10	1243	0.64 <sup>z</sup>	0.6	Low	-	-	99.5
C2 + E	20% P.R. + Reed	1399	0.8	0.75	Low	100-250 (exl. inst.)	30 (est)	90 & 100
C3 + E	30% P.R. + Reed	1399	0.8	0.75	Low	100-250 (exl. inst.)	30 (est)	90 & 100
Perforated Aluminium	sheet with absorptive core – Forster FF Products e.g. Solosar MAGNUM AL12-type	1920	0.85	0.90	60	150	40	0
Perforated (galvanised Steel)	perforated galvanized steel acoustic panel with rock wool, e.g. Ornitolink / SteelProfil type	1750	0.80	0.80	35	65	35	0
Mineral Wool/ Stone Wool	Rockfon Sonar acoustic	2000	0.85 – 0.95	0.75 – 1.00	4.15	53 – 69	50	0
Glass Fibre	Ecophon Focus A Carbon Low	2000	0.80	0.80	1.17	34 – 76	50	0
Melamine Foam	Basotect G+ / 50 mm absorber	1870	0.80 – 0.90	0.75 – 0.85	2.4 – 2.9	50 – 94	Prod. specific	0
PET Fibre Panels	9–24 mm recycled PET felt/polyester fibre wall panels	1500	0.3 – 0.8	0.45 – 1.00	6.45	75 – 160	50	0
Open-cell Polyurethane Foam	50 mm PU acoustic foam panel	1900	0.85	0.80	4.3 – 5.7	15 – 31	5 – 10	0
(Micro) Perforated Wood & MDF	Topakustik-type perforated	1860	0.70 – 0.95	0.60– 0.90	4.6	60 – 200+	30	0

Table 17: z: 3-point average is taken for the NRC of S13 (500, 1000 & 2000 Hz) Note: comparison can only be made if values are compared in the correct unit: EN 15804 is used; w: a prediction based on the curve of S3 has been made; y: based on Nabasco EPD data, see references To assess the area and compare the materials optimally, an estimation on the curvature on the frequencies in between 1600 (the end of large 100 mm samples in the impedance tube) and 2500 Hz (the end of the focus frequency range), is made. Obtained values for established materials are retrieved from the Literature Review chapter and the same as applied in table 1 and 2. (sources: see tables 1 and 2)

The main research question will be answered in this section:

**How can low carbon materials be designed and optimised to provide effective acoustic performance for noise mitigation in infrastructure and urban environments?**

Low-carbon acoustic materials can be designed by applying several acoustic principles for an optimal design. Effective performance depends on interaction between absorber thickness, pore size and structure, fibre and filler reinforcement, cavity depth, perforation rates and the back structure. Porous furan-resin foamed materials absorb sound well for certain frequencies. However, a serious competitor to mainstream outdoor infrastructural absorbers is a perforated front sheet with a perforation rate of 20% with an absorptive material behind it in combination with a 40 mm air cavity is optimal. This ensures a durable, largely biobased, nature inclusive design.

The sub-questions are answered in this section:

**(a) What are requirements for traffic noise reduction?**

Traffic noise is best mitigated on mid-frequencies. These are usually around 500 to 1000 Hz. Often small or large vehicles produce sound pollution in this band width. Especially in wet weather conditions.

Acoustic performance such as sound absorption is not sufficient to develop an outdoor mitigating product. The following aspects should be considered:

- Mechanical strength
- moisture and freeze-thaw resistance
- fire safety
- durability
- lightweight
- low environmental impact
- large scale manufacturing possibilities

**(b) How do biobased fibre composite configurations affect sound absorption and attenuation?**

Thickness is the most dominant factor in absorption design for porous biobased materials. Cavities have a small improving impact depending on absorber backing materials. Reed for the backing structure performs best for this research with a 40 mm cavity.

**(c) How do density, porosity, and binder type control acoustic response?**

The acoustic response is controlled the ease with which sound passes through a material

Important parameters are:

Porosity: what are the dimensions of the pores

Pore connectivity: how easy can air enter the material

Tortuosity: influences frictional losses

Airflow resistivity: how is sound dissipated

Density: influences stiffness and mass

Binder type: affects pore openness, moisture behaviour and mechanical properties

Surface porosity is only one of the factors influencing sound absorption. The furan resin binder appears useful because it creates a porous acoustic material which also limits rapid water uptake and it has UV resistance properties needed for outdoor durability.

**(d) How do the developed biocomposite concepts compare with conventional mitigation materials?**

Reed backing showed very strong acoustic performance and could compete with mineral wool in some configurations. However, combustibility limits usage where fire requirements are tight.

Foamed furan resin-based materials could provide a compromise. They do not outperform based on acoustical performance but have small water uptake and can withstand freeze cycles. Also, furan resin is UV resistant as stated in the previous section. This would also apply to furan-based foamed materials. Perforations do not degrade faster based on visual assessment.

**(e) How can numerical and laboratory results be interpreted in relation to real-world highway and urban contexts?**

The impedance tube tests and simulations provide early-design insights. Long-term durability testing has not been conducted, however early-stage durability testing was done.

Acoustic Modelling and Whealy form general estimations on the performance of the façade set-up design. Interpretation should be done carefully as these assumptions are based on general acoustic formulas described in the work of Allard & Atallia, and Cox & D'Antonio.

Full scale testing should be conducted to prove real world application readiness. In the recommended future research section, more on this is elaborated.

## 5.2 Societal Impact

This section elaborates on the societal impact the designed product can have. Upscaled scenarios and nationwide application is explored. An upscaled production process is illustrated in figure 98. Kneader mixing could be done continuously. Multiple presses could work automated. Large scale perforation machine could manufacture perforated sheet in larger numbers. Moulds with cavities already integrated, could offer a solution for faster production.



Figure 98: Current production process at NPSP for pressed biocomposites and a possible upscale perforation device added (source: Author)

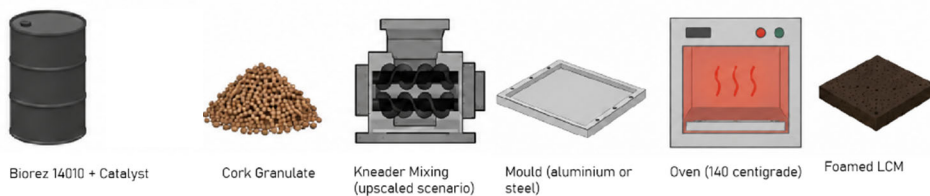


Figure 99: Current production process for foamed biocomposites (source: Author)

Figure 99 showcases the current foamed biocomposite production process. An oven at 140 centigrade is used to create optimally foamed materials.

### Wider Impact on Society:

To assess how large the societal impact could be if the proposed façade prototype were to be applied, estimations are made using calculations. In the following section it is demonstrated what the extent could be for the application of the optimal prototype for infrastructural, outdoor sound mitigation.

An exact number in square meters is not available, however the number of people suffering from noise pollution is known, as elaborated in the introduction of this research. Noise exposure assessment is based on detailed propagation models that calculate sound levels at building facades. These models evaluate most exposed facades of dwellings. Population exposure, dwelling exposure, annoyance and sleep disturbance are assessed.

The WHO takes noise exposure above 53 dB Lden as significant to health effects. The Netherlands contains approximately eight million dwellings. It can be assumed that that between 30% and 50% of these dwellings experience façade noise levels above health-based thresholds. This leads to in between 2.5 and 4 million dwellings which are affected. Typical residential buildings exhibit an external façade area in the range of approximately 100–200 m<sup>2</sup> per dwelling. This depends on housing typology, building height, and degree of façade sharing.

These assumptions yield an estimated total exposed façade surface area of:

$$A_{\text{exposed}} \approx (2.5-4.0 \times 10^6 \text{ dwellings}) \times (100-200 \text{ m}^2)$$

This corresponds to:

$$2.5 \times 10^8 \text{ to } 8.0 \times 10^8 \text{ m}^2$$

This can be translated to 250–800 million square metres of façade surface potentially exposed to environmental noise above health-relevant levels.

Not all facades on exposed buildings exceed the decibel threshold. Building orientation, floor height and surrounding urban morphology influence the exposure. This calculation is first-order and broad. Nevertheless, a large scale of the Dutch buildings is facing elevated sound exposure levels. In an upscaled scenario,  $2.5 \times 10^8$  to  $8.0 \times 10^8 \text{ m}^2$  could be used for the proposed product prototype in this research.

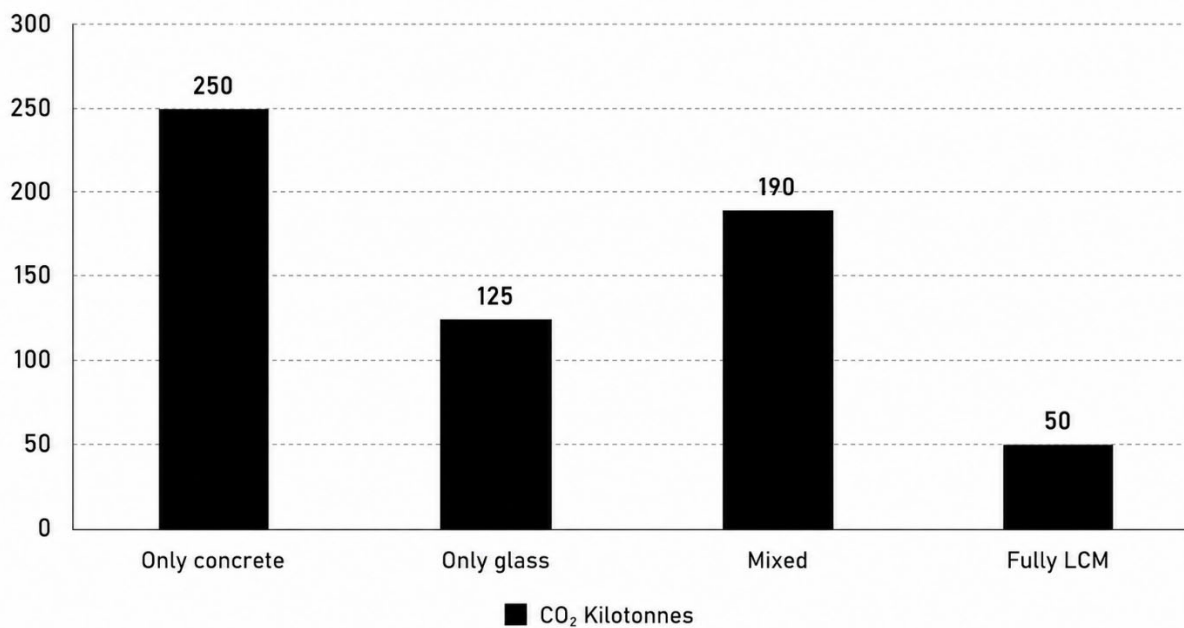


Figure 100: Impact comparison of different applied materials for noise mitigation infrastructure in the Dutch context (CO<sub>2</sub> in kilotonnes) (source: Author)

Figure 100 demonstrates the impact my designed Low Carbon Materials could have on the total highway barrier surfaces in the Netherlands. Roughly, a 4x reduction in carbon emissions could be achieved if all new highway barriers were to be made from biocomposites (8040 furan resin based) (no reed is taken into consideration in this estimation).

Reed can be locally sourced from municipalities and farmers in Dutch provinces. For this research, reed was ordered from one of the contacts within NPSP for the mock-up prototype. Thanks to Henk Lok, reed supply was conducted successfully. Reed costs around 1 EUR/kg and is abundant in most regions in the Netherlands. Local economies will benefit from the integration of this material in façade prototypes.

Supply chains for furan-resin based materials will gain importance. Currently, Belgium is the main supplier of Biorez furan resin for commercial use for this research. Potentially, fabrication hubs could be set-up for a flawless delivery chain.

The aim of this research is to reduce the number of cardiovascular and stress levels of inhabitants of the Netherlands. It is predicted, that if this prototype would be widely applied, the population in the Netherlands would increase the quality of life and duration of human life, leading to a better society.

## 5.3 Future Research

This section demonstrates which areas of research are worth continuation in the future.

### Reverberation Room Testing:

Reverberation room testing is necessary to showcase the performance of a material or prototype with the help of a mock-up. At TU Delft, Henry den Bok supervises the Reverberation Chamber. According to official ISO standards, 12 m<sup>2</sup> surface area is necessary for official testing. However, from 7 m<sup>2</sup> onwards, reliable data can be retrieved. Producing more perforated panels with a P.R. of 20% and reed backing structures could be investigated. It would also be worth diving in thinner solutions as some urban situations, would prefer reduced wall thicknesses.

### Further acoustic simulation software/ elaboration on the Grasshopper model:

The Grasshopper simulation file should be elaborated further to gain more insights into the overall geometry of the product in different urban situations. Further optimisation tools could be implemented. Other relevant simulations would be the placement of material on building facades. Related to SPLs for example. Facades above a certain threshold could be appointed a 20% or 30% open area façade with absorptive backing structure. Façade parts with less urgency for sound absorption, could use the non-perforated panels, as these are more price effective. Different distributions could be made.

### EOL foamed furan-based materials:

The End-of-Life cycle of foamed furan-based materials could be explored further. Could this new design for foamed material be grinded and used again as a filler for new materials. Or is it biodegradable when placed in earth e.g. Further research on this aspect is worth it. As from a sustainability point of view, the final stage of a product is important.

### Mechanical testing:

Mock-up scale mechanical testing would be valuable to prove that the furan based, perforated sheets are resistant to important forces. Both impact and wind resistance could be assessed. A 3-point bending test on panel scale could deliver valuable insights into the potentially brittle character of the material.

### Substitutes of furan resin e.g. sugar beet:

Furan resin is primarily sourced from Latin-American countries. If locally available substitutes could be used, this would reduce the carbon footprint of the product further. Sugar based supplies of sugar beet could form an alternative. However, UV-resistance and durability should be ensured. If chemical properties match the desired production process where the catalyst performs optimally in an acid environment. Different catalysts can be explored to find optimal performance.

### TGV real-world ageing tests:

QUV-testing has been conducted. However, to prove a products durability, real-world testing is required. A proposal could be made to place mock-ups at TGV on the TU Delft campus.

Water repellent membranes within the structure:

Water repellent membranes could be integrated in the design. This could reduce high frequency sound absorption but could increase the lifespan of the total product. In common brick building façade configurations, a cavity is designed with a water repellent layer in front of mineral wool.

The effect of water saturation of materials on the acoustic performance:

Water saturation of the porous absorptive layer could influence acoustic performance. It is valuable to gain knowledge on the absorbing properties after the water has been immersed in water.

Thermal testing:

The foamed furan resin could isolate well. It is common that sound absorbing materials could also insulate thermally. Thermal testing could be conducted. Simple box set-ups could be made, and a thermal camera could be used to assess changes over time e.g.

Real-world highway test location:

After successful mock-up testing, a larger production could be conducted to install an entire façade on common highway acoustic barrier heights. These are commonly 3 to 5 meters high. Acoustic measuring devices could assess the performance of this future set-up

A person wearing a dark jacket is holding a large, rusted metal cross. The cross is made of a dark, textured material, possibly weathered metal, and has a prominent hole in the center of its vertical beam. The person's hands are visible at the top and bottom of the cross. The background is a soft-focus landscape of mountains under a pale sky.

06

REFLECTIONS

## 6.1 Research Approaches

The research has been conducted with the objective to create low carbon materials for optimal products for sound mitigation in infrastructural outdoor environments. Targeting sound absorption in the frequency range of 400 to 2500 Hz.

The approach for this research is illustrated in figure 8. Most of the approach steps worked out. Literature on sound absorbing materials and a thorough understanding of sustainable biocomposite development led to educated guesses or more informed decision-making along the research. Impedance tube testing was a key testing method and provided valuable data. It was at first, an understanding that porous filler-based composites would show important absorption already. However, as the biocomposite plates are pressed and the resin and linseed oil spread out to the top surface, the pores are enclosed and absorption is hindered. This led to a second and third applied strategy, namely that of porous and perforated materials. These resemble current established state-of-the-art absorptive materials.

Designing on a prototype level began after several impedance tube testing on the material level. Promising results from the second batch of porous materials and reed testing, led to the final design where an optimal perforation rate is confirmed. This was then integrated into panel surface design to allow for mechanical strength, while also having perforations for the acoustic performance.

## 6.2 Moral & Ethical Considerations

Important ethical considerations are the use of furan resin. Sugarcane bagasse is used to obtain furan resin. The process, as illustrated in the SOTA, could impact farmland in subtropical regions. It is retrieved from biobased waste streams, however, if the production line would increase globally, demand in these regions could increase. This could lead to a change in farmland use to harvest the needed vegetation for furan resin. It is important to prevent ecologically damaging practices. An example of a challenging ecological farming method is that of palm oil plantations in e.g. Indonesia.

Another important factor to keep in mind is fire safety and safety in general. New building materials should be tested thoroughly before real-world implementation near residents.

## 6.3 Evaluation of Societal Impact

As described in section 5.2, impact on society could be large with this product. Creating a larger positive impact in society has always been my core motivation during the execution of this research. Fascination and interest for national problems have been a drive. If the TRL of this product were to increase over time, wider application would make this product mainstream and a standard option in noise mitigating wall infrastructure. Not only in highly urban areas, but near any noise producing source. Indoor applications have a high rate of succession as conditions are favourable for long lifespans of applied products. Upscaled production facilities will ensure the price for manufacturing would decrease. More jobs within this field would emerge. There are people needed in production plants, education on the material science, product development and R&D in general would be required. Also, maintenance will play a larger role. After 30 years, panels should be replaced or given a secondary life. Also damaged panels should be replaced. And efficient system would need to be developed. Current sub-frame systems could be improved.

# References:

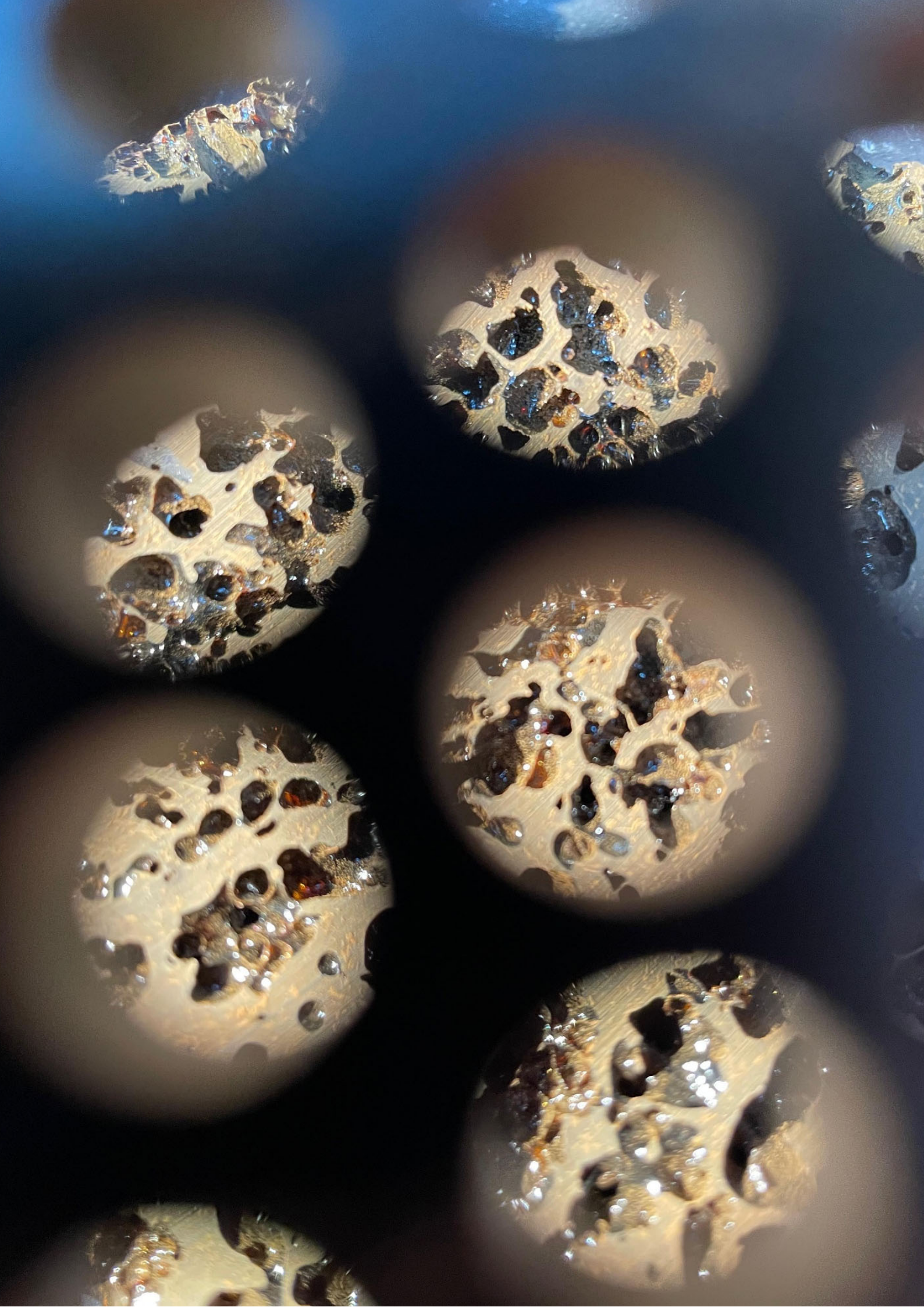
- 3DBAG Viewer*. (n.d.). <https://www.3dbag.nl/en/viewer?rdx=117852.16081044805&rdy=485817.4547115264&ox=14.264143965177936&oy=393.15611299648305&oz=404.55730376443535>
- Acoustic analysis - DigiPedia*. (2025, 5 november). DigiPedia. <https://digipedia.tudelft.nl/tutorial/acoustic-analysis/?tab=chapter-1>
- Afval Circulair. (2022). *Afvalverwerking in Nederland: Cijfers 2020*. <https://afvalcirculair.nl/actueel/nieuws/afvalnieuws/2022/afvalverwerking-nederland-cijfers-2020/>
- Ahmad, W., McCormack, S. J., & Byrne, A. (2025). Biocomposites for sustainable construction: A review of material properties, applications, research gaps, and contribution to circular economy. *Journal of Building Engineering*, 105, Article 112525. <https://doi.org/10.1016/j.jobe.2025.112525>
- Allard, J. F., & Atalla, N. (2009). *Propagation of sound in porous media: Modelling sound absorbing materials* (2nd ed.). Wiley. <https://doi.org/10.1002/9780470747339>
- American Society of Baking. (n.d.). *Dicalcium phosphate dihydrate (DCPD)*.
- Amran, M., Fediuk, R., Murali, G., Vatin, N., & Al-Fakih, A. (2021). Sound-absorbing acoustic concretes: A review. *Sustainability*, 13(19), Article 10712. <https://doi.org/10.3390/su131910712>
- Arenas, J. P., & Crocker, M. J. (2010). Recent trends in porous sound-absorbing materials. *Sound & Vibration*, 44(7), 12–17.
- Arenas, J. P., Parra, C. C., Rebolledo, J., & Venegas, R. (2025). Granular pumice stone: A natural double-porosity sound-absorbing material. *Buildings*, 15(4), Article 557. <https://doi.org/10.3390/buildings15040557>
- Argalis, P. P., Sinka, M., Andzs, M., Korjakins, A., & Bajare, D. (2024). Development of new bio-based building materials by utilising manufacturing waste. *Environmental and Climate Technologies*, 28(1), 58–70. <https://doi.org/10.2478/rtuect-2024-0006>
- Asdrubali, F. (2006). Survey on the acoustical properties of new sustainable materials for noise control. In *Proceedings of Euronoise 2006* (pp. 1–10).
- AskNature. (2020). *Biopolymer composites prevent structural failure*. <https://asknature.org/strategy/biopolymer-composites-prevent-structural-failure/>
- ASTM International. (2023). *Standard test method for sound absorption and sound absorption coefficients by the reverberation room method* (ASTM C423-23). <https://doi.org/10.1520/c0423-23>
- Atlas Leefomgeving. (2025). *Geluid in je omgeving: Wegverkeer*. <https://www.atlasleefomgeving.nl/thema/geluid-in-je-omgeving/wegverkeer>
- Attenborough, K. (1985). Acoustical impedance models for outdoor ground surfaces. *Journal of Sound and Vibration*, 99(4), 521–544. [https://doi.org/10.1016/0022-460X\(85\)90538-3](https://doi.org/10.1016/0022-460X(85)90538-3)
- Attenborough, K., Li, K. M., & Horoshenkov, K. V. (2007). *Predicting outdoor sound*. Taylor & Francis.
- Biocomposieten*. (n.d.). <https://www.biobasednederland.nl/materialen/biobased-material-3>
- Bozkurt, T. S. (2022). Meeting room acoustic design in the historical building: The example of Istanbul University Faculty of Science and Letters Building. *Journal of Architectural Sciences and Applications*. <https://dergipark.org.tr/tr/pub/jah/issue/72961/1186514>
- Budelmann, D., & Fiedler, B. (2026). Bio-based poly (furfuryl alcohol) resin as a sustainable matrix alternative for prepregs. *Materials & Design*, 265, 115866. <https://doi.org/10.1016/j.matdes.2026.115866>
- Bureau Sanering Verkeerslawaaai. (2025). *Sanering van geluidhinder*. <https://www.bureausaneringverkeerslawaaai.nl/lokale-sanering-3/sanering/geluidhinder>
- Cai, M., Zhong, S., Wang, H., Chen, Y., & Zeng, W. (2017). Study of the traffic noise source intensity emission model and the frequency characteristics for a wet asphalt road. *Applied Acoustics*, 123, 55–63. <https://doi.org/10.1016/j.apacoust.2017.03.006>
- Carruthers, J. (2012). *Technology overview: Biocomposites* [Knowledge Transfer Network report]. Technology Strategy Board. <http://www.netcomposites.com>
- Catrinck, M. N., Barbosa, P. S., Filho, H. R., Monteiro, R. S., Barbosa, M. H., Ribas, R. M., & Teófilo, R. F. (2020). One-step process to produce furfural from sugarcane bagasse over niobium-based solid acid catalysts in a water medium. *Fuel Processing Technology*, 207, 106482. <https://doi.org/10.1016/j.fuproc.2020.106482>

- Cellyph. (2025). *BASOTECT melamine foam acoustic properties* [Product data].
- Cereals & Grains Association. (n.d.). *04 acids methods*.
- Chabriac, P.-A., Gourdon, E., Glé, P., Fabbri, A., & Lenormand, H. (2016). Agricultural by-products for building insulation: Acoustical characterization and modeling to predict micro-structural parameters. *Construction and Building Materials*, *112*, 158–167. <https://doi.org/10.1016/j.conbuildmat.2016.02.162>
- Chen, J., Hočevnar, M., & Širok, B. (2011). Melt Volume Flow Measurement in the Mineral-Wool Production Process. *Strojniški Vestnik – Journal Of Mechanical Engineering*, *57*(04), 293–303. <https://doi.org/10.5545/sv-jme.2010.159>
- Cox, T. J., & D'Antonio, P. (2016). *Acoustic absorbers and diffusers: Theory, design and application* (3rd ed.). CRC Press. <https://doi.org/10.1201/9781315369211>
- Decibel.shop. (2024). *Understanding NRC ratings of wood wool panels*.
- Del Rey, R., Uris, A., Alba, J., & Candelas, P. (2017). Characterization of sheep wool as a sustainable material for acoustic applications. *Materials*, *10*(11), Article 1277. <https://doi.org/10.3390/ma10111277>
- Đuriš, R., & Labašová, E. (2021). The design of an impedance tube and testing of sound absorption coefficient of selected materials. *IOP Conference Series Materials Science And Engineering*, *1050*(1), 012003. <https://doi.org/10.1088/1757-899x/1050/1/012003>
- Electricbloomhosting. (2017, August 30). *Algorithms design Hamburg concert hall: "It would be insane to do this by hand"*. Global Construction Review. <https://www.globalconstructionreview.com/algorithms-design-hamburg-concert-hall-it-would-be/>
- European Environment Agency. (2020). *Environmental noise in Europe—2020*. Publications Office of the European Union. <https://www.eea.europa.eu/publications/environmental-noise-in-europe>
- European Environment Agency. (2023). *Health risks caused by environmental noise in Europe*. Publications Office of the European Union. <https://www.eea.europa.eu/publications/health-risks-caused-by-environmental>
- Faruk, O., Bledzki, A. K., Fink, H. P., & Sain, M. (2012). Biocomposites reinforced with natural fibers: 2000–2010. *Composites Part A: Applied Science and Manufacturing*, *43*(3), 288–297. <https://doi.org/10.1016/j.compositesa.2011.04.016>
- First Fence. (n.d.). *Timber acoustic fencing panels / Soundproof & noise reduction fencing*. Retrieved June 1, 2026, from <https://firstfence.co.uk/timber-acoustic-fencing>
- GlasBoertje. (n.d.). *Sound insulating laminated glass 55.2 (Rw in dB: 38)*. Retrieved June 1, 2026, from <https://www.glasboertje.nl/en/laminated-sound-proofing-glass-552>
- Government of the Netherlands. (n.d.). *Noise pollution from roads*. Retrieved March 27, 2026, from <https://www.government.nl/topics/environment/noise- nuisance/noise-pollution-from-roads>
- Groene Bouwmaterialen. (2024). *Geluidsisolatie met natuurlijke materialen*. <https://www.groenebouwmaterialen.nl/blogs/nieuws/geluidsisolatie-met-natuurlijke-materialen/>
- Hayward, M., & Helbich, M. (2024). Environmental noise is positively associated with socioeconomically less privileged neighbourhoods in the Netherlands. *Environmental Research*, *248*, Article 118294. <https://doi.org/10.1016/j.envres.2024.118294>
- Helmholtz calculator. (n.d.). <http://www.acousticmodelling.com/helmholtz.php>
- InnovA58. (2025). *InnovA58 unieke testomgeving voor duurzame innovaties*. <https://innova58.nl/default.aspx>
- International Organization for Standardization. (1993). *Acoustics—Attenuation of sound during propagation outdoors—Part 1: Calculation of the absorption of sound by the atmosphere* (ISO 9613-1:1993). ISO.
- International Organization for Standardization. (2024). *Acoustics—Attenuation of sound during propagation outdoors—Part 2: Engineering method for the prediction of sound pressure levels outdoors* (ISO 9613-2:2024). ISO.
- Ioannou, O., & Konijnenberg, F. (2026). Valorising food waste into functional bio-composite façade cladding: A circular approach to sustainable construction materials. *Clean Technologies*, *8*(1), Article 11. <https://doi.org/10.3390/cleantechnol8010011>
- Irvani, H., Mahabadi, H. A., Khavanin, A., Variani, A. S., & SheikhMozafari, M. J. (2025). Bamboo bio composite: A renewable and sustainable sound absorber for acoustic comfort in indoor settings. *Journal of Engineered Fibers and Fabrics*, *20*. <https://doi.org/10.1177/15589250251329457>
- Jaouen, L., Bécot, F.-X., & Chevillotte, F. (2025). Characterizations of acoustical porous media: Standardized methods, current trends and challenges. *Frontiers in Acoustics*, *3*, Article 1543456. <https://doi.org/10.3389/facou.2025.1543456>
- Kang, J. (2006). *Urban sound environment*. Taylor & Francis. <https://doi.org/10.1201/9781482265613>

- Kapicová, A., Bily, P., Fládr, J., & Šeps, K. (2024). Development of sound-absorbing pervious concrete for interior applications. *Journal of Building Engineering*, 85, Article 108697. <https://doi.org/10.1016/j.jobe.2024.108697>
- Karger-Kocsis, József, Bárány, Tamás (2019). Polypropylene Handbook (Morphology, Blends and Composites) || Foams. , 10.1007/978-3-030-12903-3(Chapter 10), 579–641
- Khomenko, S., Nieuwenhuijsen, M., Ambrós, A., Wegener, S., Mueller, N., et al. (2022). Premature mortality due to environmental noise exposure in European cities: A health impact assessment. *Environment International*, 165, Article 107304. <https://doi.org/10.1016/j.envint.2022.107304>
- Knauf Insulation. (n.d.). *Mineral wool board acoustic properties* [Product data].
- Korjakins, A., Sahmenko, G., & Lapkovskis, V. (2025). A short review of recent innovations in acoustic materials and panel design: Emphasizing wood composites for enhanced performance and sustainability. *Applied Sciences*, 15(9), Article 4644. <https://doi.org/10.3390/app15094644>
- Krimm, J. (2018). *Acoustically effective façades*. A+BE | Architecture and the Built Environment. <https://doi.org/10.7480/abe.2018.18>
- Lattice structures for acoustics applications – Zhai Group at NUS*. (n.d.). <https://blog.nus.edu.sg/zhaigroup/acoustic-lattice-structures/>
- Lehmann & Voss & Co. KG. (2024). *Chemical blowing agents to produce foamed films and sheets: Advantages and application*
- Lekshmi, Vishnudas, S., & Anil, K. (2023). Experimental investigation on acoustic performance of coir fiber and rice husk acoustic panels. *Applied Acoustics*, 204, Article 109244. <https://doi.org/10.1016/j.apacoust.2023.109244>
- Lopez, M., Dupont, T., & Panneton, R. (2024). Mass-spring model for acoustic metamaterials consisting of a compact linear periodic array of dead-end resonators. *The Journal Of The Acoustical Society Of America*, 155(1), 530–543. <https://doi.org/10.1121/10.0024212>
- Lu, J., Ding, S., Ni, Y., & Li, S. (2025). Bio-inspired acoustic metamaterials for traffic noise control: bridging the gap with machine learning. *Communications Engineering*, 4(1), 136. <https://doi.org/10.1038/s44172-025-00470-x>
- Ma, S., Li, T., Liu, X., & Zhu, J. (2015). Research progress on bio-based thermosetting resins. *Polymer International*, 65(2), 164–173. <https://doi.org/10.1002/pi.5027>
- MAGNUM AL12 – Aluminium acoustic panel for high-performance noise barriers – Solosar*. (n.d.). <https://www.solosar.fr/en/noise-barriers-uk/MAGNUMAL12-uk>
- MIT OpenCourseWare. (2012). *Chemical transformation I: Decomposition with H<sub>2</sub>O<sub>2</sub> with MnO<sub>2</sub>*.
- Mohammadi, M., Taban, E., Tan, W. H., Din, N. C., Putra, A., & Berardi, U. (2024). Recent progress in natural fiber reinforced composite as sound absorber material. *Journal of Building Engineering*, 84, Article 108514. <https://doi.org/10.1016/j.jobe.2024.108514>
- Mohammed, M., Jawad, A. J. M., Mohammed, A. M., Oleiwi, J. K., Adam, T., Osman, A. F., Dahham, O. S., Betar, B. O., Gopinath, S. C. B., & Jaafar, M. (2023). Challenges and advancement in water absorption of natural fiberreinforced polymer composites. Polymer Testing, 124, Article 108083. https://doi.org/10.1016/j.polymertesting.2023.108083*
- Mondal, M. I. H., Islam, M. M., Haque, M. I., & Ahmed, F. (2022). Natural, biodegradable, biocompatible and bioresorbable medical textile materials. In *Medical textiles from natural resources* (pp. 87–116). Elsevier. <https://doi.org/10.1016/B978-0-323-90479-7.00023-3>
- Namakka, M., Rahman, M. R., Bakri, M. K. B., Karuppasamy, B. D., Ahmmad, M. S., James, A. A., & Rahman, I. M. M. (2025). Advancements in acoustic properties of natural waste biocomposites: Current trends, applications, and future perspectives. *Advanced Composites and Hybrid Materials*, 8(5). <https://doi.org/10.1007/s42114-025-01427-6>
- National Center for Biotechnology Information. (2024). *PubMed Central*. <https://pmc.ncbi.nlm.nih.gov/articles/PMC11642230/>
- Nazari, S., Ivanova, T. A., Mishra, R. K., Müller, M., Akhbari, M., & Hashjin, Z. E. (2024). Effect of natural fiber and biomass on acoustic performance of 3D hybrid fabric-reinforced composite panels. *Materials*, 17(23), Article 5695. <https://doi.org/10.3390/ma17235695>
- Neuhaus, L., Ioannou, O., & Overend, M. (2025). Bulk fillers from food waste for polymeric bio-composites: The influence of filler type, particle size and volume ratio on furan-matrix composites. Construction and Building Materials, 502, Article 144303. https://doi.org/10.1016/j.conbuildmat.2025.144303*
- NPSP B.V. (n.d.-a). Nabasco. https://www.npsp.nl/en/nabasco NPSP B.V. (n.d.-b). Nabasco 8010. https://www.npsp.nl/en/material/nabasco-8010*











- Nwankwo, C. O., & Mahachi, J. (2025). Bio-based polymer composites used in the building industry: A review. In M. Kioumarsis & B. Shafei (Eds.), *The 1st International Conference on Net-Zero Built Environment (NTZR 2024)* (Lecture Notes in Civil Engineering, Vol. 237). Springer. [https://doi.org/10.1007/978-3-031-69626-8\\_71](https://doi.org/10.1007/978-3-031-69626-8_71)
- Odiyi, D. C., Sharif, T., Choudhry, R. S., Mallik, S., & Shah, S. Z. H. (2023). A review of advancements in synthesis, manufacturing and properties of environment friendly biobased polyfurfuryl alcohol resin and its composites. *Composites Part B: Engineering*, 267, Article 111034. <https://doi.org/10.1016/j.compositesb.2023.111034>
- Okhrimenko, L., & Okhrimenko, L. (2022, 4 juli). *New futuristic perforated sheet metal designs*. Arrow Metal. <https://www.arrowmetal.com.au/new-futuristic-perforated-sheet-metal-designs/>
- Ornitolink. (n.d.). *Acoustic cladding panel to reduce the noise up to 31 decibels*. Retrieved June 1, 2026, from <https://ornitolink.com/gb/enclosures-panels-doors/340001000-55675-acoustic-cladding-panel-with-perforated-sheet.html>
- Park, J. W., Lee, Y. W., Yun, C. H., Park, H. K., Chang, S. I., & Lee, I. P. (2010). Cloud computing for online visualisation of GIS applications in ubiquitous city. In *CLOUD COMPUTING 2010: The First International Conference on Cloud Computing, GRIDS, and Virtualisation*.
- Parool. (2023, 23 Juni). <https://www.parool.nl/cs-b5c8368e/> <https://www.parool.nl/cs-b5c8368e/>
- Perforated aluminum acoustic sheet for highway noise barrier and buildings*. (n.d.). [www.specifiedby.com](http://www.specifiedby.com). Requested 25 May 2026, van <https://www.specifiedby.com/shanda-noise-barrier-engineering-co/perforated-aluminum-acoustic-sheet-for-highway-noise-barrier-and-buildings>
- Perruchoud, V., Alderliesten, R., & Mosleh, Y. (2024). Enhancing fatigue performance of structural biocomposites by pre-straining and pre-creeping methods. In C. Binetury & F. Jacquemin (Eds.), *Proceedings of the 21st European Conference on Composite Materials: Volume 3—Material and structural behaviour: Simulation & testing* (Vol. 3, pp. 1512–1519). The European Society for Composite Materials and the Ecole Centrale de Nantes.
- Przybek, A. (2025). The role of natural fibers in the building industry—The perspective of sustainable development. *Materials*, 18(16), Article 3803. <https://doi.org/10.3390/ma18163803>
- Raad van State. (2021). *Case 202104562/1/R4*. <https://www.raadvanstate.nl>
- Rajappan, S., Bhaskaran, P., & Ravindran, P. (2017). An insight into the composite materials for passive sound absorption. *Journal of Applied Sciences*, 17(7), 339–356. <https://doi.org/10.3923/jas.2017.339.356>
- Rakesh, K. M., Srinidhi, R., Gokulkumar, S., Nithin, K. S., Madhavarao, S., Sathish, S., Karthick, A., Muhibbullah, M., & Osman, S. M. (2021). Experimental study on the sound absorption properties of finger millet straw, darbha, and ripe bulrush fibers. *Advances in Materials Science and Engineering*, 2021, Article 7382044. <https://doi.org/10.1155/2021/7382044>
- Rijksinstituut voor Volksgezondheid en Milieu. (2014). *Omvang van de effecten op gezondheid en welbevinden door omgevingsgeluid in Nederland* (RIVM Report 2014-0100). <https://www.rivm.nl/publicaties/omvang-van-effecten-van-omgevingsgeluid-op-gezondheid>
- Rijksinstituut voor Volksgezondheid en Milieu. (2018). *Volksgezondheid Toekomst Verkenning 2018: Een gezond vooruitzicht*. <https://www.vtv2018.nl>
- Rijksinstituut voor Volksgezondheid en Milieu. (2022). *Geluid en gezondheid* [Factsheet]. <https://www.rivm.nl/geluid/gezondheid>
- Rijksoverheid. (n.d.). *Geluidsoverlast van wegen*. Retrieved March 27, 2026, from <https://www.rijksoverheid.nl/onderwerpen/geluidsoverlast/geluidsoverlast-van-wegen>
- Rijkswaterstaat. (n.d.-a). *Design of noise barriers*. Retrieved March 27, 2026, from <https://www.rijkswaterstaat.nl/wegen/projectenoverzicht/meerjarenprogramma-geluidsanering-mjpg-aanpak-geluidsoverlast-woningen/aanpak/vormgeving-geluidschermen>
- Rijkswaterstaat. (n.d.-b). *Measures against increasing noise along national roads*. Retrieved March 27, 2026, from <https://www.rijkswaterstaat.nl/leefomgeving/leefbaarheid-en-milieu/milieukwaliteit/geluid-langs-rijkswegen/maatregelen-tegen-toename-geluid>
- RIVM & Atlas Leefomgeving. (2025). *Geluid in Nederland* [Interactive maps]. <https://www.atlasleefomgeving.nl>
- Röck, M., Saade, M. R. M., Balouktsi, M., Rasmussen, F. N., Birgisdottir, H., Frischknecht, R., Habert, G., Lützkendorf, T., & Passer, A. (2020). Embodied GHG emissions of buildings—The hidden challenge for effective climate change mitigation. *Applied Energy*, 258, Article 114107. <https://doi.org/10.1016/j.apenergy.2019.114107>
- Rudin, A., & Choi, P. (2012). Biopolymers. In *Elsevier eBooks* (pp. 521–535). <https://doi.org/10.1016/b978-0-12-382178-2.00013-4>
- Ruiz, J. A. R., Vincent, M., Agassant, J., Sadik, T., Pillon, C., & Carrot, C. (2014). Polymer foaming with chemical blowing agents: Experiment and modeling. *Polymer Engineering And Science*, 55(9), 2018–2029. <https://doi.org/10.1002/pen.24044>











- Saçlı, C., et al. (2019). Acoustic and mechanical properties of PET fiber panels.
- Sandberg, U., & Ejsmont, J. A. (2002). *Tyre/road noise reference book*. Informex.
- Schreurs, E. M., Jabben, J., Verheijen, E. N. G., & Rijksinstituut voor Volksgezondheid en Milieu. (2010). *STAMINA—Model description* (RIVM Report No. 680740003). RIVM. <https://www.rivm.nl/bibliotheek/rapporten/680740003.pdf>
- Shankar, M. V., Padmaraj, N. H., Hegde, S., Yash, G. M., & Kini, C. R. (2025). Analysis of effect of thickness and surface treatment on sound transmission loss characteristics of natural fibres. *Scientific Reports*, 15, Article 28957. <https://doi.org/10.1038/s41598-025-14210-w>
- Sound Absorption Coefficient Chart (125 Hz–4 KHz)*. (2025, 6 oktober). Acoustic Supplies. <https://www.acoustic-supplies.com/absorption-coefficient-chart>
- Sound Acoustic Solutions. (2018). *NRC of fiberglass and mineral wool board*.
- SteelProfil. (n.d.). *Acoustic wall insulation mineral wool sandwich panel 80mm*. Retrieved 5 March 2026, from <https://www.steelprofil.eu/en/shop/acoustic-wall-insulation-mineral-wool-sandwich-panel-80mm/>
- TU Delft. (2017). *Noise barriers in the Netherlands* [Repository report]. <https://repository.tudelft.nl>
- United Nations Environment Programme, & Yale Center for Ecosystems + Architecture. (2023). *Building materials and the climate: Constructing a new future*. United Nations Environment Programme. <https://www.unep.org/resources/report/building-materials-and-climate-constructing-new-future>
- Van Kempen, E., Casas, M., Pershagen, G., & Foraster, M. (2018). WHO environmental noise guidelines for the European region: A systematic review on environmental noise and cardiovascular and metabolic effects. *International Journal of Environmental Research and Public Health*, 15(2), Article 379. <https://doi.org/10.3390/ijerph15020379>
- Van Renterghem, T. (2014). Guidelines for optimizing road traffic noise shielding by non-deep tree belts. *Ecological Engineering*, 69, 276–286. <https://doi.org/10.1016/j.ecoleng.2014.04.029>
- Van Renterghem, T., Forssén, J., Attenborough, K., Jean, P., Defrance, J., Hornikx, M., & Kang, J. (2015). Using natural means to reduce surface transport noise during propagation outdoors. *Applied Acoustics*, 92, 86–101. <https://doi.org/10.1016/j.apacoust.2015.01.004>
- Wan, J., Wan, J., & Wan, J. (2020, 18 oktober). *The Fractal® acoustic barrier*. IPAM - Institute For Pure & Applied Mathematics. <https://www.ipam.ucla.edu/research-articles/fractal-acoustic-barrier/>
- Wikipedia contributors. (n.d.). *Noise reduction coefficient*. In *Wikipedia*. Retrieved March 27, 2026, from [https://en.wikipedia.org/wiki/Noise\\_reduction\\_coefficient](https://en.wikipedia.org/wiki/Noise_reduction_coefficient)
- World Health Organization. (2011). *Burden of disease from environmental noise: Quantification of healthy life years lost in Europe*. WHO Regional Office for Europe. <https://www.who.int/europe/publications/i/item/WHO-EURO-2011-2970-42707-59667>
- World Health Organization. (2018). *Environmental noise guidelines for the European Region*. WHO Regional Office for Europe. <https://www.who.int/europe/publications/i/item/9789289053563>
- Xie, Y., Hill, C. A. S., Xiao, Z., Miltz, H., & Mai, C. (2010). Silane coupling agents used for natural fiber/polymer composites: A review. *Composites Part A: Applied Science and Manufacturing*, 41(7), 806–819. <https://doi.org/10.1016/j.compositesa.2010.03.005>
- Yamane, & Takeo. (2026, May 1). *Sugarcane | Description, Grass, planting, harvesting, pests, & Diseases*. Encyclopedia Britannica. <https://www.britannica.com/plant/sugarcane>
- Yang, T., Hu, L., Xiong, X., Petrů, M., Noman, M. T., Mishra, R., & Miltký, J. (2020). Sound absorption properties of natural fibers: A review. *Sustainability*, 12(20), Article 8477. <https://doi.org/10.3390/su12208477>
- Zuidasdok, S. B.-., & Zuidasdok, S. B.-. (2026, 19 april). *Kilometers schermen beperken geluid van A10 Zuid*. Zuidas. <https://zuidas.nl/blog/2023/03/15/kilometers-schermen-beperken-geluid-van-a10-zuid/>
- 廣澤, 邦. (2008). Acoustic absorbers and diffusers—Theory, design and application— [Book review of *Acoustic absorbers and diffusers: Theory, design and application*, by T. J. Cox & P. D'Antonio]. *日本音響学会誌 [Journal of the Acoustical Society of Japan]*, 64(5), 328–329. <https://ci.nii.ac.jp/naid/110006664436>



## Appendix:

TABLE 8 PRODUCED MATERIALS (ADDITIONAL TO THE TABLE IN THE REPORT):

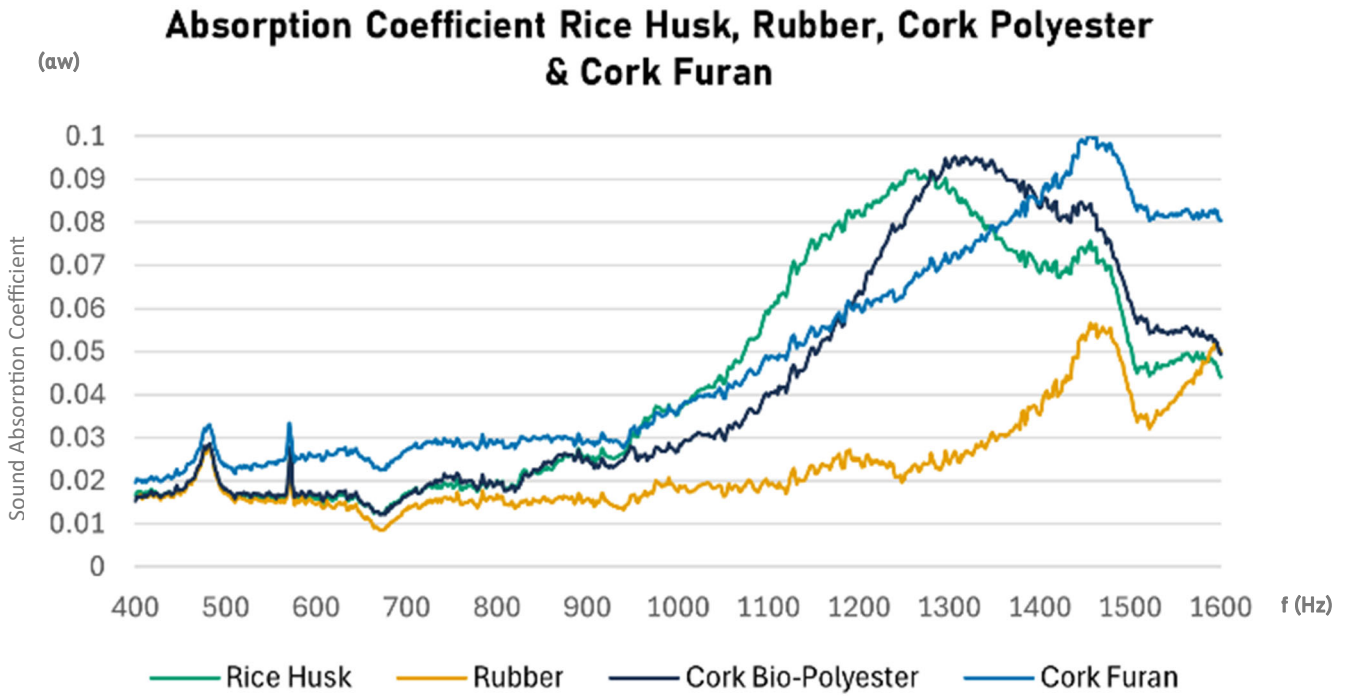
	<p>A1</p>	<p><b>8012 Bio-Polyester</b>  T: 145 centigrade  Time: 6 min  Thickness: 6 mm  Weight: 77 g  Density: 1.634 g/cm<sup>3</sup>  With Mould</p>	
	<p>A2</p>	<p><b>8040 Furan Resin based Fire Hemp</b>  T: 145 centigrade  Time: 15 min  Thickness: 6.5 mm  Weight: 69 g  Density: 1.464 g/cm<sup>3</sup>  With Mould</p>	
	<p>B1</p>	<p><b>Rice Husk</b>  Furan Resin (wt%)  Rice husk (wt%)  T: 145 centigrade  Time: 15 min  Thickness: 6 mm  Weight: 58 g  Density: 1.218 g/cm<sup>3</sup>  With Mould</p>	
	<p>B2</p>	<p><b>Rubber</b>  Furan Resin (wt%)  Rubber (5wt%) (180mu)  (50% petroleum-based rubber and 50% natural)  T: 145 centigrade  Time: 15 min  Thickness: 6.5 mm  Weight: 71 g  Density: 1.369 g/cm<sup>3</sup>  With Mould</p>	
	<p>B3</p>	<p><b>Cork &amp; Bio-Polyester</b>  Bio-Polyester (wt%)  Cork 0.5mm (wt%)  T: 145 centigrade  Time: 6 min  Thickness: 6 mm  Weight: 54 g  Density: 0.885 g/cm<sup>3</sup>  With Mould</p>	

	<b>B4</b>	<b>Glass Bubbles</b> Bio-Polyester (wt%) Glass Bubbles (wt%) T: 145 centigrade Time: 6 min Thickness: 6 mm Weight: 33 g Density: 0.713 g/cm <sup>3</sup> With Mould	
	<b>B5</b>	<b>Cork 10 bar</b> Furan Resin (wt%) Cork 0.5mm (wt%) T: 145 centigrade Time: 15 min Thickness: 6 mm Weight: 55 g Density: 1.167 g/cm <sup>3</sup> With Mould	
	<b>B6</b>	<b>Glass Bubbles 20 bar</b> Bio-Polyester (wt%) Glass Bubbles (wt%) T: 145 centigrade Time: 6 min Thickness: 6 mm Weight: 30 g Density: 0.637 g/cm <sup>3</sup> With Mould	
	<b>B7</b>	<b>Glass Bubbles 40 bar</b> Bio-Polyester (wt%) Glass Bubbles (wt%) T: 145 centigrade Time: 6 min Thickness: 6 mm Weight: 33 g Density: 0.70 g/cm <sup>3</sup> With Mould	
	<b>S1</b>	<b>Foamed Cork 1</b> Furan Resin (90wt%) Cork 0.5mm (10wt%) T: 140 centigrade Thickness: 3-5 mm (mostly 3 mm) Weight: 15 g Density: 0.637 g/cm <sup>3</sup>	

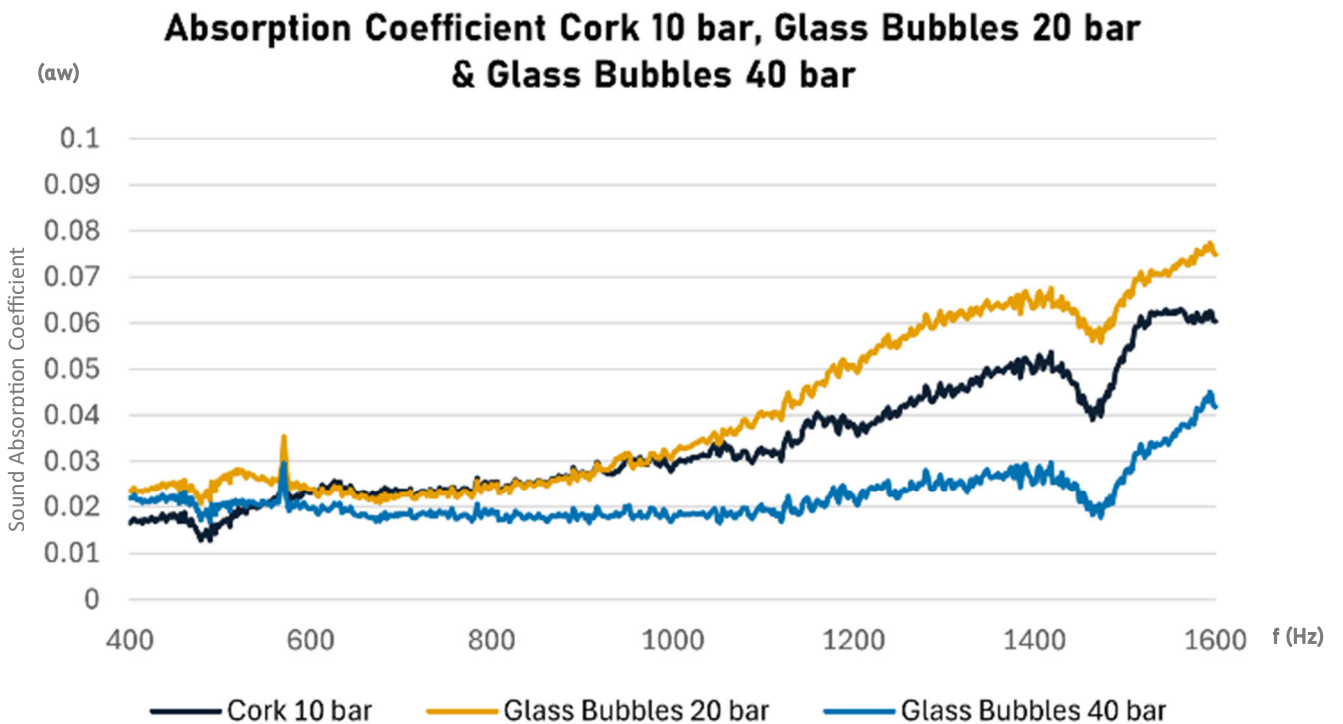
	<p>S2</p>	<p><b>Foamed Cork 2</b>  Furan Resin (80wt%)  Cork 0.5mm (20wt%)  T: 140 centigrade  Thickness: 7-12 mm (mostly 10 mm)  Weight: 54 g  Density: 0.688 g/cm<sup>3</sup></p>	
	<p>S4</p>	<p><b>Foamed Cork 4</b>  Furan Resin (95wt%)  Cork 0.5mm (5wt%)  T: 140 centigrade  Thickness: 6-8 mm  Weight: 11 g  Density: 0.200 g/cm<sup>3</sup>  With Mould</p>	
	<p>S5</p>	<p><b>Foamed Cork 5</b>  Furan Resin (95wt%)  Cork 0.5mm (5wt%)  T: 140 centigrade  Thickness: 11 mm  Weight: 19 g  Density: 0.220 g/cm<sup>3</sup>  Low Moisture (less than 2%)  With Mould</p>	
	<p>S6</p>	<p><b>Foamed Cork 6</b>  Furan Resin (90wt%)  Cork 0.5mm (10wt%)  T: 160 centigrade  Thickness: 2-7 mm  Weight: 9 g  Density: 0.164 g/cm<sup>3</sup>  Low Moisture (less than 2%)  With Mould</p>	
	<p>S7</p>	<p><b>Foamed Cork 7</b>  Furan Resin (80wt%)  Cork 0.5mm (20wt%)  T: 160 centigrade  Thickness: 9 mm  Weight: 39 g  Density: 0.552 g/cm<sup>3</sup>  Low Moisture (less than 2%)  With Mould</p>	

Table 8: Overview Produced Materials (additionally to overview in the thesis) (source: Author)

## IMPEDANCE TUBE TESTING RESULTS



*Figure 101: Impedance Tube test – Absorption Coefficient Rice Husk, Rubber, Cork Bio-Polyester & Cork Furan (source: Author)*



*Figure 102: Impedance Tube test – Absorption Coefficient Cork low pressure, Glass Bubbles different pressures (source: Author)*

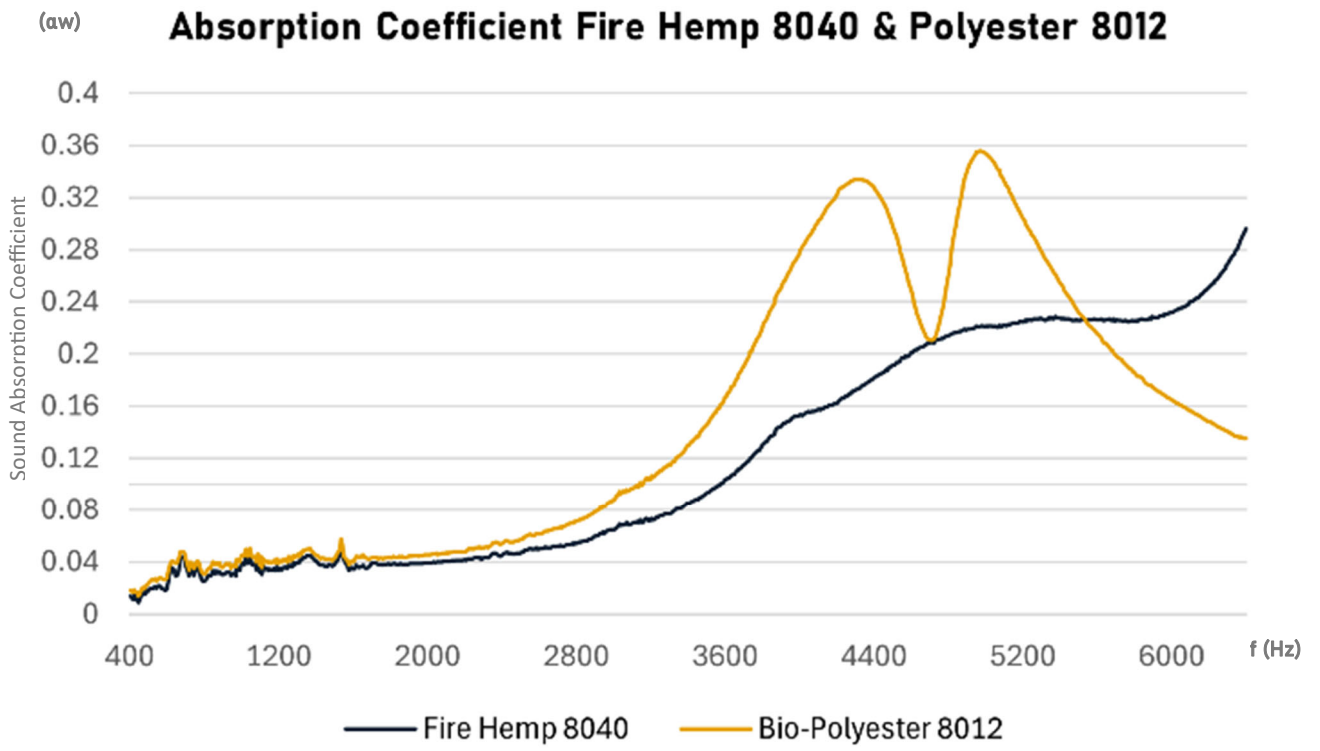


Figure 103: Impedance Tube test - Absorption Coefficient Fire Hemp 8040 (source: Author)

# IMPEDANCE TUBE TESTING – KU LEUVEN

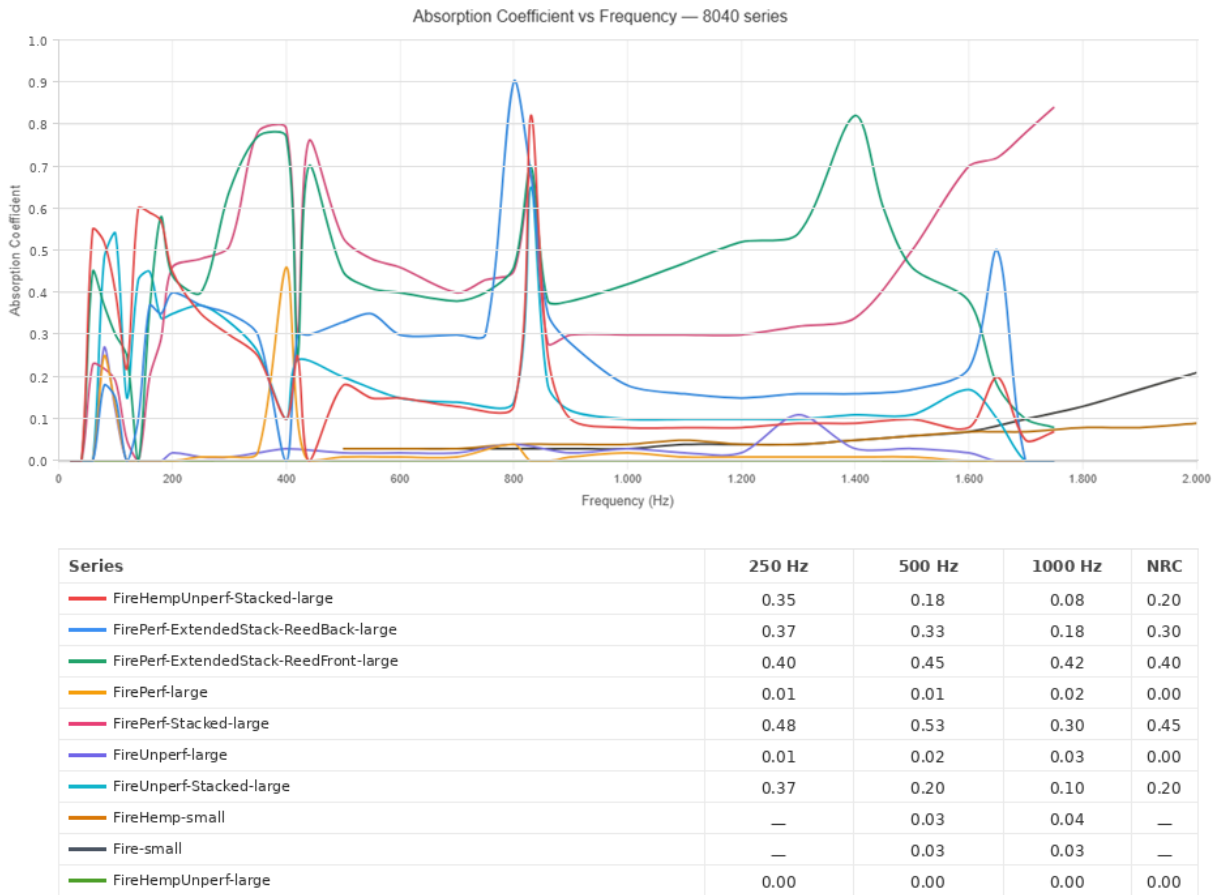


Figure 104: Impedance Tube test – absorption coefficient combinations conducted at the KU Leuven – 8040 series (source: Author)

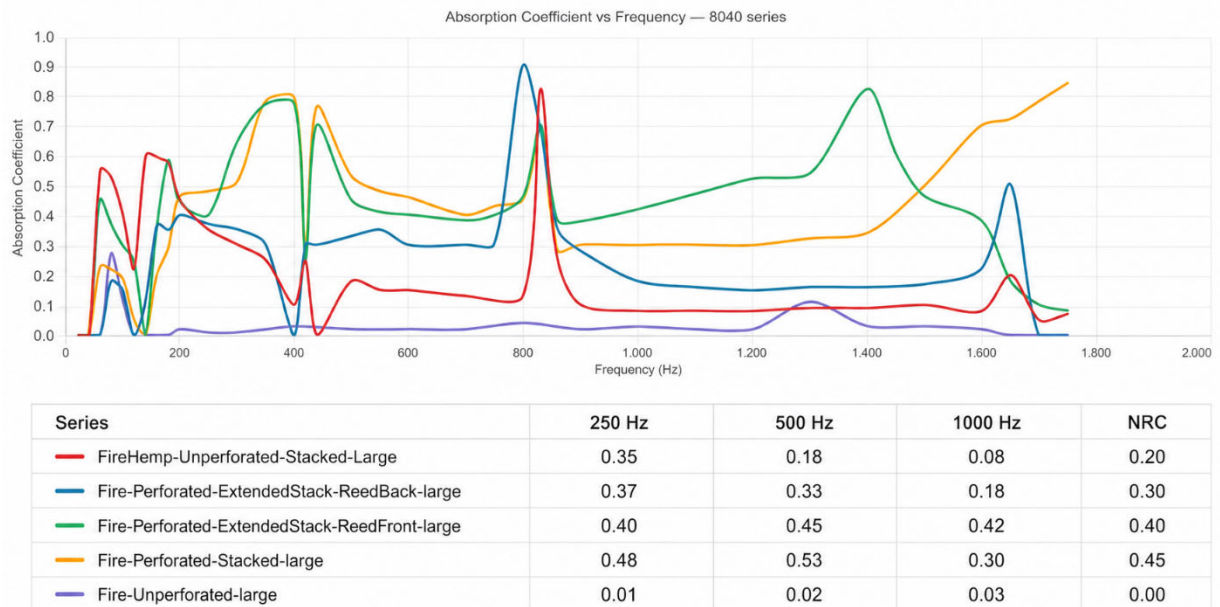
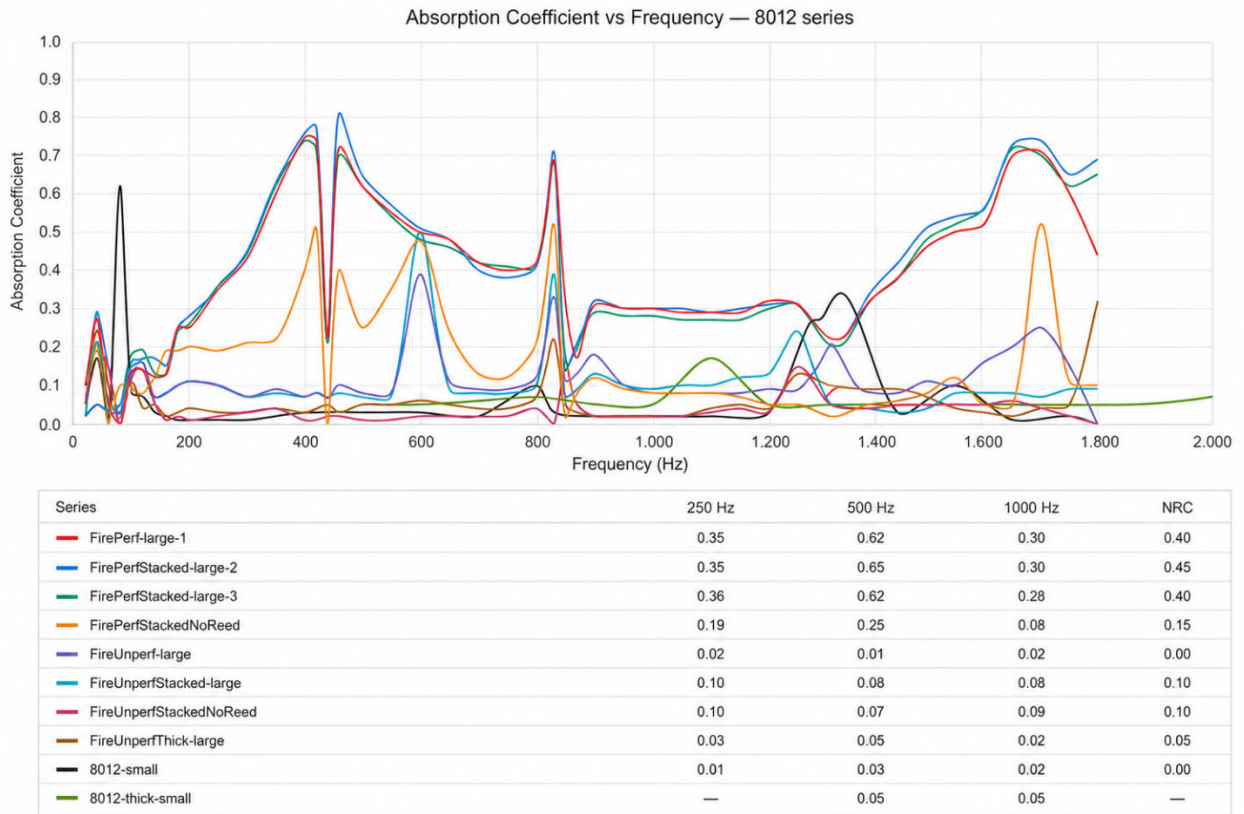
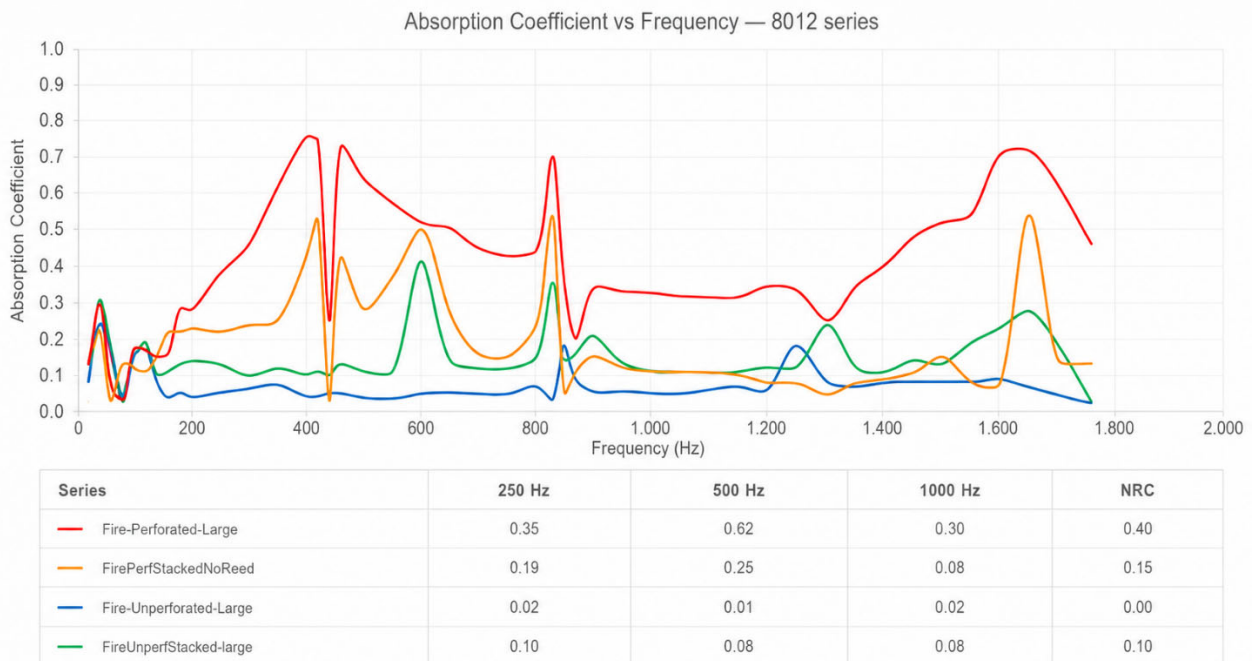


Figure 105: Impedance Tube test – absorption coefficient combinations conducted at the KU Leuven selection – 8040 series (source: Author)



**Figure 106: Impedance Tube test – absorption coefficient combinations conducted at the KU Leuven – 8012 series (source: Author)**



**Figure 107: Impedance Tube test – absorption coefficient combinations conducted at the KU Leuven selection – 8012 series (source: Author)**

# ABSORPTION TESTING TU DELFT

Table 18: Water Basin Capillary Water Conductivity:

Data pH Absorption Testing	Pt1000	Pt1000 (microS/cm)
Troom: 26 centigrade		
Twater: 23 centigrade		
pH before testing	6.17	41.38
pH after testing	7.68	487.4

Table 18: (source: Author)

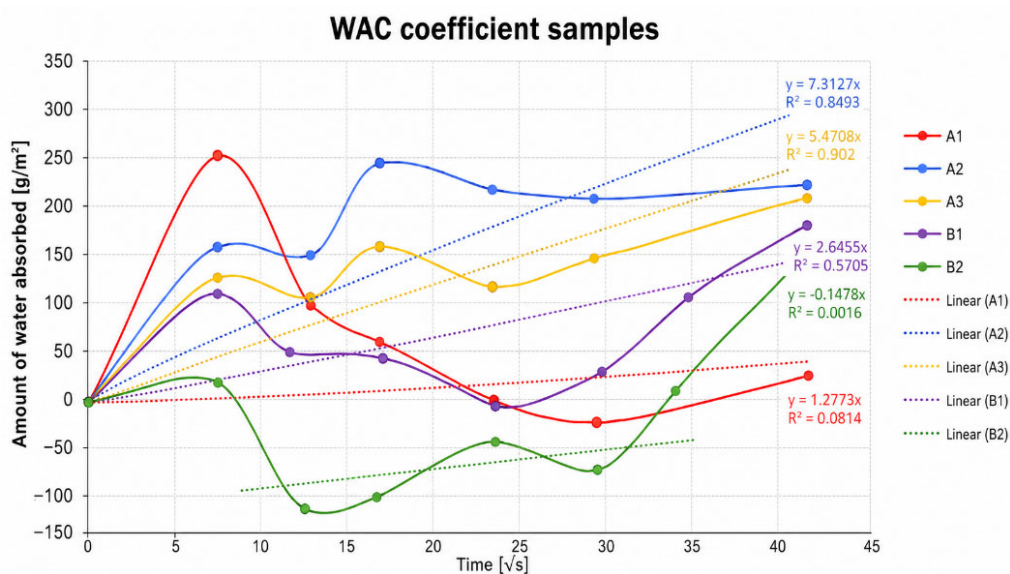


Figure 108: Amount of water absorbed for each sample after 8h (A1, A2, A3, B1, B2) (observations: no decrease of weight is possible; this is likely to be caused by the cord under the weighing scale which touched the perforated table the scale was placed on; according to B. Lubelli) (source: Author)



Figure 109: WA (Water absorption) test close-up (source: Author)

**Capillary water absorption test**

Material

Furan resin based porous samples (S3,S9,S10,S11,S13)

Source

Belgium

Sample Code

A1	A2	A3
----	----	----

Note

with tape with tape with tape

Dry mass (without tape) Md [g]

101.98 31.12 53.89

Immersed surface area A [m<sup>2</sup>]

0.00785 0.00785 0.00785

seconds	t(i)=√s	time	S10 (bamboo)			S3 (cork)			S9 (almond shell)		
			M=m(i) [g]	W=m(i)-m(0) [g]	W/A [g/m <sup>2</sup> ]	M=m(i) [g]	W=m(i)-m(0) [g]	W/A [g/m <sup>2</sup> ]	M=m(i) [g]	W=m(i)-m(0) [g]	W/A [g/m <sup>2</sup> ]
0	0.0	0 min	104.15	0.00	0.00	32.21	0.00	0.00	55.92	0.00	0.00
60	7.7	1 min	106.13	1.98	252.23	33.42	1.21	154.14	56.89	0.97	123.57
180	13.4	3 min	106.88	2.73	347.77	33.37	1.16	147.77	56.73	0.81	103.18
300	17.3	5 min	107.33	3.18	405.10	34.13	1.92	244.59	57.14	1.22	155.41
600	24.5	10 min	107.33	3.18	405.10	33.91	1.70	216.56	56.82	0.90	114.65
900	30.0	15 min	107.21	3.06	389.81	33.84	1.63	207.64	57.06	1.14	145.22
1,800	42.4	30 min	107.42	3.27	416.56	33.9	1.69	215.29	57.55	1.63	207.64
2,700	52.0	45 min	108.99	4.84	616.56	34.79	2.58	328.66	58.32	2.40	305.73
3,600	60.0	60 min	109.24	5.09	648.41	34.14	1.93	245.86	57.77	1.85	235.67
5,400	73.5	90 min	108.29	4.14	527.39	33.95	1.74	221.66	57.27	1.35	171.97
7,200	84.9	2 h	107.73	3.58	456.05	34.47	2.26	287.90	57.57	1.65	210.19
10,800	103.9	3 h	108.34	4.19	533.76	34.54	2.33	296.82	58.01	2.09	266.24
14,400	120.0	4 h	108.18	4.03	513.38	34.61	2.40	305.73	57.67	1.75	222.93
18,000	134.2	5 h	108.28	4.13	526.11	34.93	2.72	346.50	58.07	2.15	273.89
21,600	147.0	6 h	110.01	5.86	746.50	35.78	3.57	454.78	60.74	4.82	614.01
28,800	169.7	8 h	110.08	5.93	755.41	34.40	2.19	278.98	58.84	2.92	371.97

**Capillary water absorption test**

Material

Furan resin based porous samples (S3,S9,S10,S11,S13)

Source

Dom. Republic, NPSP, Belgium, etc.

Sample Code

B1	B2
----	----

Note

with tape with tape

Dry mass (without tape) Md [g]

69.11 73

Immersed surface area A [m<sup>2</sup>]

0.00785 0.00785

seconds	t(i)=√s	time	S13 (tall furan)			S11 (cork)		
			M=m(i) [g]	W=m(i)-m(0) [g]	W/A [g/m <sup>2</sup> ]	M=m(i) [g]	W=m(i)-m(0) [g]	W/A [g/m <sup>2</sup> ]
0	0.0	0 min	75.41	0.00	0.00	77.01	0.00	0.00
60	7.7	1 min	76.26	0.85	108.28	77.15	0.14	17.83
180	13.4	3 min	76.64	0.38	48.41	76.1	-0.91	-115.92
300	17.3	5 min	76.96	0.32	40.76	76.19	-0.82	-104.46
600	24.5	10 min	76.87	-0.09	-11.46	76.66	-0.35	-44.59
900	30.0	15 min	77.09	0.22	28.03	76.45	-0.56	-71.34
1,800	42.4	30 min	78.46	1.37	174.52	78.1	1.09	138.85
2,700	52.0	45 min	77.76	-0.70	-89.17	78.22	1.21	154.14
3,600	60.0	60 min	77.73	-0.03	-3.82	77.09	0.08	10.19
5,400	73.5	90 min	78.64	0.91	115.92	78.67	1.66	211.46
7,200	84.9	2 h	78.74	0.10	12.74	77.57	0.56	71.34
10,800	103.9	3 h	78.24	-0.50	-63.69	77.07	0.06	7.64
14,400	120.0	4 h	78.48	0.24	30.57	77.68	0.67	85.35
18,000	134.2	5 h	79.16	0.68	86.62	77.79	0.78	99.36
21,600	147.0	6 h	79.46	0.30	38.22	78.47	1.46	185.99
28,800	169.7	8 h	80.13	0.67	85.35	80.04	3.03	385.99

Figure 110: Data capillary water absorption (source: Author)

## ABSORPTION TESTING NPSP

Table 19: 8040 Water Absorption:

Recipes	Water Absorption (%) – 96h
Biochar – Profagus – Furan	0.94 – 1.05
Almond Shell – Furan	0.97 – 1.13
Biochar – Profagus – UPE	0.3
Activated Carbon Coconut	0.5

*Table 19: (source: NPSP)*

Table 20: Swelling/Shrinkage change in plates:

Recipe	Length before water absorption (cm)	Length after water absorption (cm)	Length after drying (cm)
Biochar – Profagus	29.3	29.42 (0.41%)	29.32
Lignocellulosic filler (base)	29.28	29.38 (0.34%)	29.29
Biochar – Profagus – UPE	29.51	29.55 (0.14%)	29.51

*Table 20: Swelling/Shrinkage change in plates (Length Mould: 29.65 cm) (source: NPSP)*

Table 21: Mechanical Properties NPSP materials:

Recipe	Flexural Strength (MPa)	Flexural Modulus (GPa)	Flexural Strain (%)	Impact Strength (kJ/m <sup>2</sup> )	Density (g/cc)
Biochar	36	4.4	0.81	2.4	1.37
Biochar – 96h water	26 (27%)	4.8	0.59	1.8	1.42
Biochar – 96h water + dried	32 (11%)	4.7	0.75	1.9	1.37
Almond Shell	72	5.3	1.4	5.7	1.38
Almond Shell – 96h water	50.1 (31%)	5.4	1.2	4.1	1.41
Almond Shell 96h water + dried	64 (11%)	5.3	1.2	4.9	1.38
Almond Shell + oven dried	64.7	5.3	1.23	5.1	1.37
Almond Shell + hemp + App	53	4.6	1.3		1.43
Almond Shell + hemp + App + dried	42 (26%)	5	0.92		1.47
Mica	32	10.6	0.44	3	1.53
Mica – 96h water	15	4.1	0.49	1.5	1.58
Biochar – 2.5% Borchi	23	3	0.98	2	1.52
Activated Coconut biochar	73	8.45	0.8		1.55
Activated Coconut biochar – 96h water	69	8.3	0.86		1.57

*Table 21: Mechanical properties (Data on Almond Shell water absorption e.g.) (source: NPSP)*

Table 22: Water Absorption (source: NPSP):

Recipe	Water absorption (%) – 96h
Biochar - Profagus	1.05
Mica	0.71
Almond Shell (base)	1.13

*Table 22: Water Absorption (source: NPSP)*

Table 23: Swelling/Shrinkage change in plates:

Recipe	Length before water absorption (cm)	Length after water absorption
Biochar – Profagus	29.3 (1.1%)	29.42 (0.76%)
Mica	29.35 (1%)	29.45 (0.65%)

*Table 23: Swelling/Shrinkage change in plates (source: NPSP)*

## POROUS FILLER-BASED MATERIAL PRODUCTION

Table 24: Overview of the produced porous filler-based materials:


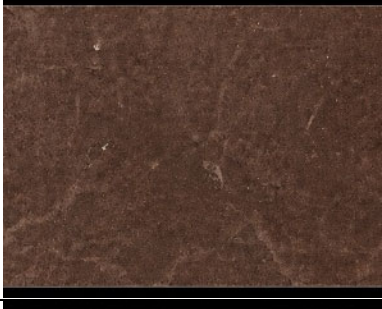



Rubber & Almond Shell	
Cork 0-0.5mm	
Cork 0.1mm	
Rice Husk	
Glass Bubbles	

Table 24: (source: Author)

# MECHANICAL PROPERTIES PRODUCED POROUS FILLER MATERIALS

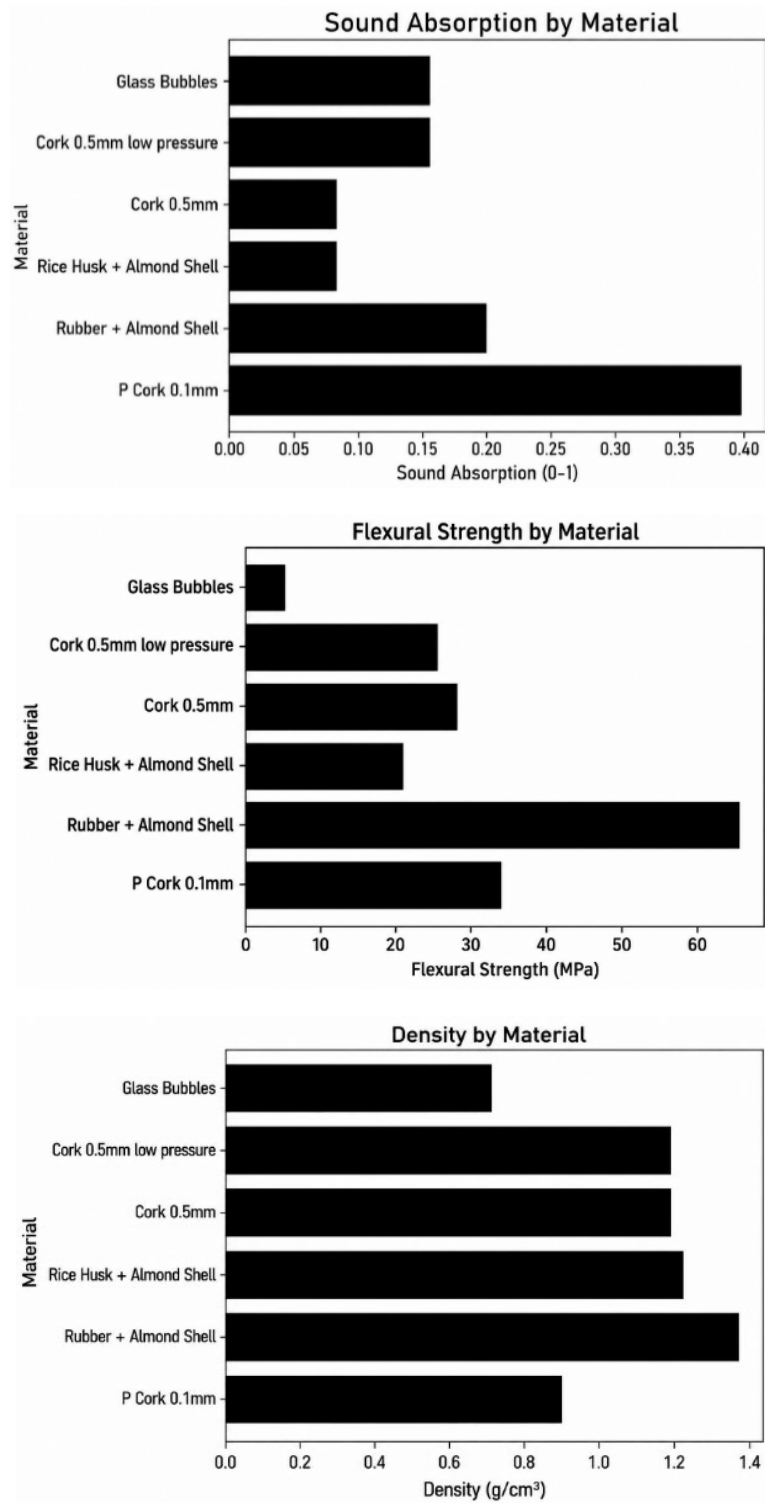


Figure 111: Mechanical Properties Overview; 3-point bending test results of different porous filler materials (source: Author)

Table 25: Mechanical properties porous filler-based materials production:

Material	Flexural Strength (MPa)	S.D. (MPa)	Flexural Strain (%)	Flex modulus (GPa)	Density (g/cm <sup>3</sup> )	Filler (%)	Pressure (bar)	Price (EUR/m <sup>2</sup> )	Details
Rubber + Almond Shell	65.8	3.73	1.1	6.51	1.369	5	40	185	5% rubber (filler), 44% almond shell (filler)
Rice Husk + Almond Shell	20.8	6.16	0.78	3.08	1.218	34	10	185	34% almond shell, 11% rice husk
Cork 0.5mm	27.7	8.24	1.5	2.16	1.188	25	40	185	25% cork
Cork 0.5mm low pressure	25	3.56	1.4	2.09	1.188	25	10	185	25% cork
Cork 0.1mm	33.6	1.53	1.3	3.26	0.885	28	40	185	28% cork
Glass Bubbles	4.68	1.6	0.33	2.08	0.713	44	40	185	44% glass bubbles, 9% hemp fibre

Table 25: (source: Author)

DIGITAL MICROSCOPIC IMAGES – TU DELFT



Figure 112: **S3** Particle Size Assessment (source: Author)

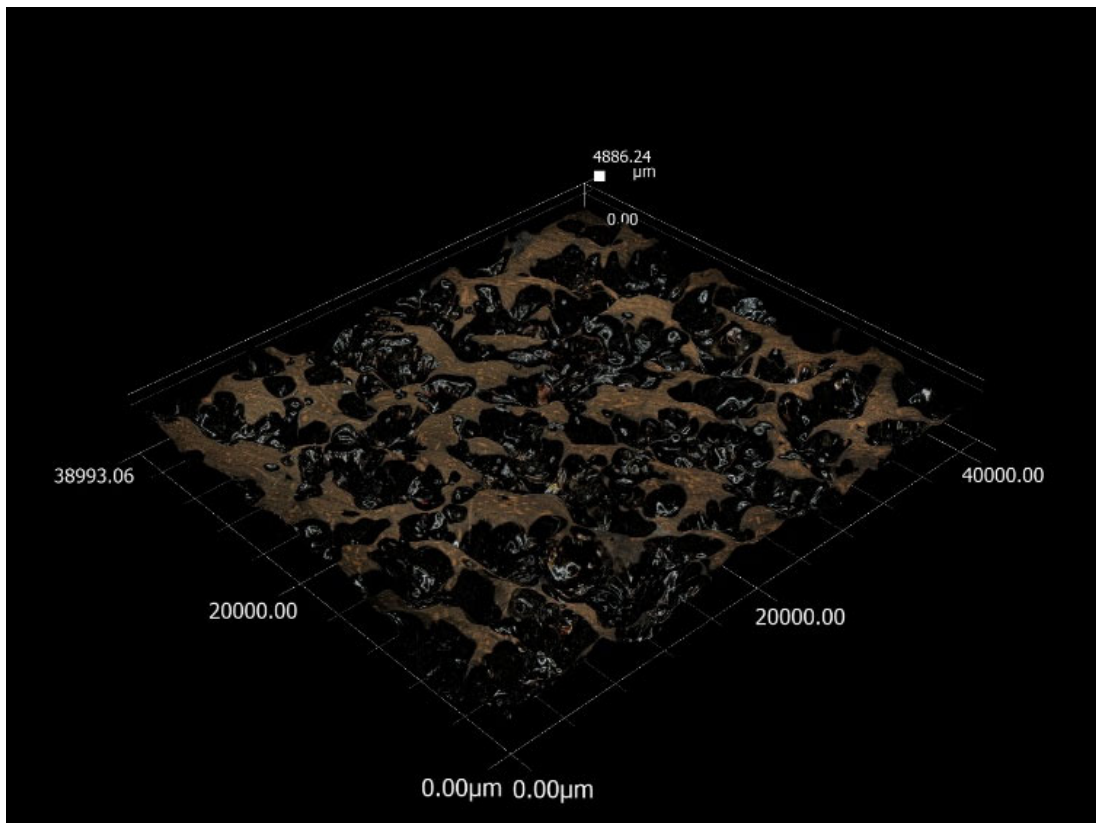


Figure 113: **S10** Depth Assessment (source: Author)

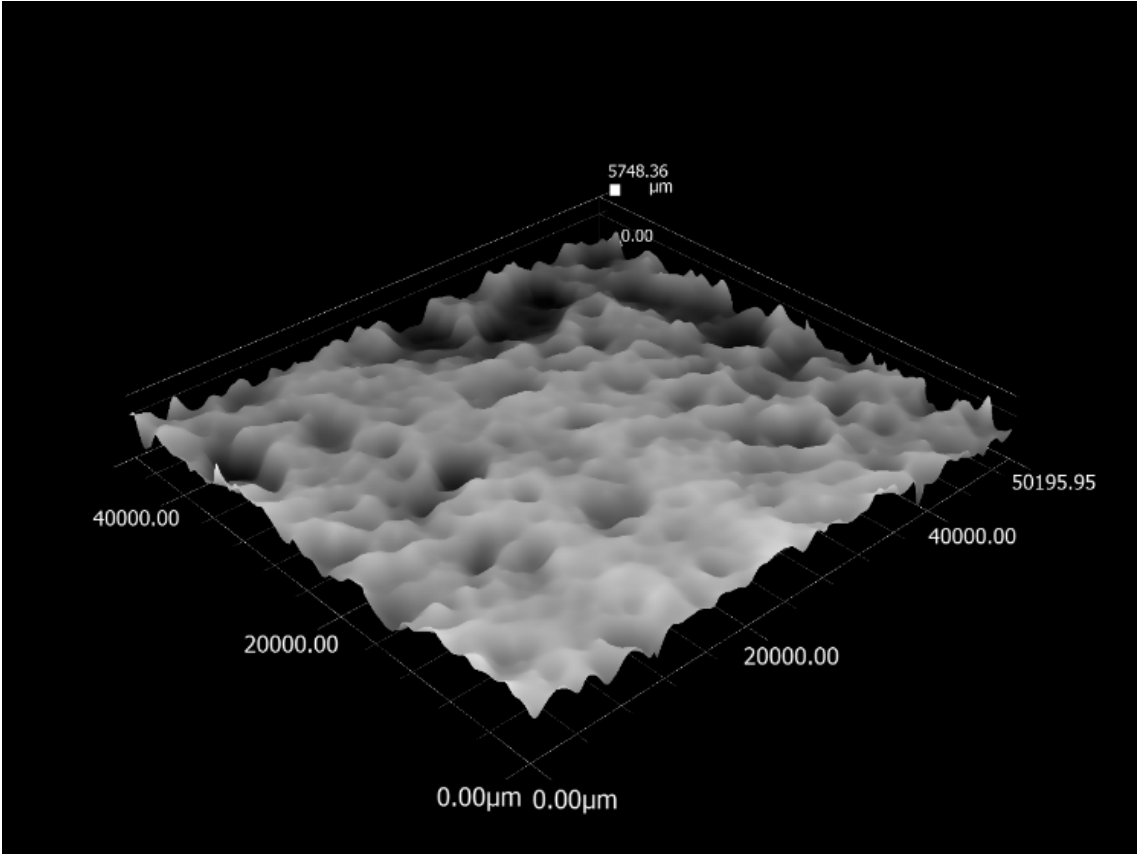


Figure 114: **S11** Depth Assessment black & white (source: Author)

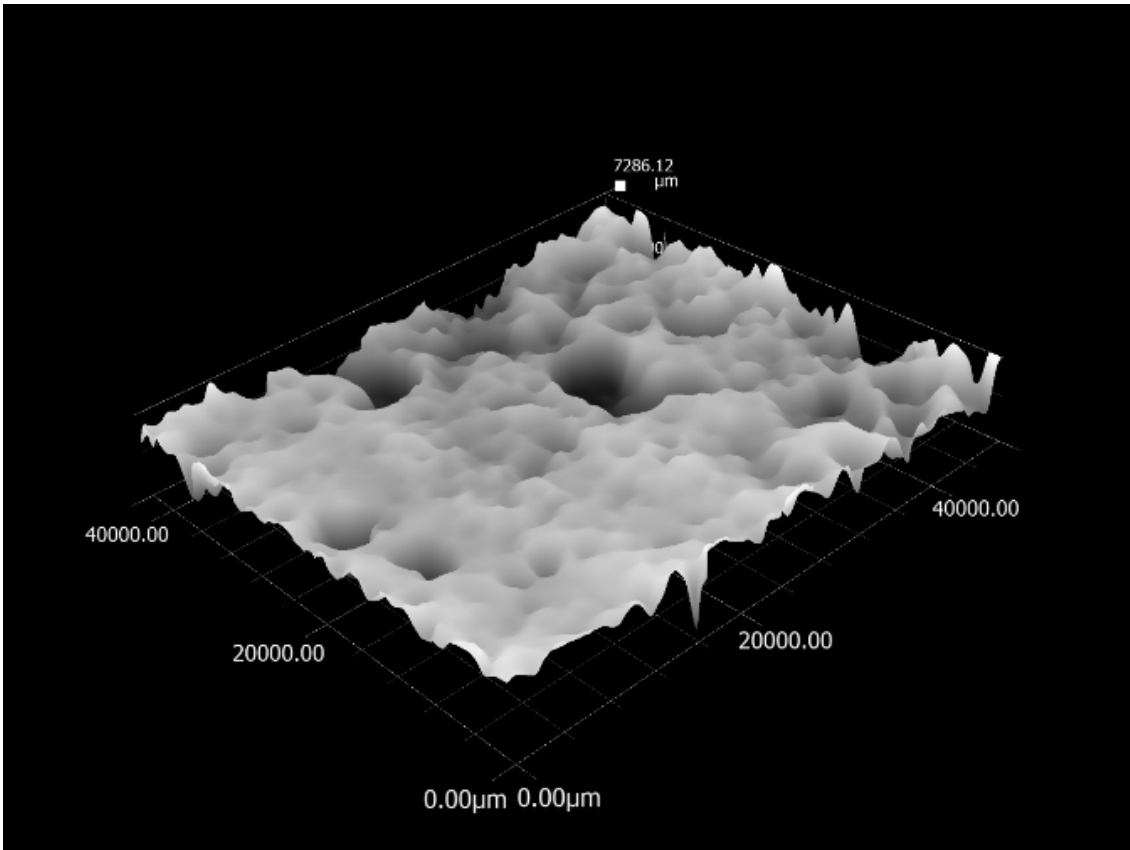


Figure 115: **S13** Depth Assessment black & white (source: Author)

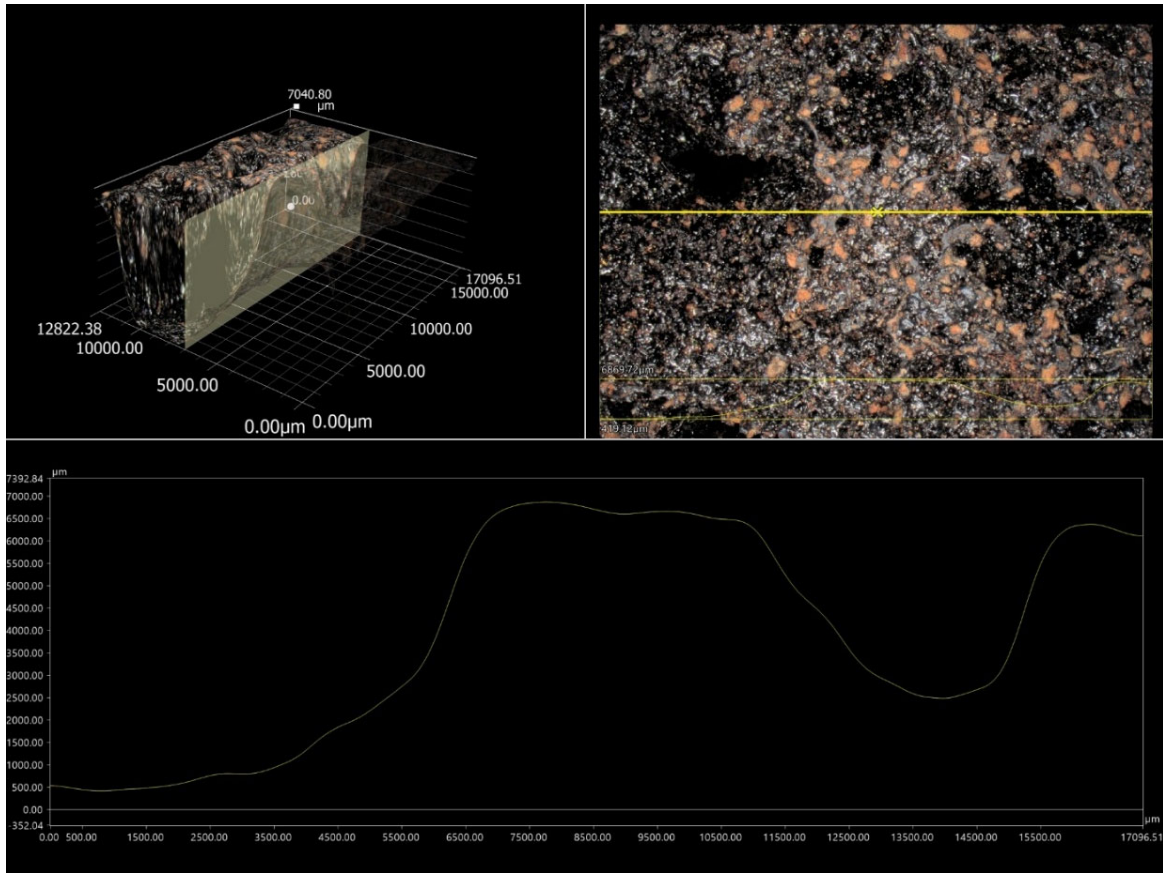


Figure 116: S3 Depth Assessment (source: Author)

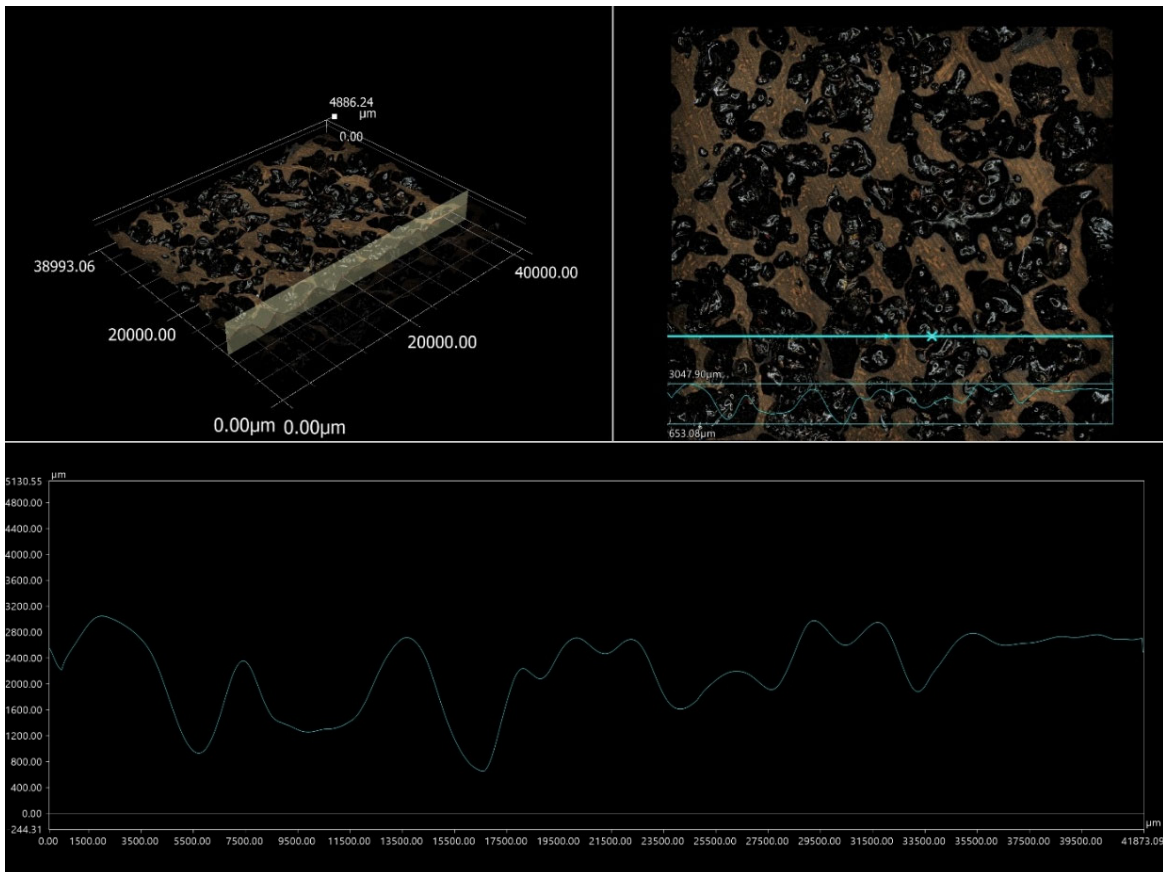


Figure 117: S10 Depth Assessment (source: Author)

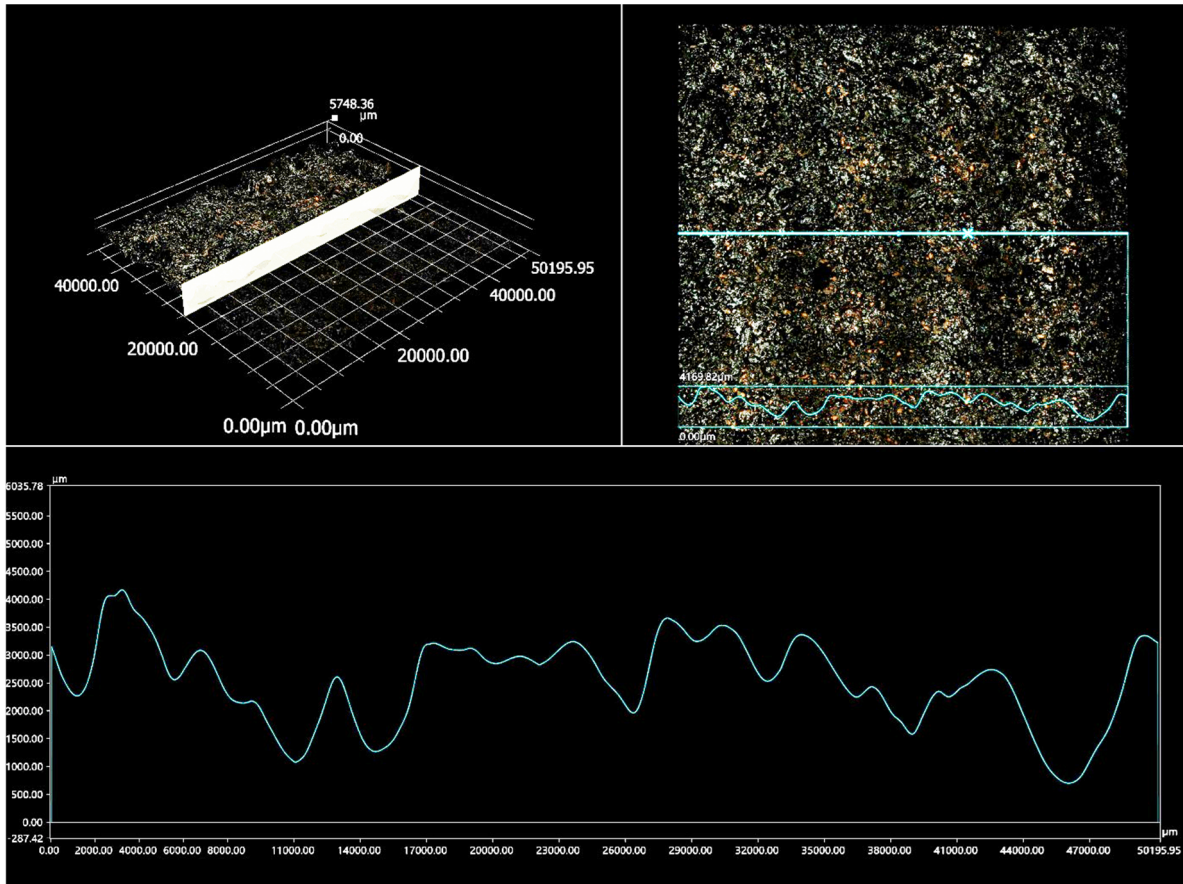


Figure 118: S13 Depth Assessment (source: Author)

FOAMED MATERIALS IMAGES

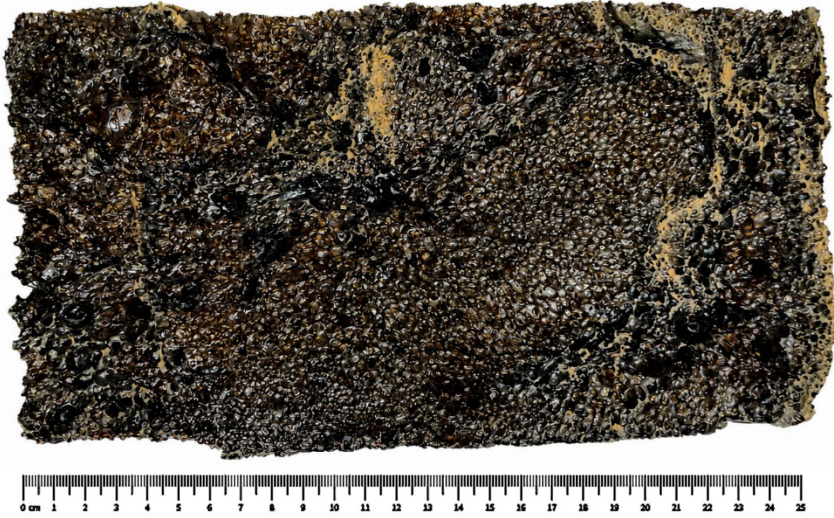


Figure 119: Foamed Material Production **S9**: Almond Shell & Furan Resin (Biorez 14010) (source: Author)

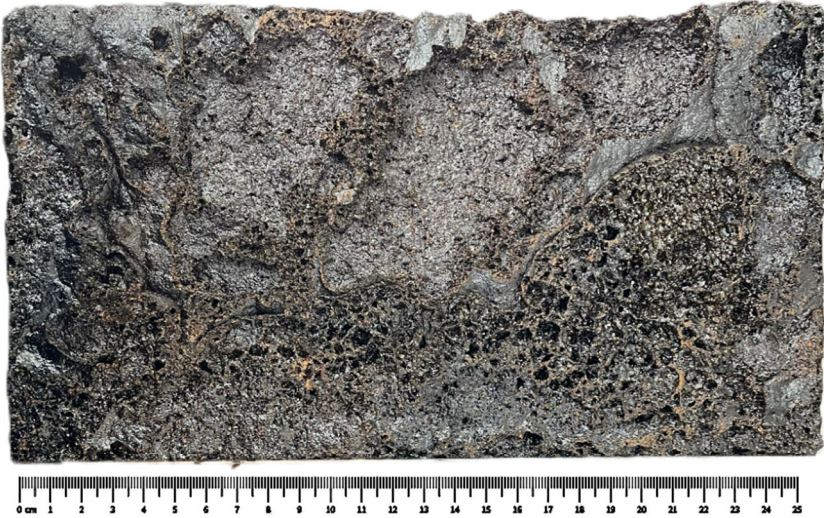


Figure 120: Foamed Material Production **S11**: Cork (0.5 mm) & Furan Resin (Biorez 14010) (source: Author)

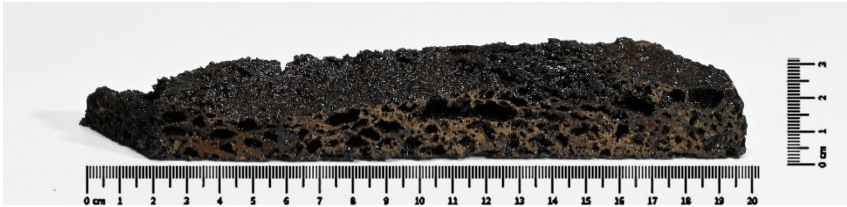


Figure 121: **S11** foamed material (source: Author)



*Figure 122: S1 Foamed Material Production (source: Author)*



*Figure 123: S1 Foamed Material Production (source: Author)*

## GRASSHOPPER SCRIPT OVERVIEW PARAMETRIC MODEL

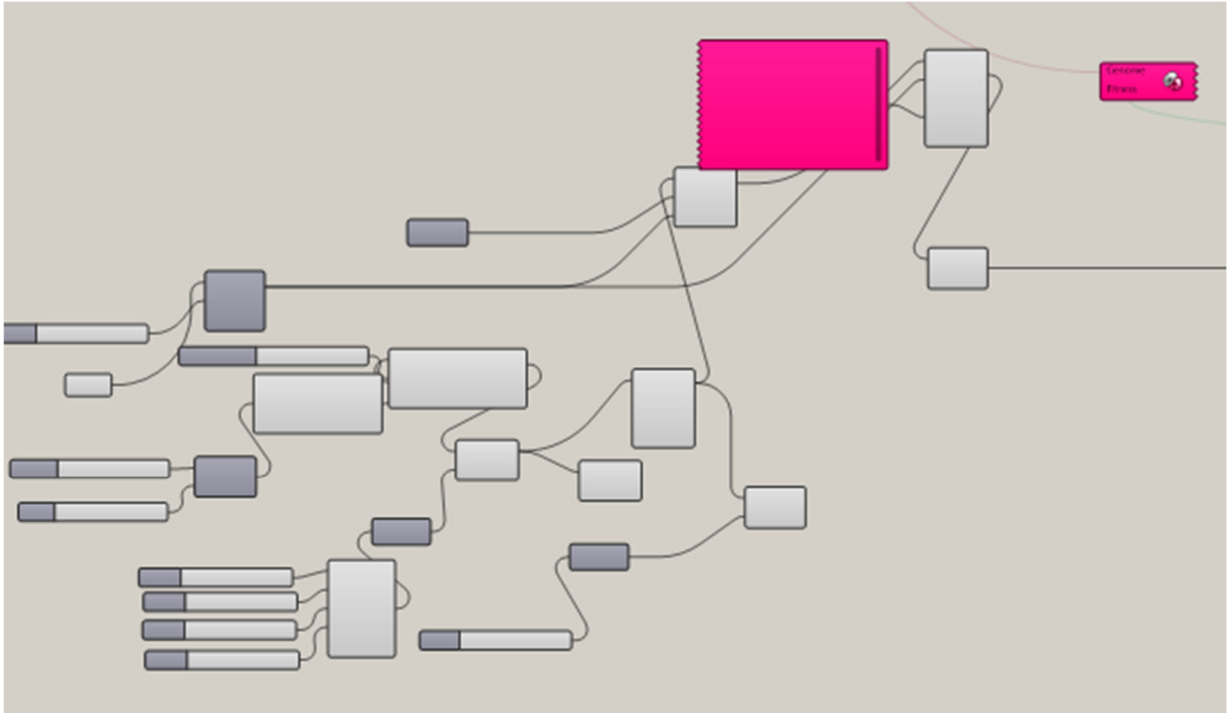


Figure 124: Grasshopper script geometry parametric model (source: Author)

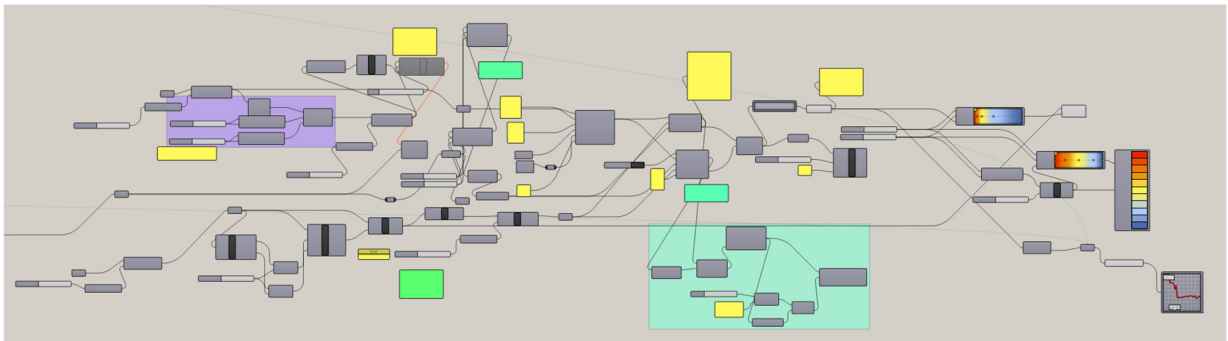


Figure 125: Grasshopper script geometry parametric model (source: Author)